Modélisation de la propagation des fissures hydrauliques par la méthode des éléments finis étendue

patrick.massin@ensta-paristech.fr

Collaborations
Richard Giot ,Université de Poitiers
Fabrice Golfier, Université de Lorraine
Nicolas Moës, Ecole Centrale Nantes
Daniele Colombo, IFPEN
Alexandre Martin, IMSIA

Doctorants
Maximilien Siavelis, Guilhem Ferté, Marcel Ndeffo, Maxime Faivre, Bertrand Paul

Objectives of the work

- The aim of our work is the development of an efficient numerical tool in EDF R&D's industrial finite element free software *Code_Aster* for the simulation of fluid-driven fracture networks in porous rock formations.

- In particular, we would like to stress the following peculiarities:
  - simulate a full hydromechanical coupling
  - extend our model to 3D geometries
  - handle complex crack geometries
  - simulate crack-propagation on non-predefined paths
  - include the possibility to model crack networks

- Wide range of applications:
  - CO_2 geological storage
  - nuclear waste geological storage
  - recovery of hydrocarbons in fractured reservoirs
  - deep geothermal energy

M. Faivre, Ph.D LABEX-GéoRessources 2012-2016, *Modélisation du comportement hydrogéomécanique d'un réseau de failles sous l'effet des variations de l'état de contrainte.*

B. Paul, Ph.D GéoRessources 2013-2016, Modélisation de la propagation de fractures hydrauliques par la méthode des Éléments finis étendus

Context and applications

- Hydraulic fracturing (left) and Enhanced Geotermal Systems (right)
  → generate the most dense and extended fracture network

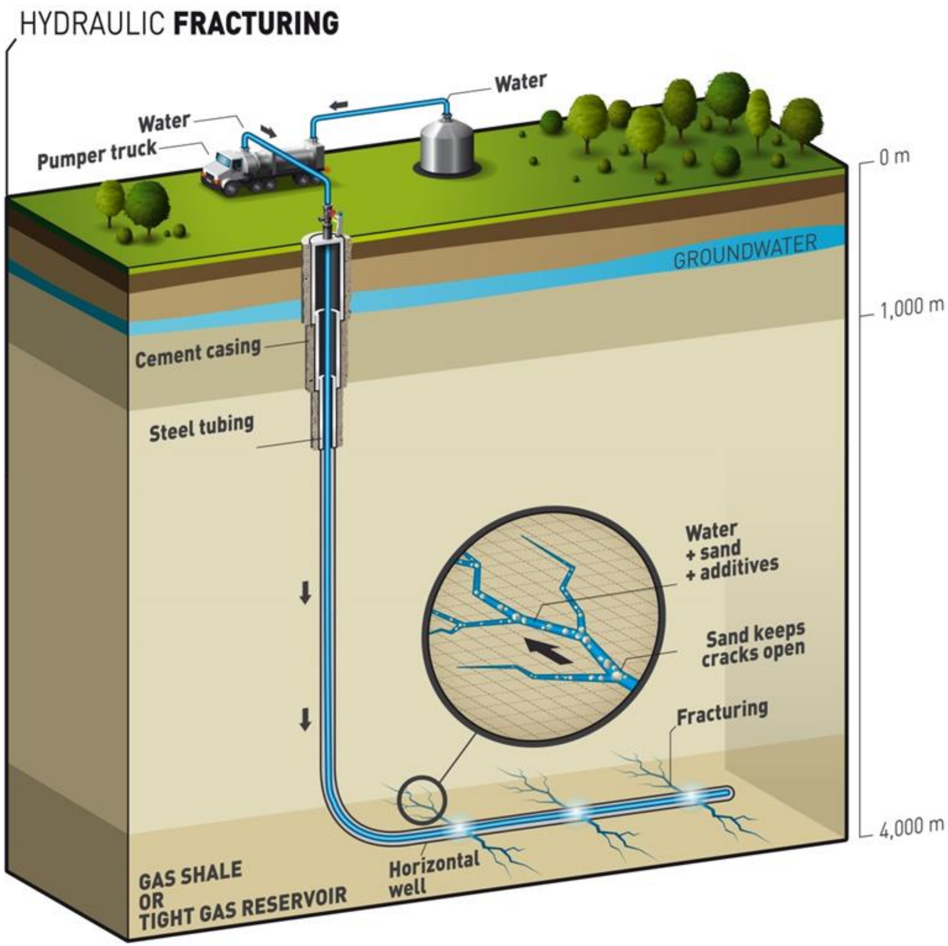

source: Total

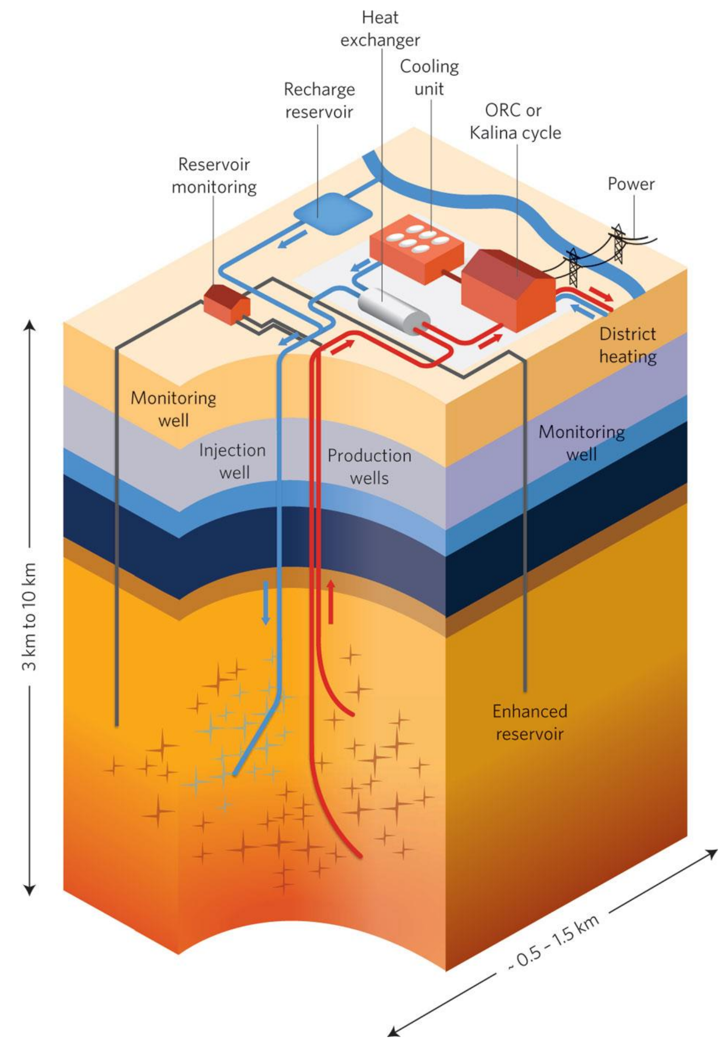

source: Nature

Context and applications

- CO_2 geological storage
  → the propagation of fluid driven cracks constitutes a threat

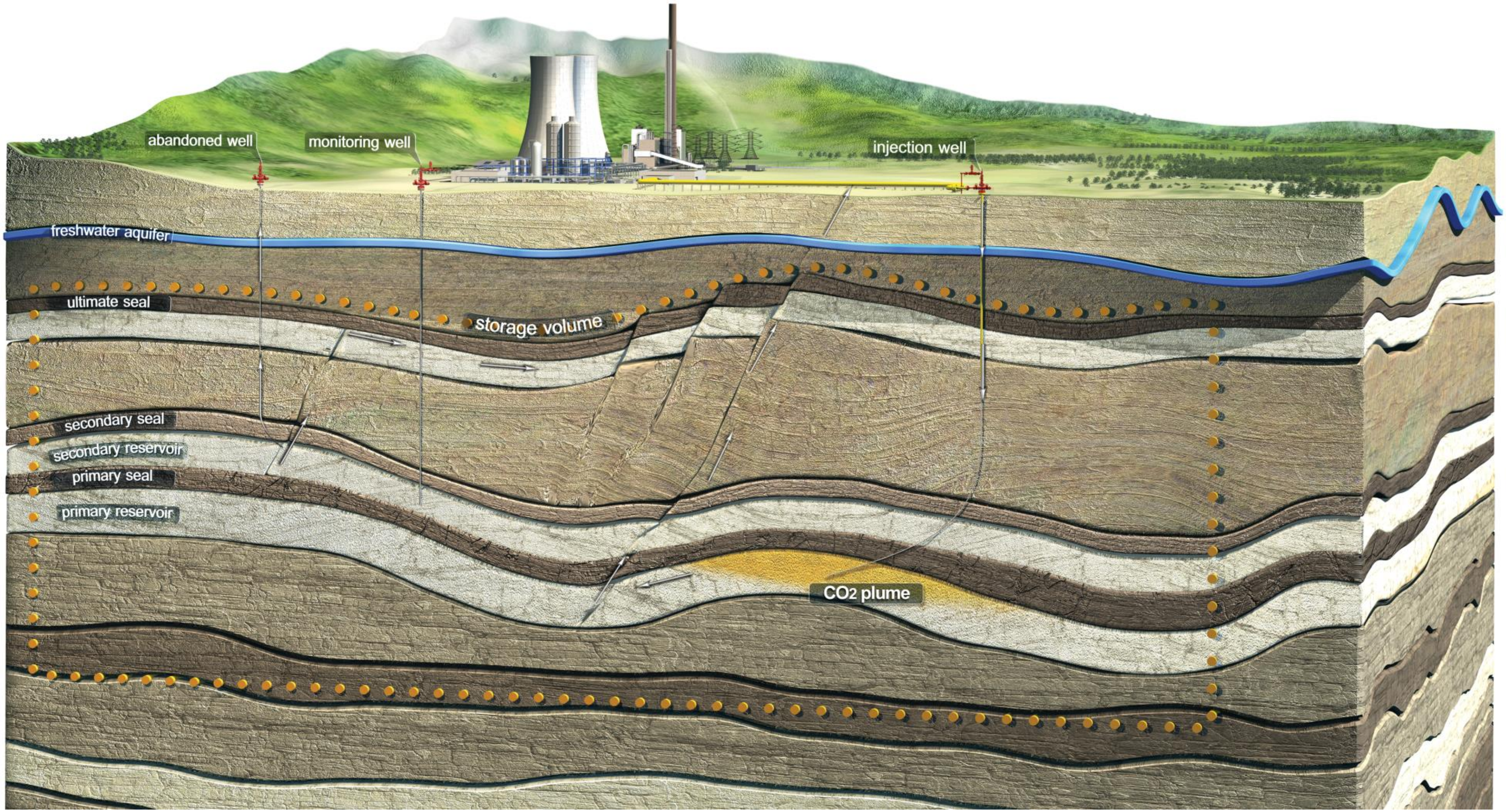

source: DNVGL

Context and applications

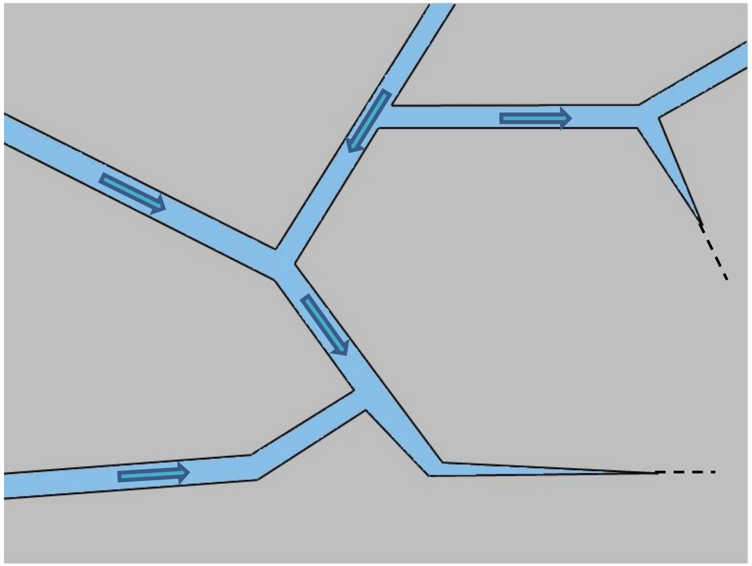

Context and applications

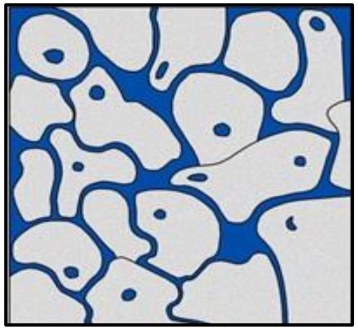

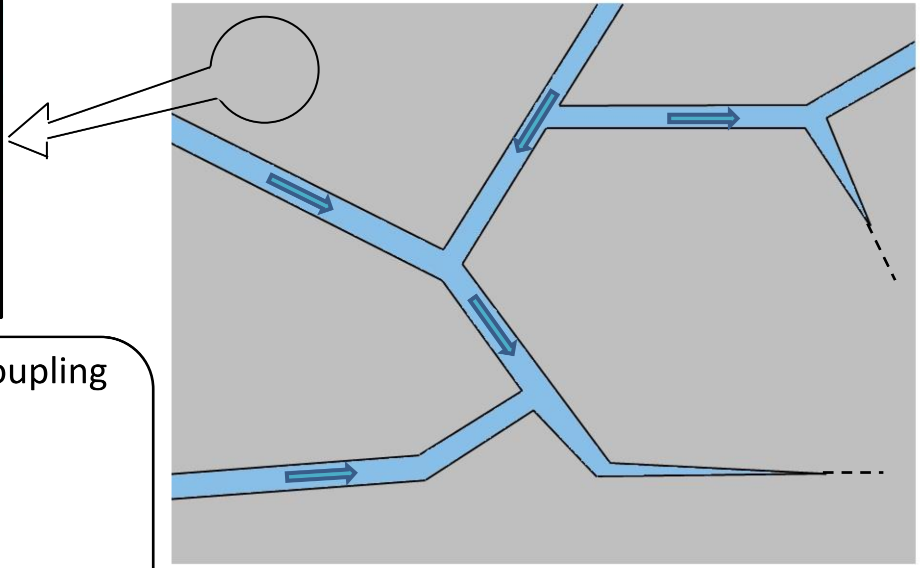

- Hydromechanical coupling
- Mass exchanges
- Heat transfers
- Dynamics
- Multiple phases
- Inhomogeneity/anisotropy

Context and applications

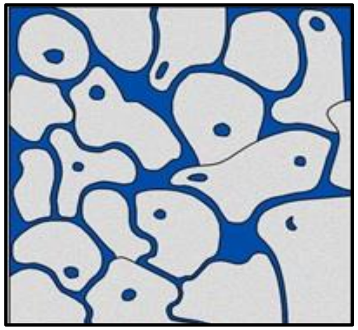

- Hydromechanical coupling
- Mass exchanges
- Heat transfers
- Dynamics
- Multiple phases
- Inhomogeneity/anisotropy

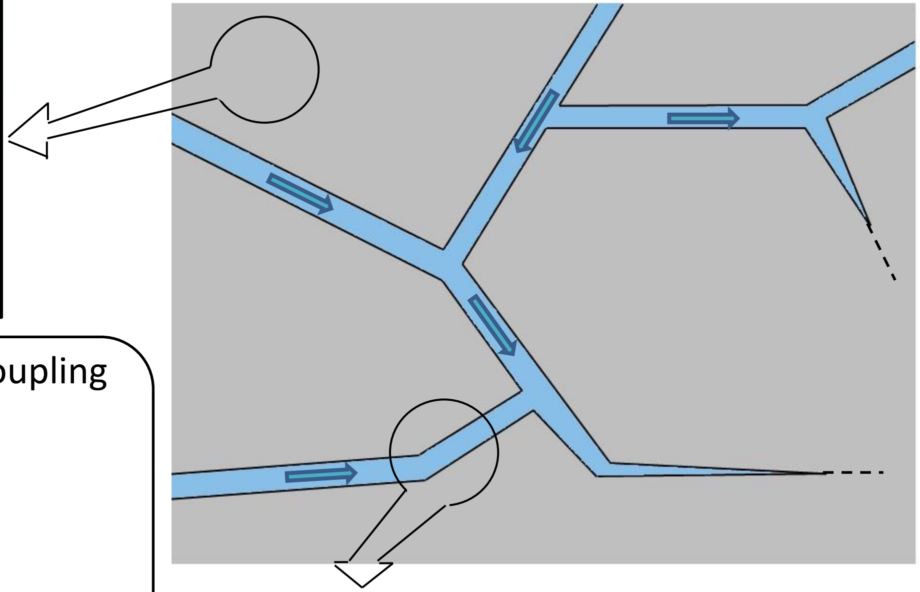

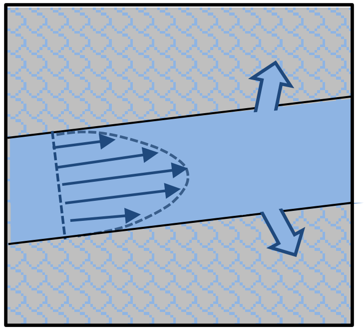

- Preferential flow in the fractures
- Hydromechanical coupling between the fracture and the surrounding porous media
- Multiple phases

Context and applications

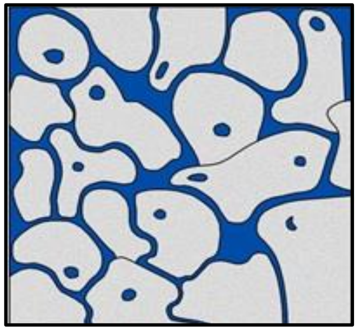

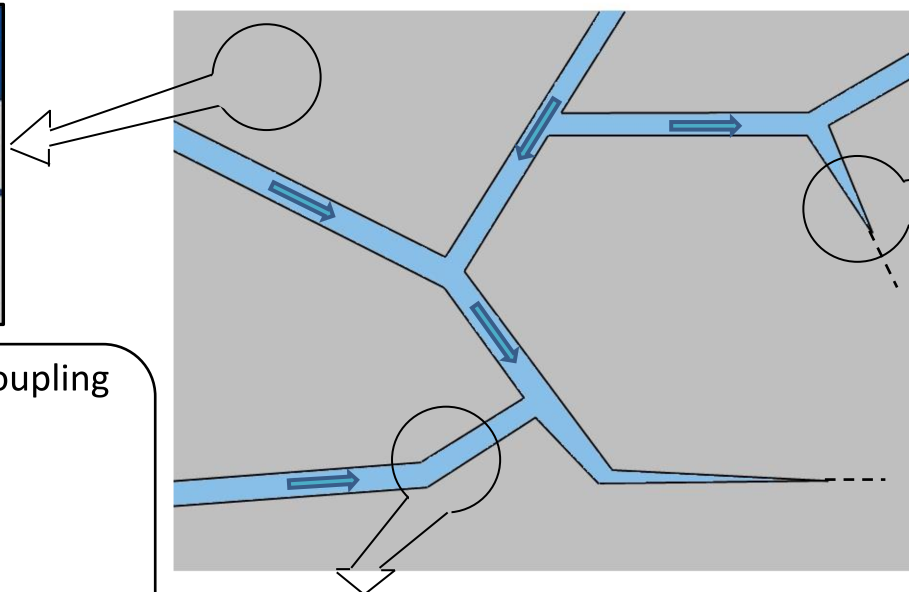

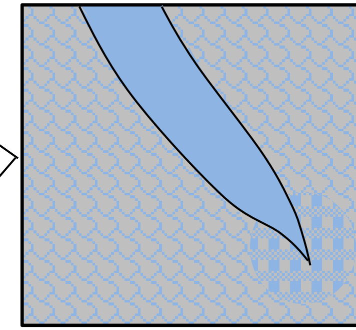

- Hydromechanical coupling
- Mass exchanges
- Heat transfers
- Dynamics
- Multiple phases
- Inhomogeneity/anisotropy

- Crack extension
- Crack reorientation
- Heat discharge
- Fluid lag
- Damage process/plasticity

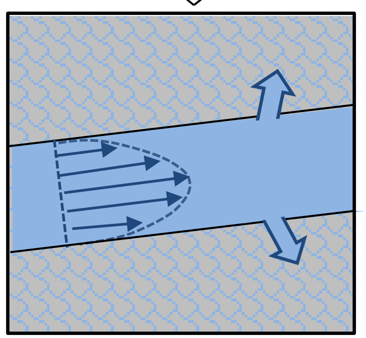

- Preferential flow in the fractures
- Hydromechanical coupling between the fracture and the surrounding porous media
- Multiple phases

Context and applications

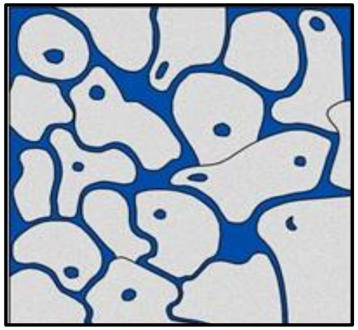

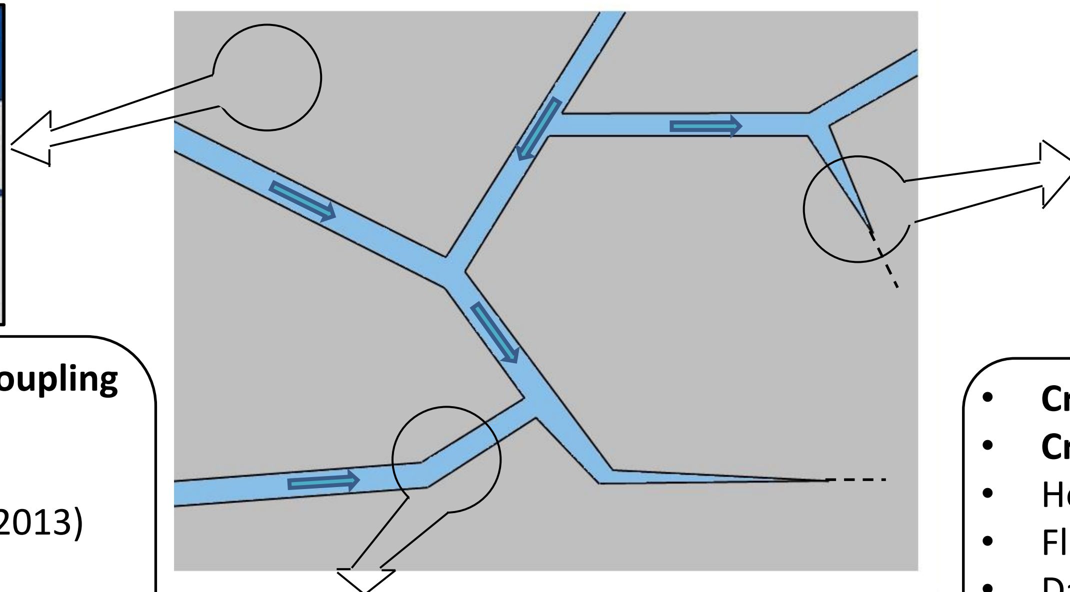

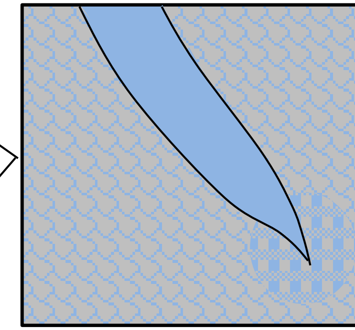

- **Hydromechanical coupling**
- **Mass exchanges**
- Heat transfers (Mohammadnejad 2013)
- Dynamics
- Multiple phases (Younes 2014)
- Inhomogeneity/anisotropy

- **Crack extension**
- **Crack bifurcation**
- Heat discharge
- Fluid lag (Lecampion 2007)
- Damage process/plasticity (Wang 2009)

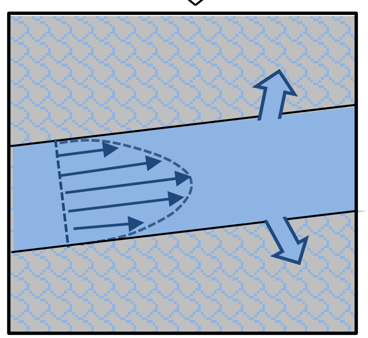

- **Preferential flow in the fractures**
- **Hydromechanical coupling between the fracture and the surrounding porous media**
- Multiple phases

- A. Younes, P. Nunez, A. Makradi, Q. Shao, L. Bouhala, S. Belouettar, *An xfem model for cracked porous media: effects of fluid flow and heat transfer*, Int. J. Fracture 2014
- B. Lecampion, E. Detournay, *An implicit algorithm for the propagation of a hydraylic fracture with a fluid lag,* Comp. Meth. Appl. Meth. Eng. 2007
- S.Y. Wang, L. Sun, A.S.K. Au, T.H. Yang, C.A. Tang, *2D-numerical analysis of hydraulic fracturing in heterogenenous geo-materials*, Construction and Building Materials 2009
- T. Mohammadnejad, A. R. Khoei, *Hydro-mechanical modeling of cohesive crack propagation in multiphase porous media using the extended finite element method*, Int. J. Numer. Meth. Engng. 2013

Context and applications

- Analytical asymptotic solutions exist for the propagation of plane fluid-driven cracks in elastic brittle materials:

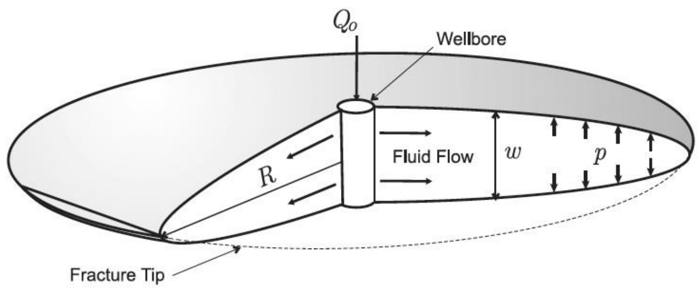

The penny shaped model (Adachi 2007)

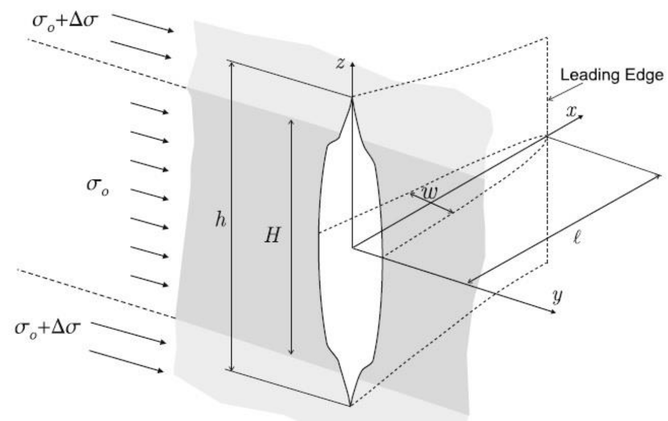

The P3D model (Adachi 2010)

- In particular, the analytical solution predicts distinct fracture profile depending on the propagation regime:

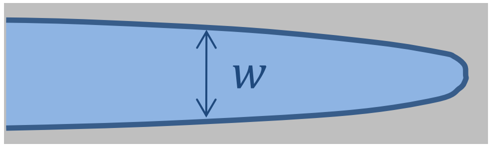

toughness dominated regime $w \sim r^{1/2}$

r : distance from the tip

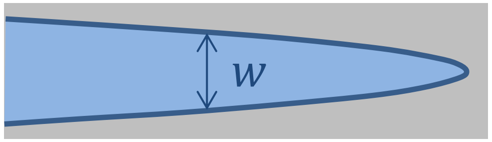

viscosity dominated regime $w \sim r^{2/3}$

- The existence of these asymptotic regimes has been confirmed experimentally (Bunger 2008).

- J. Adachi, E. Siebrits, A. Pierce, J. Desroches, *Computer simulation of hydraulic fractures*, Int. J. Rock. Mech. & Mining Sciences 2007
- J. Adachi, E. Detournay, A. Pierce, *Analysis of the classical pseudo-3d model for hydraulic fracture with equilibrium height growth accross stress barriers*, Int. J. Rock. Mech. & Mining Sciences 2010
- A. Bunger, E. Detournay, *Experimental validation of the tip asymptotics for a fluid-driven crack,* J. Mech Phys. Solids 2008

Meshing discontinuities

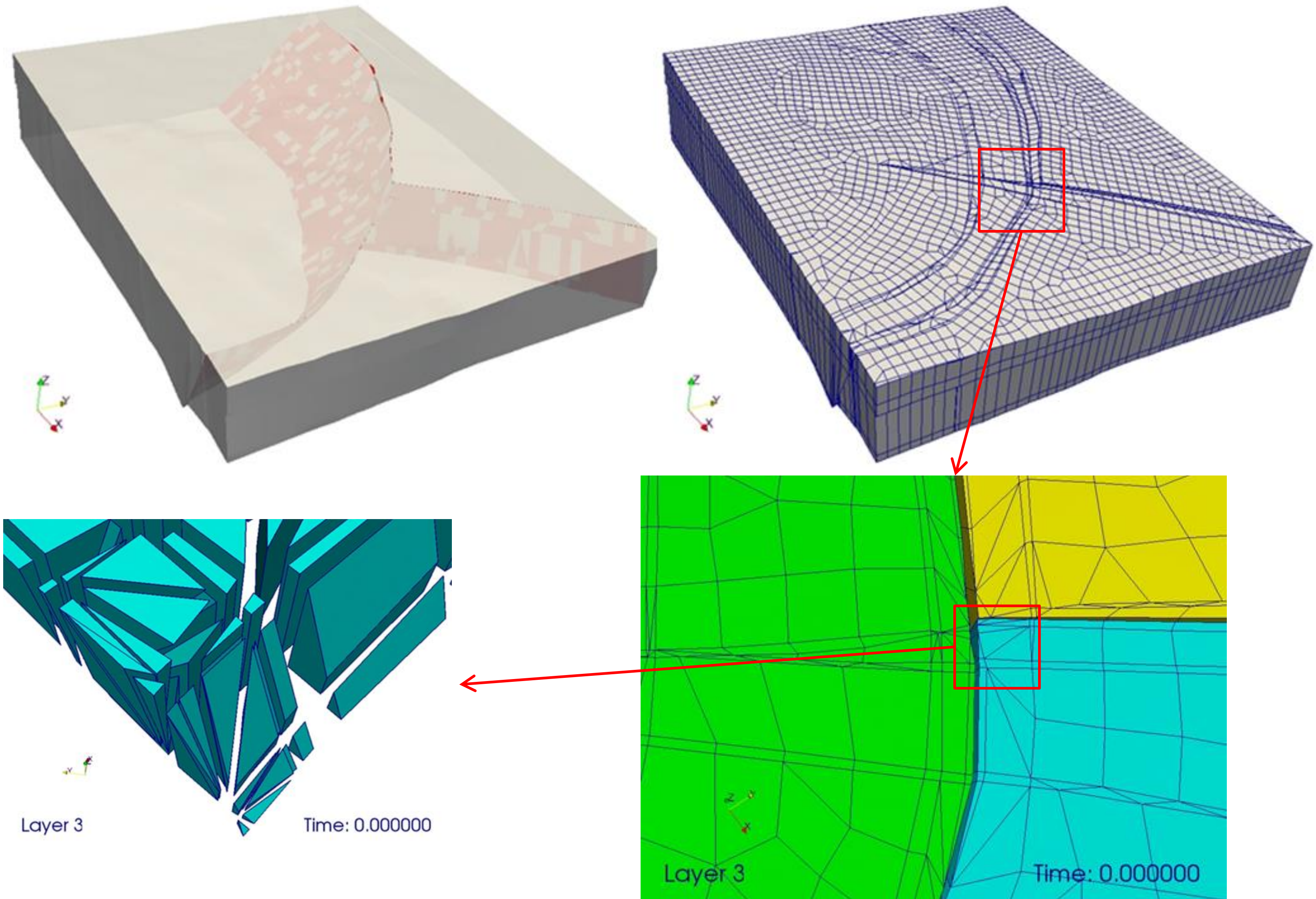

source: IFPEN

The eXtended Finite Element Method

- In order to model continous media intersected by arbitrary discontinuities, we favor the XFEM, which consists in introducing additional degrees of freedom associated to discontinous shape functions.

- The discontinuities are located in the mesh thanks to level set functions (*level-set-method*).

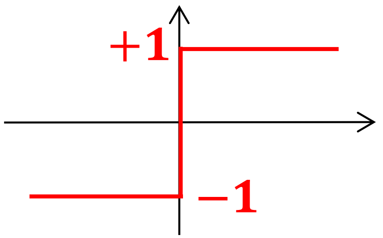

The generalized Heaviside function

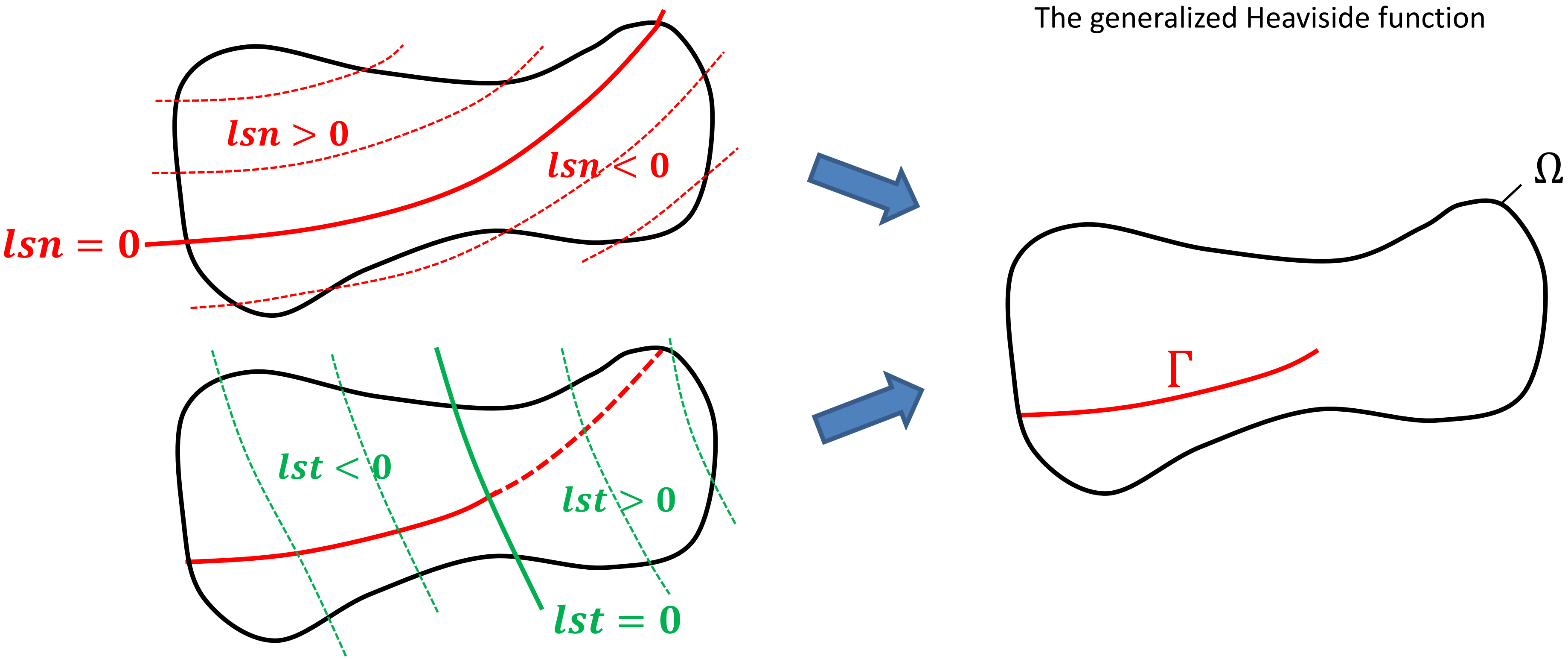

lsn: normal level set lst: tangential level set

The eXtended Finite Element Method

→ No more need for a conforming mesh
→ No need to generate a new mesh each times the crack evolves

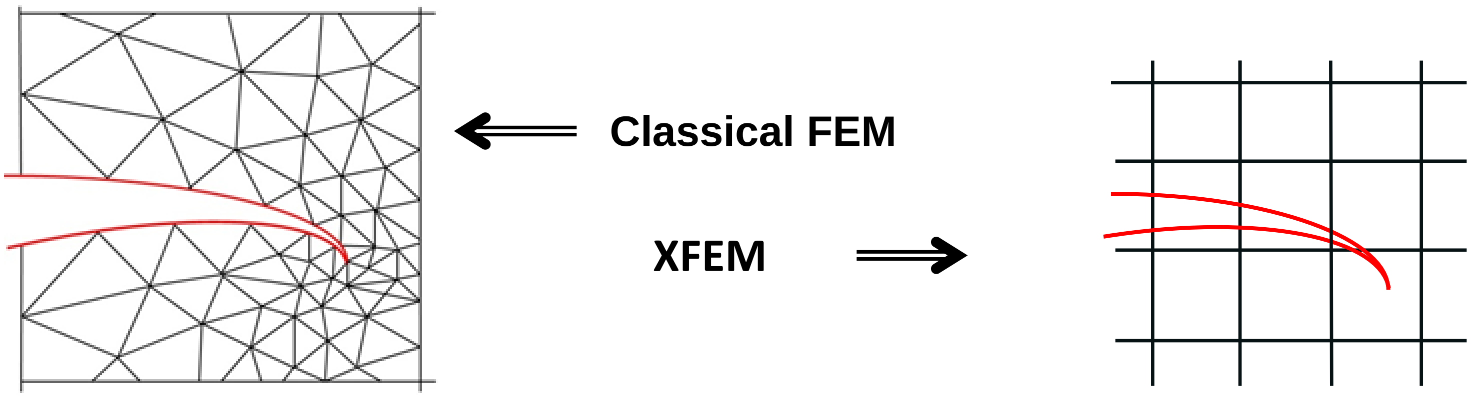

The eXtended Finite Element Method

→ No more need for a conforming mesh
→ No need to generate a new mesh each times the crack evolves

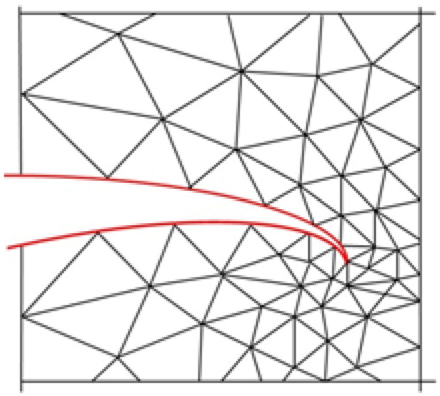

⟸ **Classical FEM**

XFEM ⟹

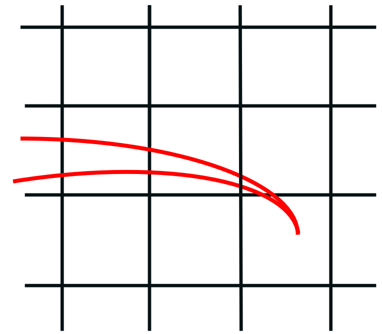

- Extension of this approach to branched discontinuities:

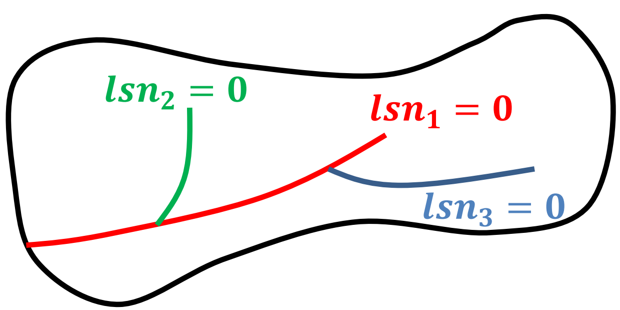

Layered normal level set fields modeling branched discontinuities

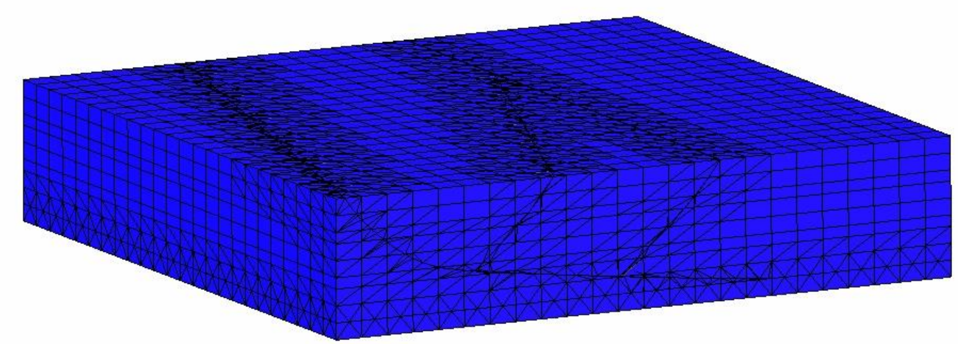

Basin modeling with XFEM (Siavelis 2011)

M. Siavelis, Ph.D IFPEN, *Modélisation numérique X-FEM de grands glissements avec frottement le long d'un réseau de discontinuités*, 2011

The eXtended Finite Element Method

- The enrichment strategy we rely on has been developped by Ndeffo (Ndeffo 2015). It allows to confine the conditioning issues.

- We developped a quadratic integration procedure for 3D curved branched interfaces in the framework of the eXtended Finite Element Method. The overall procedure is the object of a publication (Paul, 2016). We obtained optimal convergence rates in 2D and 3D for the resolution of the interface.

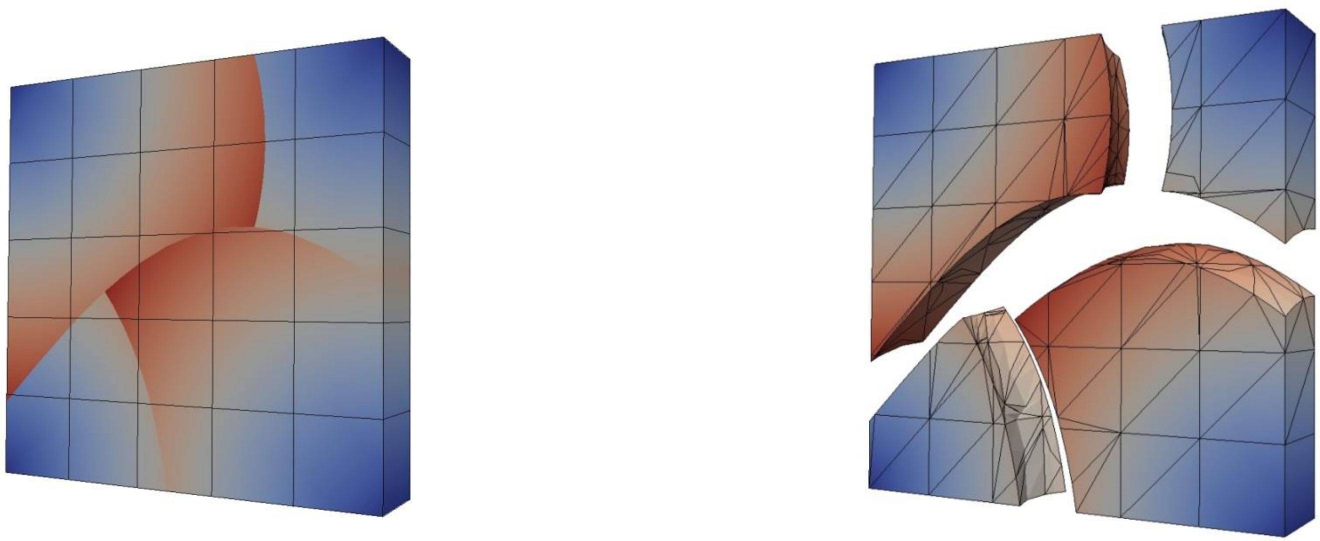

approximation mesh *integration mesh and amplified deformed shape*

Curved branched interfaces (Paul, 2016)

- M. Ndeffo, Ph.D Ecole Centrale de Nantes, *Modélisation numérique de la propagation de fissures avec des éléments 2D et 3D quadratiques,* 2015
- B. Paul, M. Ndeffo, P. Massin, N. Moës, *An integration technique for 3D curved cracks and branched discontinuities within the eXtended Finite Element Method*, Finite Element Analysis and Design 2016

Notations

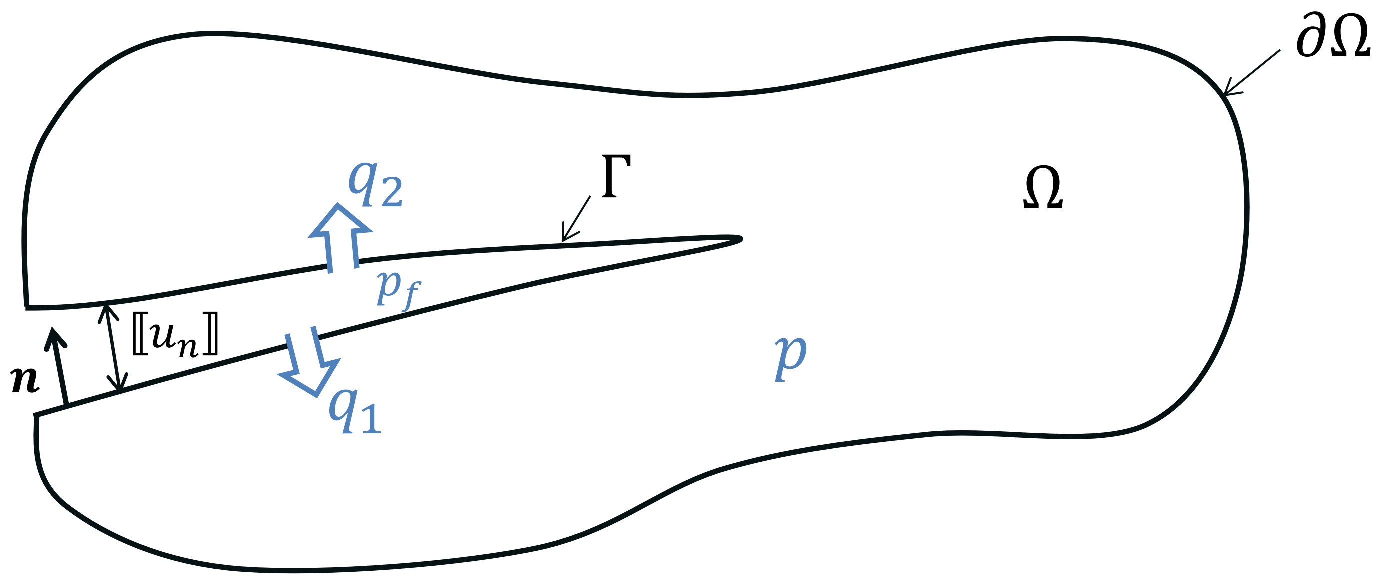

Porous matrix Ω

- The displacements are denoted $\boldsymbol{u}$
- The pore pressure is denoted p

Fluid-filled fracture Γ

- The aperture or normal displacement jump is denoted $[\![u_n]\!]$
- The pressure of the fluid in the fracture is denoted p_f
- The fluid fluxes from the fracture to the lower and upper part of the surrounding porous matrix are denoted q_1 and q_2

3 distinct approximation spaces

- The displacement field $\boldsymbol{u}$ is quadratic and enriched.

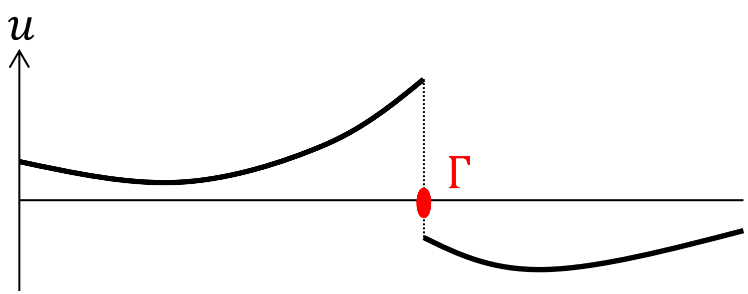

$$\mathbf{u}_h(\mathbf{x}) = \sum_{i \in N} \mathbf{a}_i \psi_i(\mathbf{x}) + \sum_{j \in N \cap N_H} \mathbf{b}_j \psi_j(\mathbf{x}) H_j(lsn(\mathbf{x}))$$

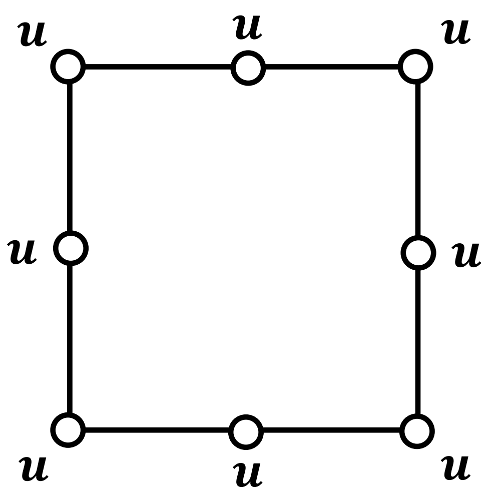

3 distinct approximation spaces

- The displacements field $\boldsymbol{u}$ is quadratic and enriched.

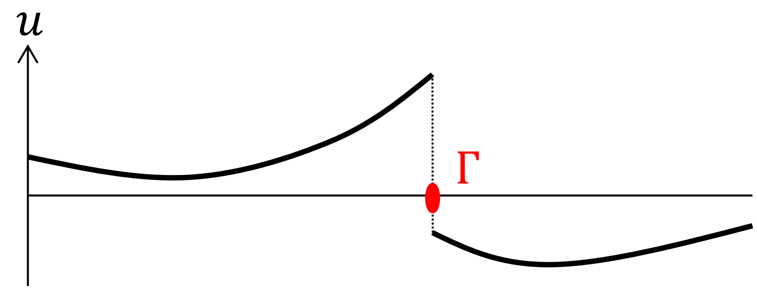

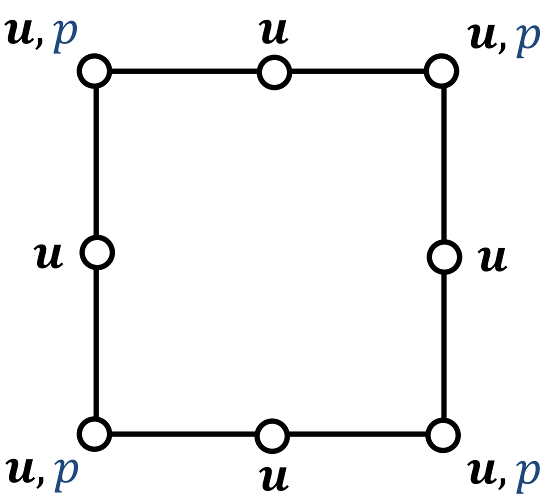

- The pore pressure field p is linear and enriched.

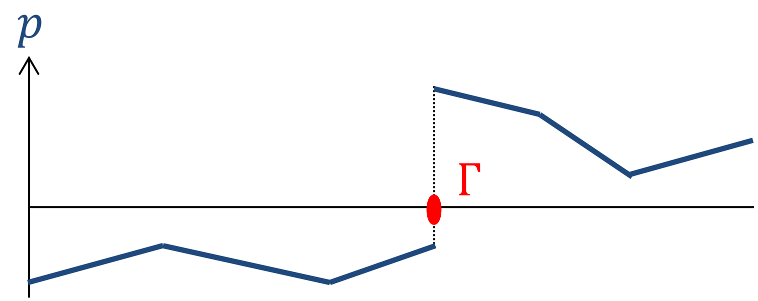

3 distinct approximation spaces

- The displacements field $\boldsymbol{u}$ is quadratic and enriched.

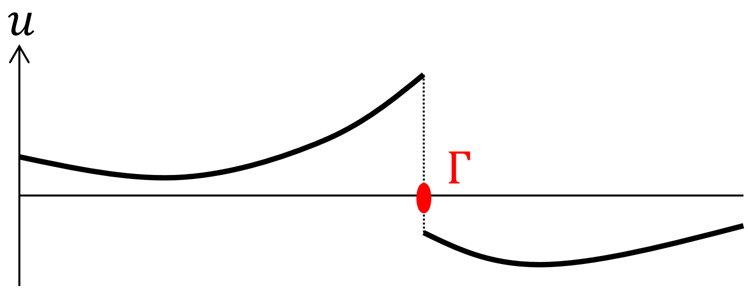

- The pore pressure field p is linear and enriched.

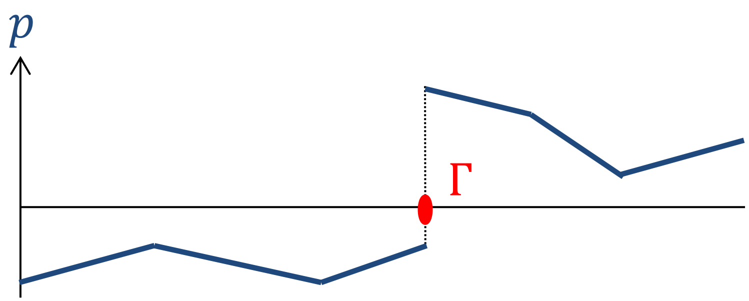

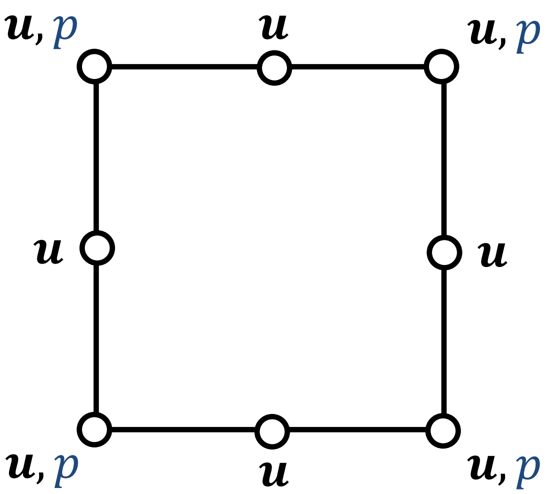

→ as demonstrated by Ern (2009), this mixed interpolation is necessary to reduce the oscillations in the numerical solution.

- A. Enr, S. Meunier, *A posteriori error analysis of euler-galerkin approximations to coupled elliptic-parabolic problems*, ESAIM: M2AN 2009

3 distinct approximation spaces

- The fields associated to the fluid-filled fracture (p_f, q_1, q_2, λ) are carried by the vertex nodes of the edges interstected by the discontinuity.

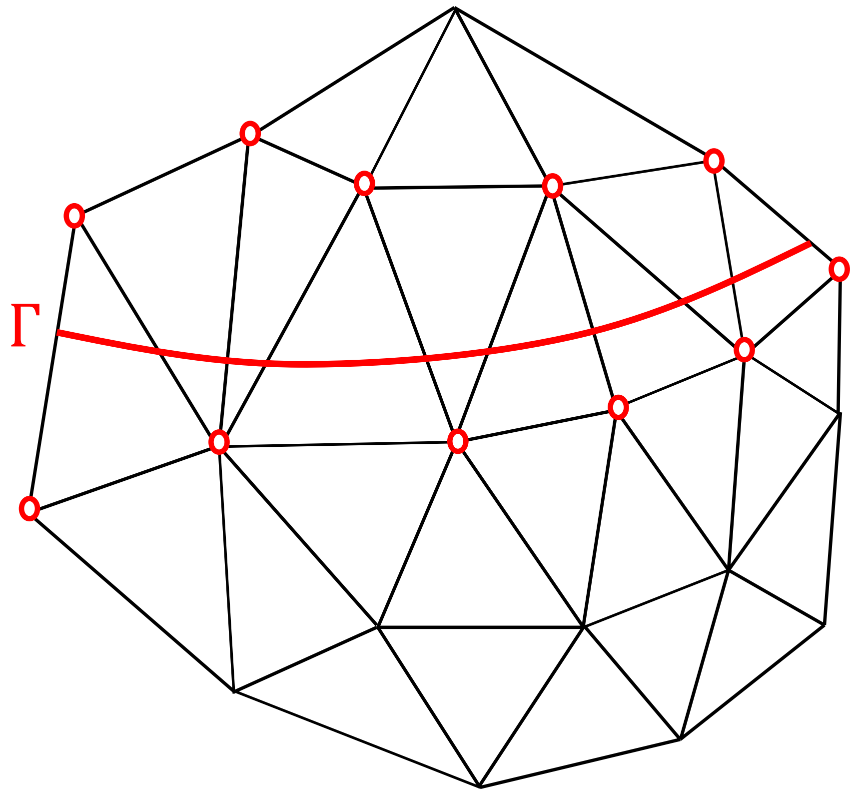

o : node carrying the fields associated to the fluid-filled fracture.

3 distinct approximation spaces

- The fields associated to the fluid-filled fracture (p_f, q_1, q_2, λ) are carried by the vertex nodes of the edges interstected by the discontinuity.
- In order to reduce the approximation space and satisfy the LBB stability condition (Béchet 2009), equality relations are prescribed accross the discontinuity based on the approach of Géniaut (2012).

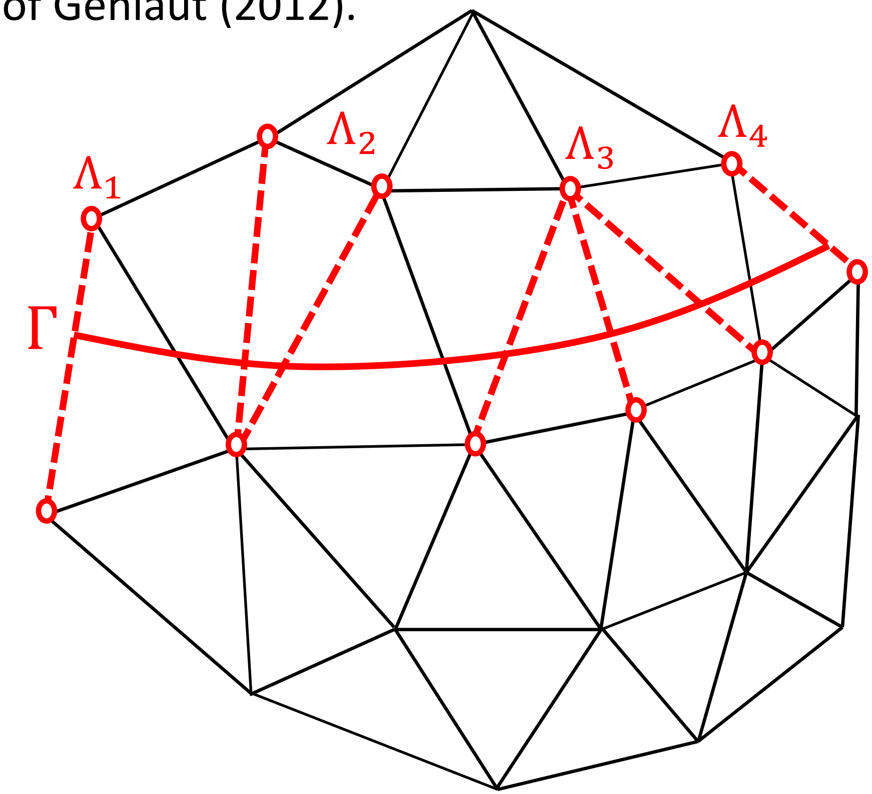

: node carrying the fields associated to the fluid-filled fracture.

: intersected edge whose vertex nodes are submitted to equality relations for the fields associated to the fluid-filled fracture.

- E. Béchet, N. Moës, B. Wohlmuth, *A stable Lagrange multipliers space for stiff interface conditions within the Extended Finite Element Method*, Int. J. Numer. Meth. Engng. 2009
- S. Géniaut, P. Massin. N. Moës, *A stable 3D contact formulation using XFEM,* European Journal of Computational Mechanics, 2012

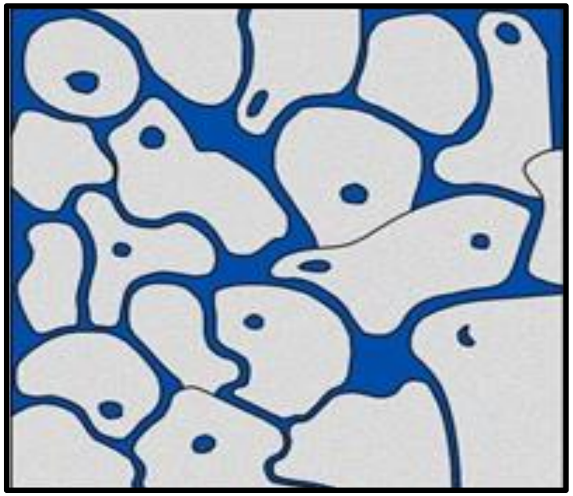

Hydromechanical coupling

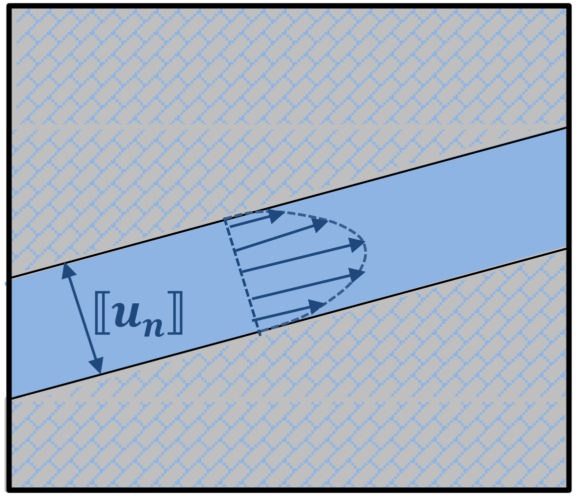

Fluid flow in the fracture

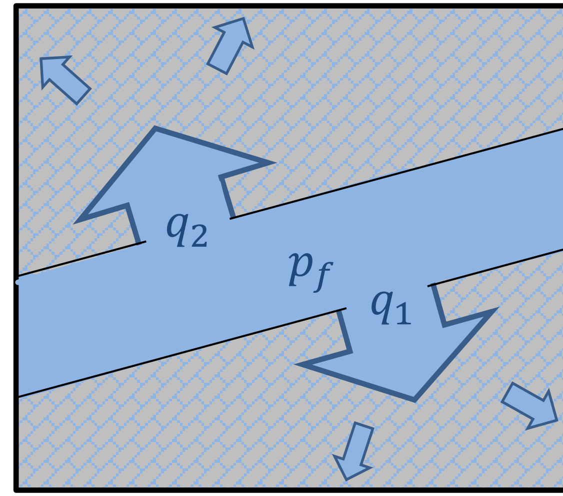

Mass exchanges between the fracture and the porous matrix and in the porous matrix

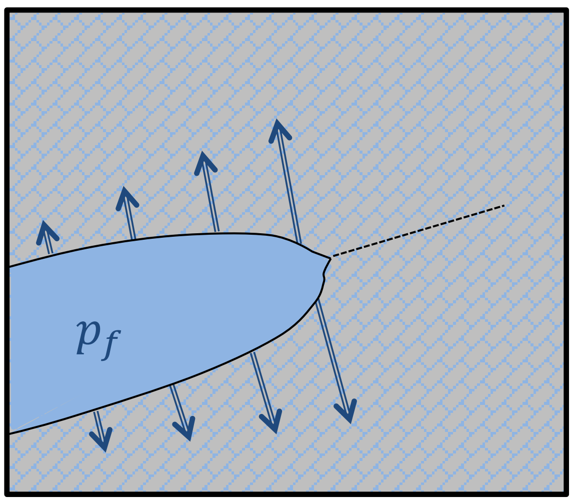

Crack extension

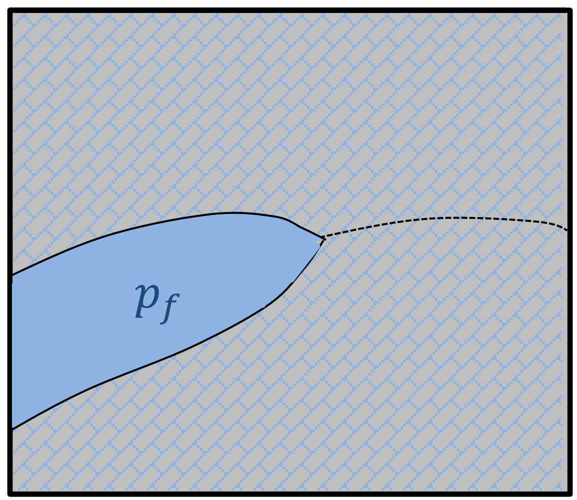

Crack reorientation

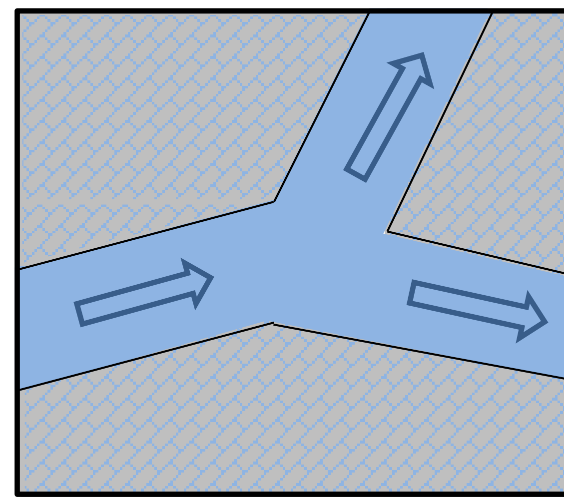

Fracture junction

[3D coupled HM-XFEM modeling with cohesive zone model and applications to non planar hydraulic fracture propagation and multiple hydraulic fractures interference](), B. Paul, M. Faivre, P. Massin, R. Giot, D. Colombo, F. Golfier, A. Martin, *Comput. Methods Appl. Mech. Engrg. Vol. 342 Pages 321–353, 2018*.

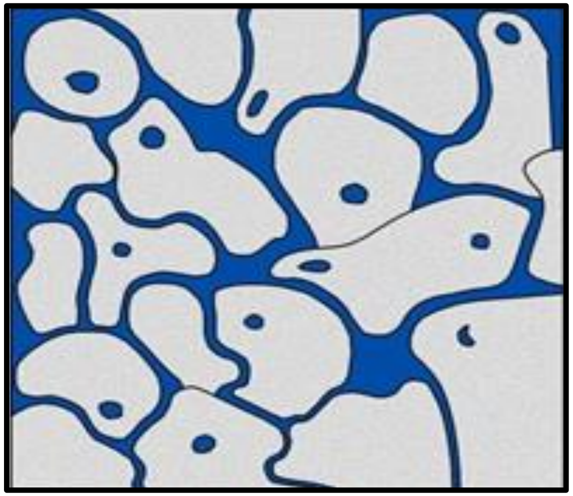

Hydromechanical coupling in the porous matrix

Hydromechanical coupling in the porous matrix

- We work under the assumption of small strains.
- The hydromechanical coupling in the porous matrix is handled within the framework of the generalized Biot theory (Coussy 2004).

Solid matrix characteristics:
- Density $\boldsymbol{\rho_s}$
- Young's modulus $\boldsymbol{E}$
- Poisson ratio $\boldsymbol{\nu}$
- Porosity $\boldsymbol{\varphi}$
- Permeability $\boldsymbol{k}$

Interstitial fluid characteristics:
- Density $\boldsymbol{\rho_l}$
- Dynamic viscosity $\boldsymbol{\mu}$

- The solid matrix is saturated by the monophasic interstitial fluid. The fluid then fills a fraction φ of the entire volume.
- The global equilibrium equation reads:

$$\boxed{Div\left(\underline{\underline{\boldsymbol{\sigma}}}' - bp\underline{\underline{\mathbf{1}}}\right) + [(1-\varphi)\rho_s + \varphi\rho_l]\underline{\boldsymbol{g}} = \underline{\mathbf{0}}}$$

b: Biot coefficient

- The solid matrix is supposed elastic:

$$\boxed{\underline{\underline{\boldsymbol{\sigma}}}' = \frac{E}{1+\nu}\left(\underline{\underline{\boldsymbol{\varepsilon}}} + \frac{\nu}{1-2\nu}Tr\left(\underline{\underline{\boldsymbol{\varepsilon}}}\right)\underline{\underline{\mathbf{1}}}\right)}$$

(Hooke's law)

- O. Coussy, *Poromechancis*, John Wiley & Sons 2004

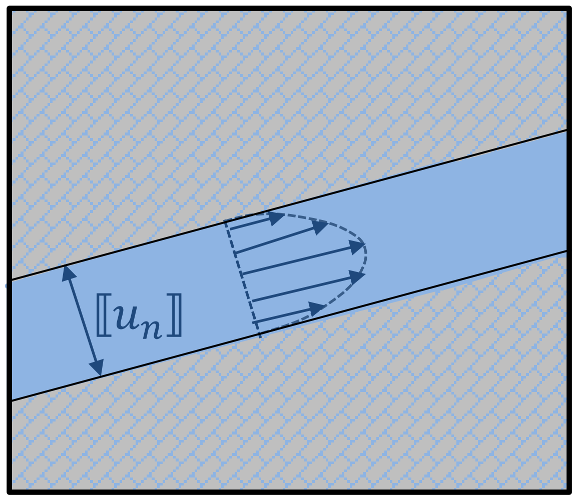

Fluid flow in the fracture

Fluid flow in the fracture

- We use the cubic law to model the fluid flux in the fractures. This is justified by Iwai et al (1980).

- The fluid flux in the fracture $\boldsymbol{W}$ then only depends on the fracture aperture and on the pressure gradient:

$$\underline{\boldsymbol{W}} = \frac{-\rho[\![u_n]\!]^3}{12\mu}\underline{\boldsymbol{\nabla}}p_f$$

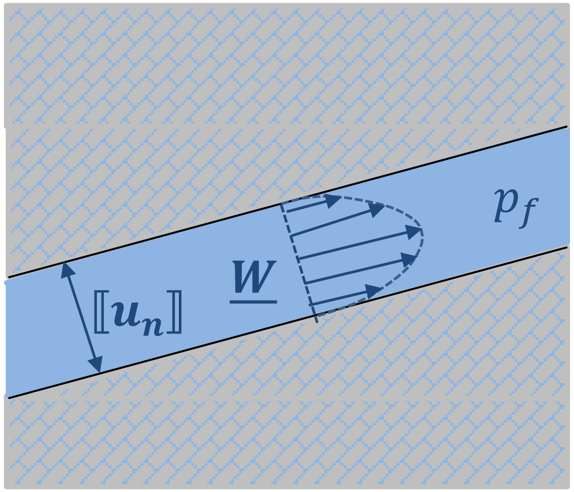

- K.J.E. Iwai, P.A. Witherspoon, J.S.Y. Wang, J.E. Gale, *Validity of cubic law for fluid flow in a deformable rock fracture*, Water Ressources 1980

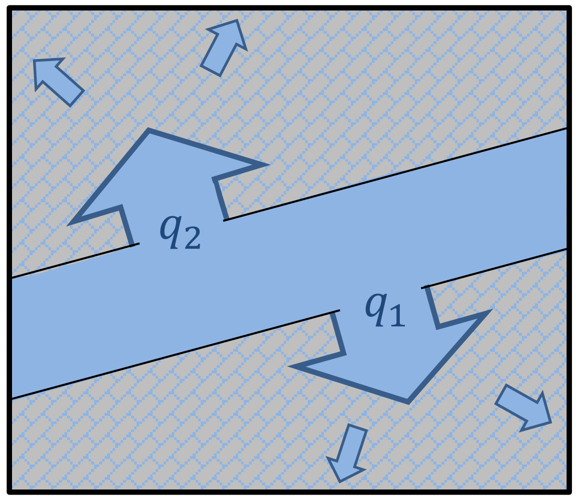

Mass exchanges between the fracture and the porous matrix and in the porous matrix

Fluid exchanges between the fracture and the porous matrix and in the porous matrix

Fluid flow in the porous matrix

- We use Darcy's law to model the fluid flow in the porous matrix $\boldsymbol{M}$:

$$\underline{\boldsymbol{M}} = \rho_l \frac{k}{\mu}(-\underline{\boldsymbol{\nabla}} p + \rho_l \underline{\boldsymbol{g}})$$

- Mass conservation for the fluid in the porous matrix:

$$\frac{\partial(\rho_l \varphi(1+\varepsilon_v))}{\partial t} + Div(\underline{\boldsymbol{M}}) = 0$$

Fluid flow in the fracture

- Flow in the fracture:

$$\underline{\boldsymbol{W}} = \frac{-\rho[\![u_n]\!]^3}{12\mu}\underline{\boldsymbol{\nabla}} p_f$$

- Mass conservation for the fluid in the porous matrix:

$$\frac{\partial(\rho_l [\![u_n]\!])}{\partial t} + Div\left(\underline{\boldsymbol{W}}\right) + q_1 + q_2 = 0$$

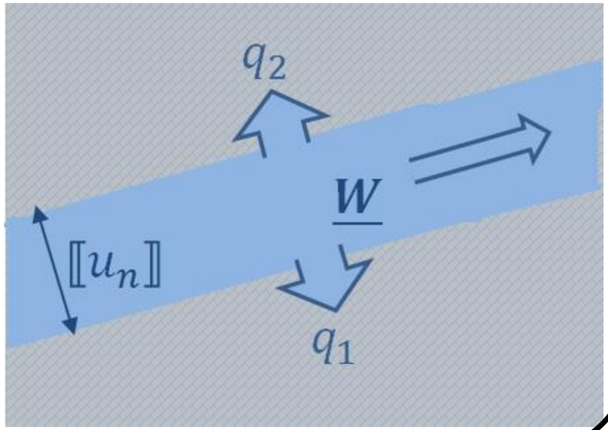

Fluid exchanges between the fracture and the porous matrix and in the porous matrix

- Finally, at each fracture wall, we impose the continuity of the fluid pressure:

$$\boxed{p = p_f \text{ on } \Gamma_{1,2}}$$

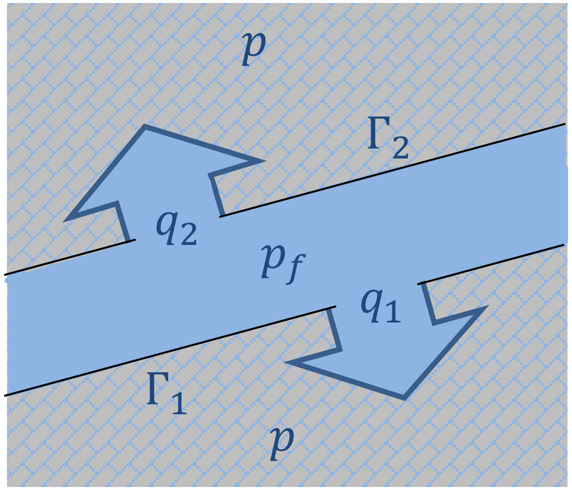

- This condition is weakly enforced:

$$\boxed{\int_{\Gamma_i} (p - p_f) q_i^* \, d\Gamma_i = 0 \quad \forall\, q_i^* \in M_0 \quad \text{for} \quad i \in \{1,2\}}$$

M_0: set of functions kinematically admissible for the fields associated to the fracture

- The pore pressure on both sides of the discontinuity is then connected to p_f:

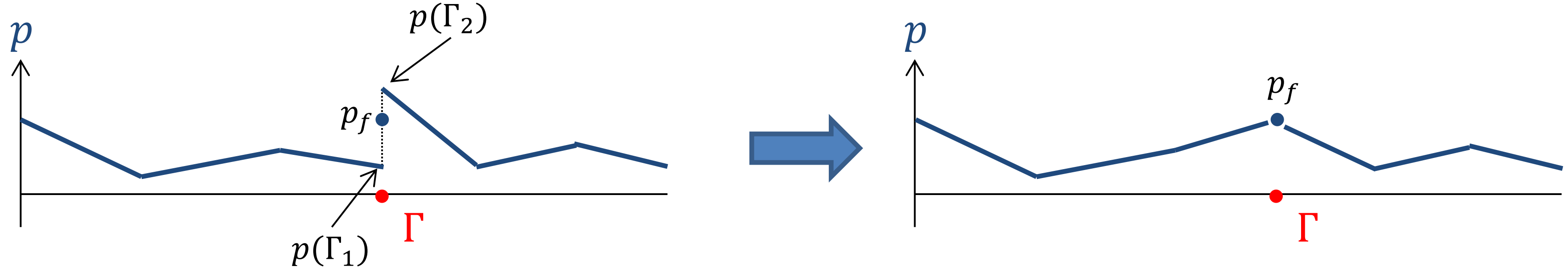

- Other models (Wang 2015) suggests that fluxes q_1 and q_2 are proportional to the pressure gap at the fracture walls: $q_i \propto [p_f - p(\Gamma_i)]$.

- H. Wang, *Numerical modeling of non-planar hydraulic fractures propagation in brittle and ductile rocks using XFEM with cohesive zone method*, Journal of Petroleum Science and Engineering 2015

Enrichment strategy for the pore pressure field

- Sukumar et al (2001) proposed to enrich the pore pressure field with $abs(lsn)$.

→ bad convergence properties.

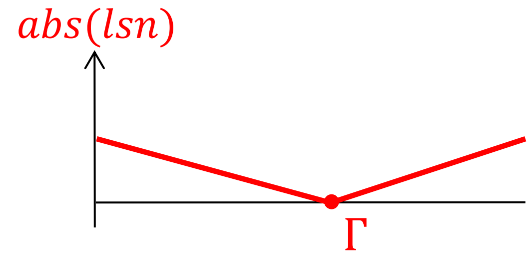

- Moës et al (2003) then suggested to use Ridge enrichment functions.

→ allows to recover optimal convergence rates.

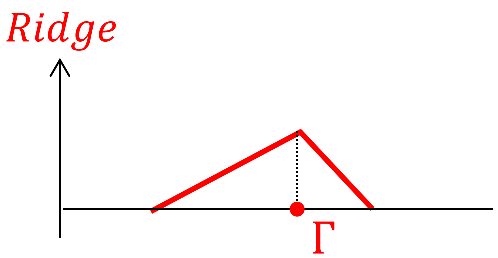

- Hansbo and Hansbo (2000) suggested to let a strong discontinuity and then force the continuity.

→ allows to recover optimal convergence rates.

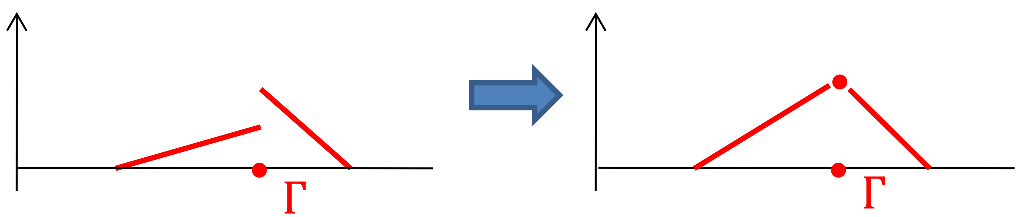

- N. Sukumar, D.L. Chopp, N. Moës and T. Belytschko, *Modeling holes and inclusions by level sets in the extended finite element method,* Comp. Meth. Appl. Mech. Engng. 2001
- N. Moës, M. Cloirec, P. Cartraud, J.F. Remacle, *A computational approach to handle complex microstructure geometries,* Comp. Meth. Appl. Mech. Engng. 2003
- A. Hansbo, P. Hansbo, *An unfitted finite element method, based on nitsche's method for elliptic interface problems,* Comp. Meth. Appl. Mech. Engng. 2000
- M. Ndeffo, P. Massin, N. Moës, A. Martin and S. Gopalakrishnan, On the construction of approximation space to model discontinuities and cracks with linear and quadratic extended finite elements, *Adv. Model. and Simul. in Eng. Sci., 4:6, https://doi.org/10.1186/s40323-017-0090-3, 51 Pages, 2017.*

Fluid exchanges between the fracture and the porous matrix and in the porous matrix

→ Fully coupled hydromechanical model

<u>Material parameters</u>

$E = 5800\ MPa$

$\nu = 0{,}2$

$\varphi = 0{,}1$

$k = 10^{-18} m^2$

$b = 1$

${}^{1}/_{K_l} = 5.10^{-10} Pa^{-1}$

$\mu = 10^{-3} Pa.s$

$G_c = 9000\ Pa.m$

$\sigma_c = 0{,}5\ MPa$

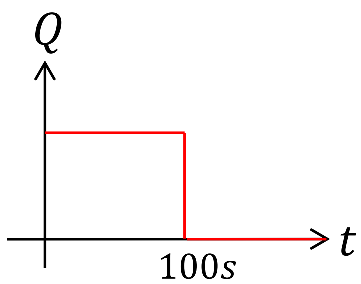

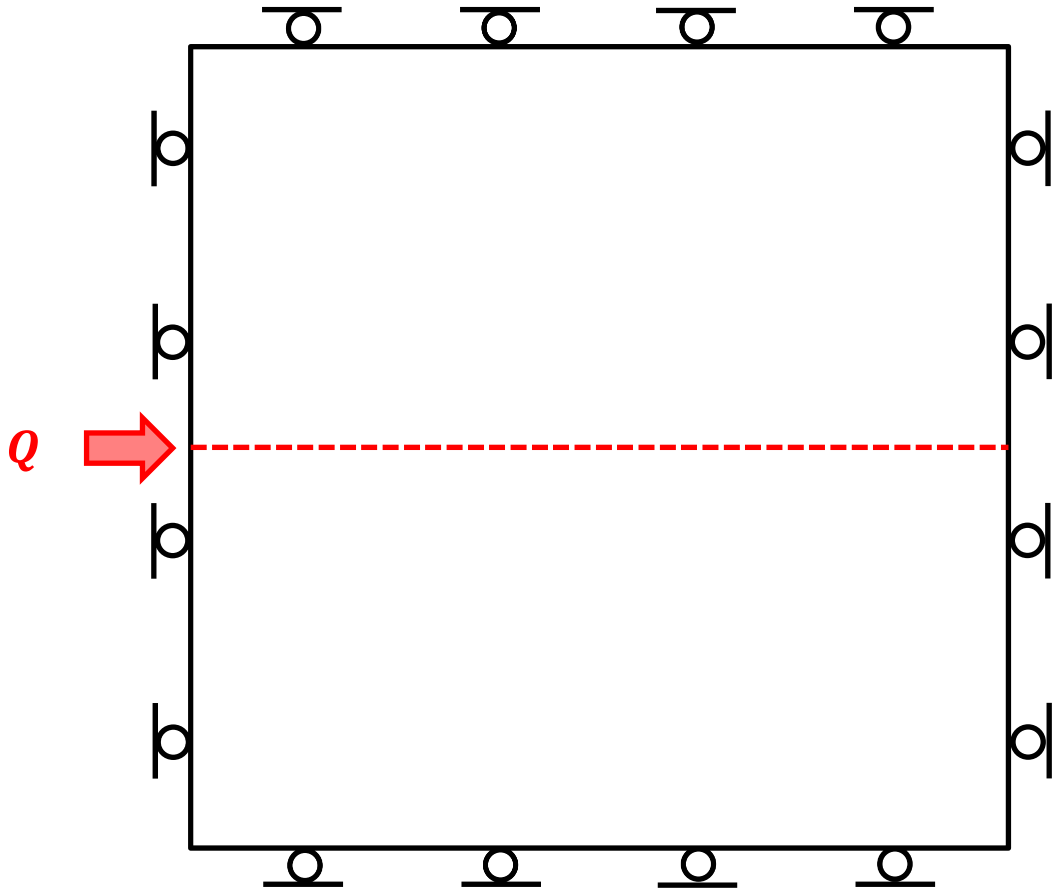

Fluid exchanges between the fracture and the porous matrix and in the porous matrix

→ Fully coupled hydromechanical model

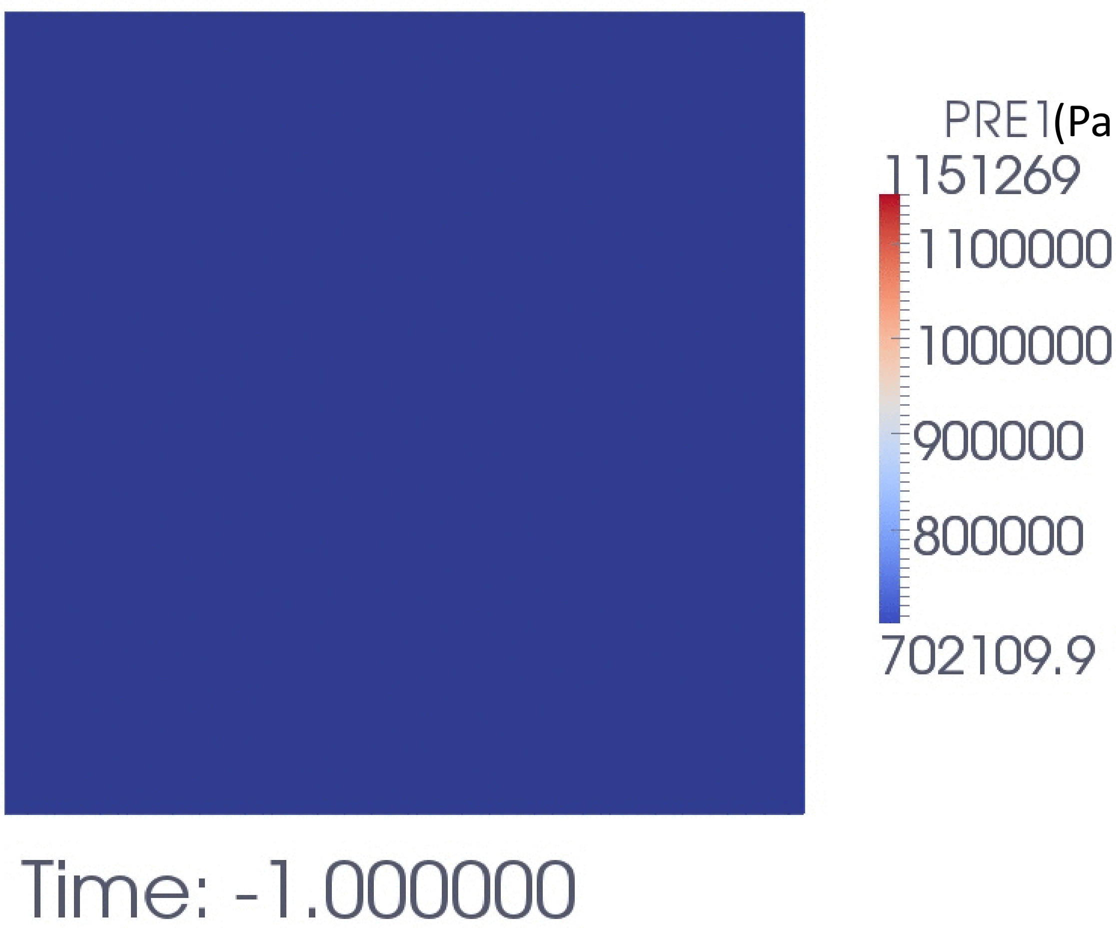

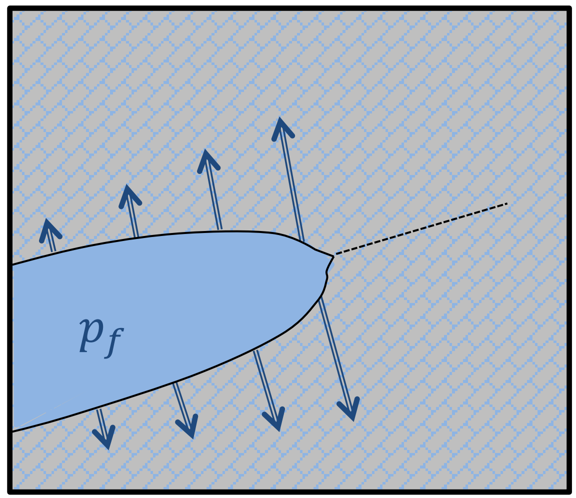

Crack extension

Cohesive zone model

- To govern the crack extension and opening, we adopt a cohesive zone model.
- The crack surface is then divided into 3 zones:

  - The **adherent zone** is undamaged.

  - In the **fracture processing zone**, cohesive traction efforts t'_c resist to the crack opening.

  - The **traction free zone** is fully opened.

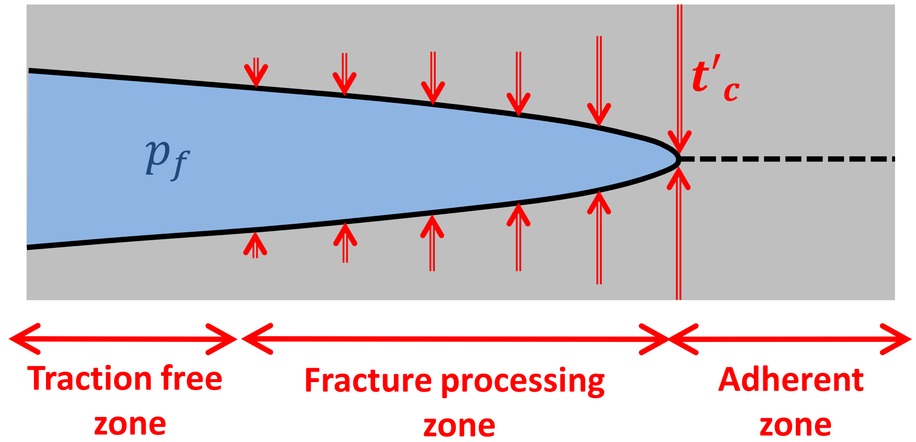

- The cohesive traction is directly related to the displacement jump via a linear mixed cohesive law.
- Once the cohesive traction reaches the critical stress σ_c, the damage process starts irreversibly.
- The crack extension is thus allowed throughout a mechanical load step.

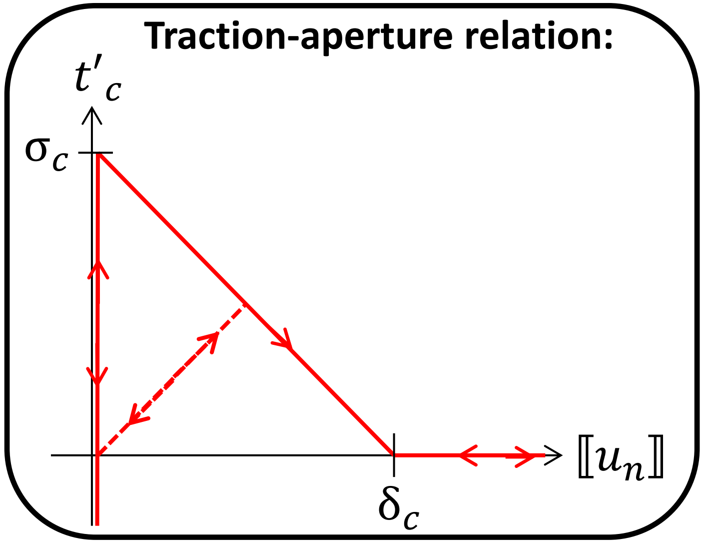

Cohesive zone model

- To include the cohesive zone in our model, we adopt the « mortar » formalism developped by Ferté (2016).
- The displacements jump $\boldsymbol{w}$ and the cohesive traction $\boldsymbol{\lambda}$ are introduced as new unknowns of the problem discretized over the same approximation space as p_f, q_1 and q_2, adapted to the fracture.

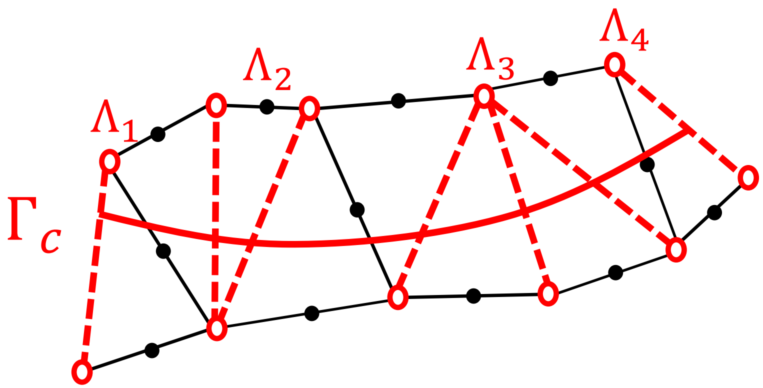

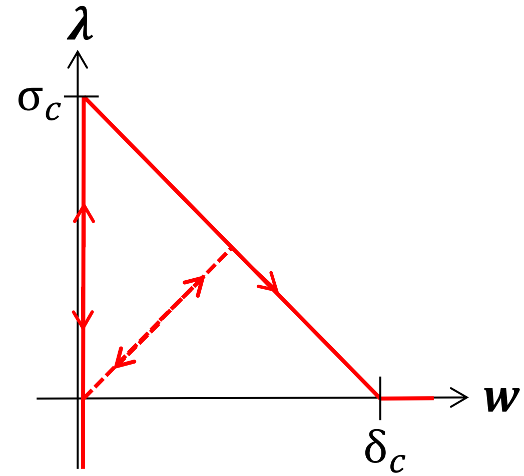

- The total energy of the system is then:

$$E(\boldsymbol{u},\boldsymbol{w},\boldsymbol{\lambda}) = \underbrace{\frac{1}{2}\int_{\Omega} \boldsymbol{\varepsilon}(\boldsymbol{u}):\boldsymbol{C}:\boldsymbol{\varepsilon}(\boldsymbol{u})d\Omega}_{\text{elastic energy}} - \underbrace{\int_{\Gamma_t} \boldsymbol{t}.\boldsymbol{u}d\Gamma_t}_{\text{external loads}} + \underbrace{\int_{\Gamma_c} \Pi(\boldsymbol{w},\boldsymbol{\lambda})d\Gamma_c}_{\text{cohesive energy}}$$

- G. Ferté, P. Massin, N. Moës, *3D crack propagation with cohesive elements in the extended finite element method,* Comput. Meth. Appl. Mech. Eng., 2016

Weak formulation of the mechanical problem

- In order to minimize this energy, we introduce the Lagrangian:

$$\mathcal{L}(\boldsymbol{u},\boldsymbol{w},\boldsymbol{\lambda},\boldsymbol{\mu}) = \frac{1}{2}\int_{\Omega} \boldsymbol{\varepsilon}(\boldsymbol{u}):\boldsymbol{C}:\boldsymbol{\varepsilon}(\boldsymbol{u})d\Omega - \int_{\Gamma_t} \boldsymbol{t}.\boldsymbol{u}d\Gamma_t + \int_{\Gamma_c} \Pi(\boldsymbol{w},\boldsymbol{\lambda})d\Gamma_c + \overbrace{\int_{\Gamma_c} \boldsymbol{\mu}.(\llbracket \boldsymbol{u} \rrbracket - \boldsymbol{w})d\Gamma_c}^{\text{mortar term}}$$

- $\boldsymbol{\mu}$ is an additional Lagrange multiplier discretized over the same space as p_f, q_1 and q_2.

- The four optimality conditions are:

$$\boxed{\int_{\Omega} \boldsymbol{\sigma}(\boldsymbol{u}):\boldsymbol{\varepsilon}(\boldsymbol{u}^*)d\Omega - \int_{\Gamma_t} \boldsymbol{t}.\boldsymbol{u}^* d\Gamma_t + \int_{\Gamma_c} \boldsymbol{\mu}.\llbracket \boldsymbol{u}^* \rrbracket d\Gamma_c = 0 \quad \forall \boldsymbol{u}^* \in \boldsymbol{U}_0 \quad \text{(global equilibrium equation)}}$$

$$\boxed{\int_{\Gamma_c} \boldsymbol{\mu}^*.(\llbracket \boldsymbol{u} \rrbracket - \boldsymbol{w})d\Gamma_c = 0 \quad \forall \boldsymbol{\mu}^* \in \boldsymbol{M}_0 \quad \text{(displacement jump projection)}}$$

$$\boxed{\int_{\Gamma_c} \boldsymbol{w}^*.(\boldsymbol{\mu} - \boldsymbol{t}_c)d\Gamma_c = 0 \quad \forall \boldsymbol{w}^* \in \boldsymbol{M}_0 \quad \text{(total cohesive stress projection)}}$$

$$\boxed{\int_{\Gamma_c} -\boldsymbol{\lambda}^*.\frac{(\boldsymbol{\lambda} - \boldsymbol{t'}_c)}{r}d\Gamma_c = 0 \quad \forall \boldsymbol{\lambda}^* \in \boldsymbol{M}_0 \quad \text{(interfacial law)}}$$

- Under the asumption of Biot effective stress: $\begin{cases} \boldsymbol{\sigma} = \boldsymbol{\sigma}' - bp\mathbf{1} \\ \boldsymbol{t_c} = \boldsymbol{t'}_c - p_f\boldsymbol{n} \end{cases}$

Loadings and boundary conditions

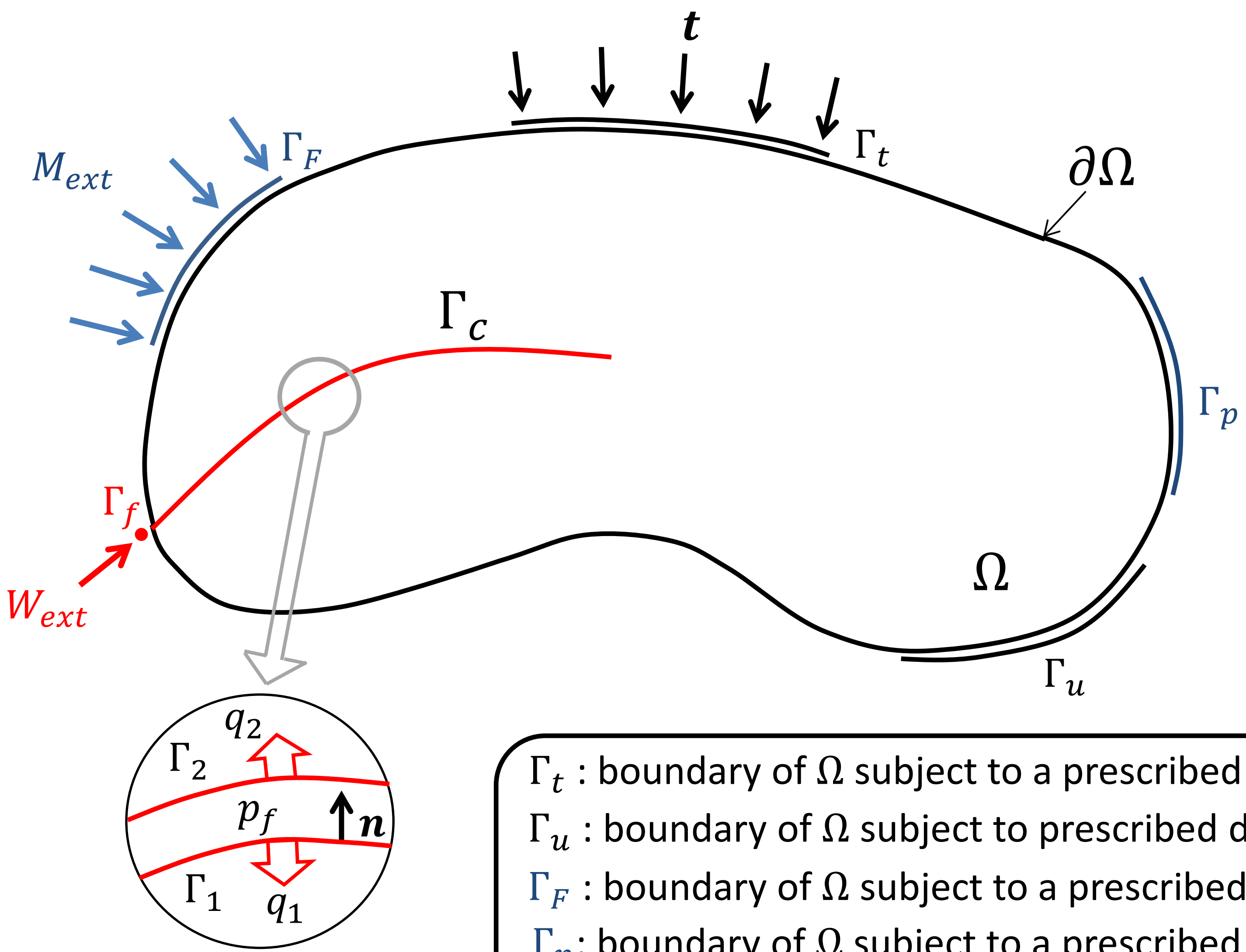

Γ_t : boundary of Ω subject to a prescribed stress $\boldsymbol{t}$

Γ_u : boundary of Ω subject to prescribed displacements

Γ_F : boundary of Ω subject to a prescribed external flux M_{ext}

Γ_p: boundary of Ω subject to a prescribed pore pressure

Γ_f : inlet of the fracture Γ_c subject to a prescribed flux W_{ext}

Weak formulation of the hydromechanical problem

The mass conservation equations are discretized in time with a θ-scheme.

- Mass conservation in the fluid-filled cohesive fracture:

$$-\int_{\Gamma_c} \frac{w^+ - w^-}{\Delta t} p_f{}^* d\Gamma_c + \theta \int_{\Gamma_c} \boldsymbol{W}^+ . \boldsymbol{\nabla} p_f{}^* d\Gamma_c + (1-\theta) \int_{\Gamma_c} \boldsymbol{W}^- . \boldsymbol{\nabla} p_f{}^* d\Gamma_c = \int_{\Gamma_f} W_{ext} p_f{}^* d\Gamma_f$$
$$+\theta \int_{\Gamma_1} q_1{}^+ p_f{}^* d\Gamma_1 + (1-\theta) \int_{\Gamma_1} q_1{}^- p_f{}^* d\Gamma_1 + \theta \int_{\Gamma_2} q_2{}^+ p_f{}^* d\Gamma_2 + (1-\theta) \int_{\Gamma_2} q_2{}^- p_f{}^* d\Gamma_2 \quad \forall \in p_f{}^* M_0$$

with $w^+ - w^- = \rho_l{}^+ [\![u_n]\!]^+ - \rho_l{}^- [\![u_n]\!]^-$

- Mass conservation in the porous matrix:

$$-\int_{\Omega} \frac{m_w{}^+ - m_w{}^-}{\Delta t} p^* d\Omega + \theta \int_{\Omega} \boldsymbol{M}^+ . \boldsymbol{\nabla} p^* d\Omega + (1-\theta) \int_{\Omega} \boldsymbol{M}^- . \boldsymbol{\nabla} p^* d\Omega = \int_{\Gamma_F} M_{ext} p^* d\Gamma_F$$
$$-\theta \int_{\Gamma_1} q_1{}^+ p^* d\Gamma_1 - (1-\theta) \int_{\Gamma_1} q_1{}^- p^* d\Gamma_1 - \theta \int_{\Gamma_2} q_2{}^+ p^* d\Gamma_2 - (1-\theta) \int_{\Gamma_2} q_2{}^- p^* d\Gamma_2 \quad \forall \in p^* P_0$$

with $m_w{}^+ - m_w{}^- = \rho_l{}^+ \varphi^+ (1 + \varepsilon_v{}^+) - \rho_l{}^- \varphi^- (1 + \varepsilon_v{}^-)$

- Pressure continuity condition at the fracture walls:

$$\int_{\Gamma_i} (p - p_f) q_i{}^* d\Gamma_i = 0 \quad \forall \in q_i{}^* M_0 \quad \text{for} \quad i \in \{1, 2\}$$

Validation

- We perform an analytical validation of our model based on the penny shaped model depicted in Bunger (2005).

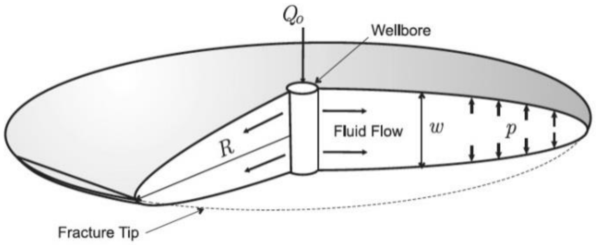

- Depending on two dimensionless parameters $\mathcal{C}$ and $\mathcal{K}$, we identify the propagation regime (tougness dominated or viscosity dominated) :

$$\boxed{\mathcal{C} = 2C_L\left(\frac{Et}{12(1-\nu^2)\mu Q^3}\right)^{1/6}}$$

$$\boxed{\mathcal{K} = 4\sqrt{\frac{G_c}{\pi}}\left(\frac{1-\nu^2}{3QE\mu}\right)^{1/4}}$$

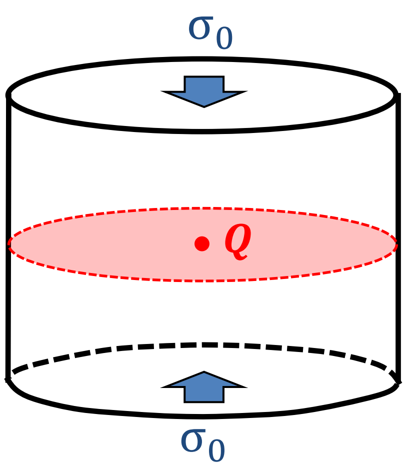

Loadings

$Q = 0{,}005\ m^3.s^{-1}$

$\sigma_0 = 3{,}7\ MPa$

Material parameters

$E = 17\ GPa$	$\mu = 10^{-4} Pa.s$
$\nu = 0{,}2$	$1/K_l = 0\ Pa^{-1}$
$\varphi = 0{,}2$	
$k = 10^{-16} m^2$	$G_c = 120\ Pa.m$
$b = 0{,}75$	$\sigma_c = 1{,}25\ MPa$

- We only present the radial case, the 2D case is abundantly documented in Faivre, Paul (2016)

- A. P. Bunger, E. Detournay, D. I. Garagash, *Toughness dominated hydraulic fracture with leak-off,* International Journal of Fracture, 2005
- M. Faivre, B. Paul, F. Golfier, R. Giot, P. Massin, D. Colombo, *2D coupled HM-XFEM modeling with cohesive zone model and applications to fluid-driven fracture networks,* Engineering Fracture Mechanics, 2016

Equivalent leak-off coefficient

$$g(r,t) = \frac{2C_L}{\sqrt{t - t_0(r)}}$$

$g(r,t)$: fluid flux transiting from the fracture to the porous matrix per unit area

C_L: leak-off coefficient

$t_0(r)$: time it takes for the fracture to reach r

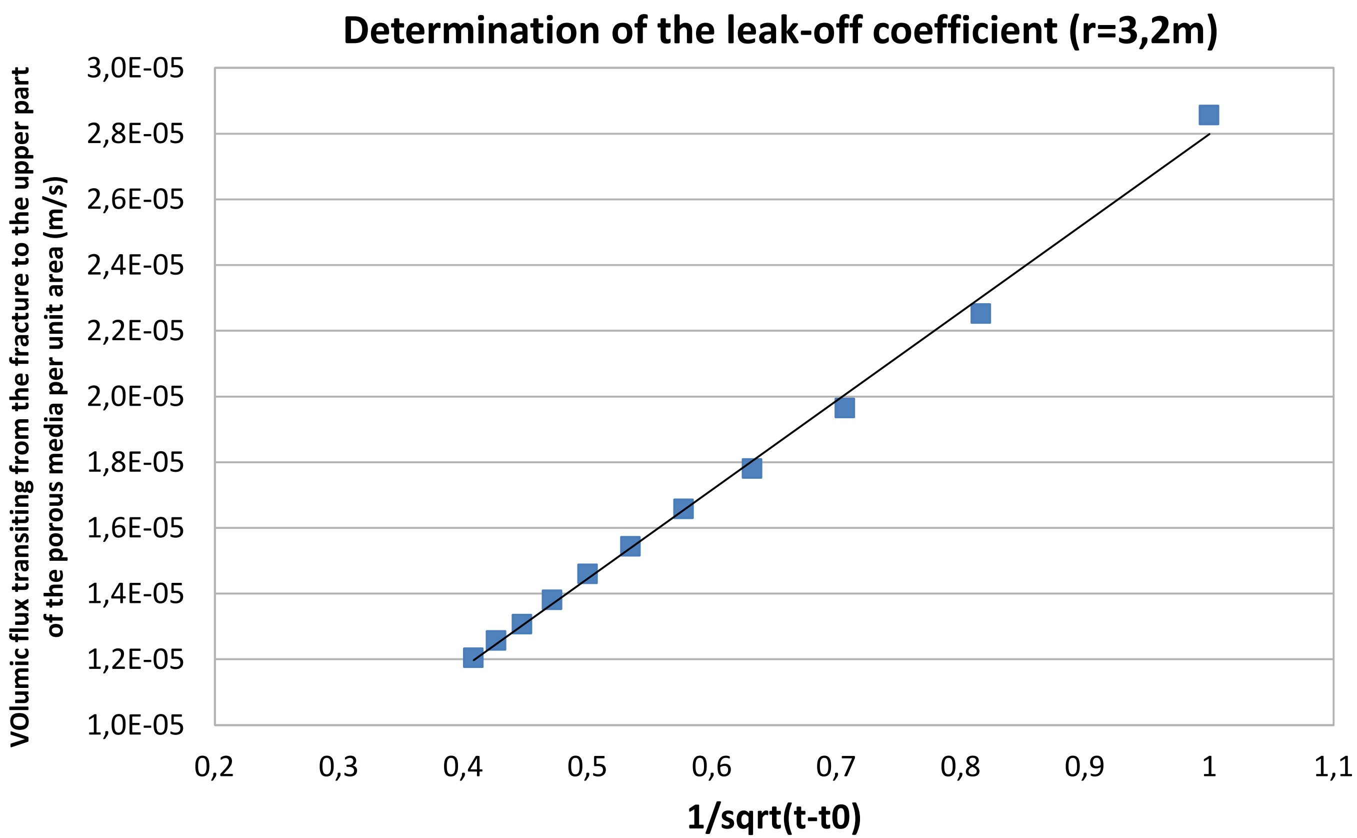

Validation

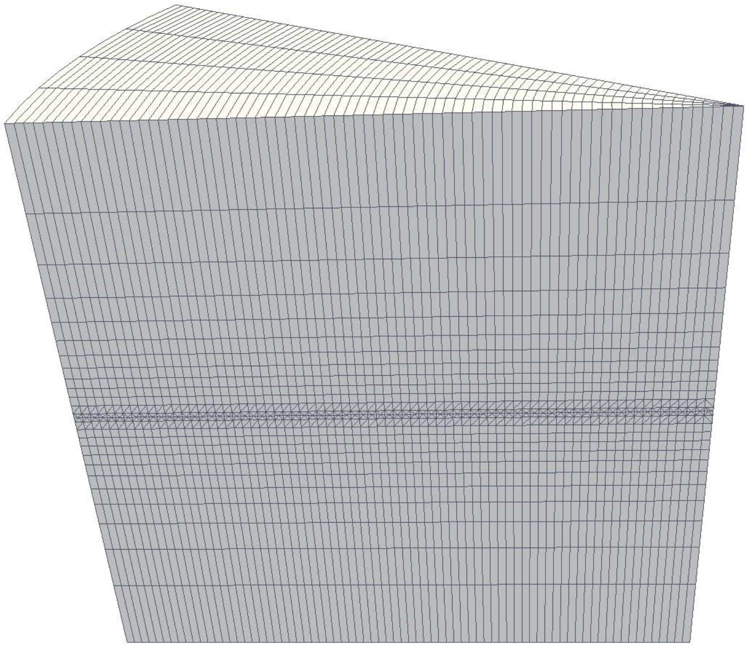

mesh used

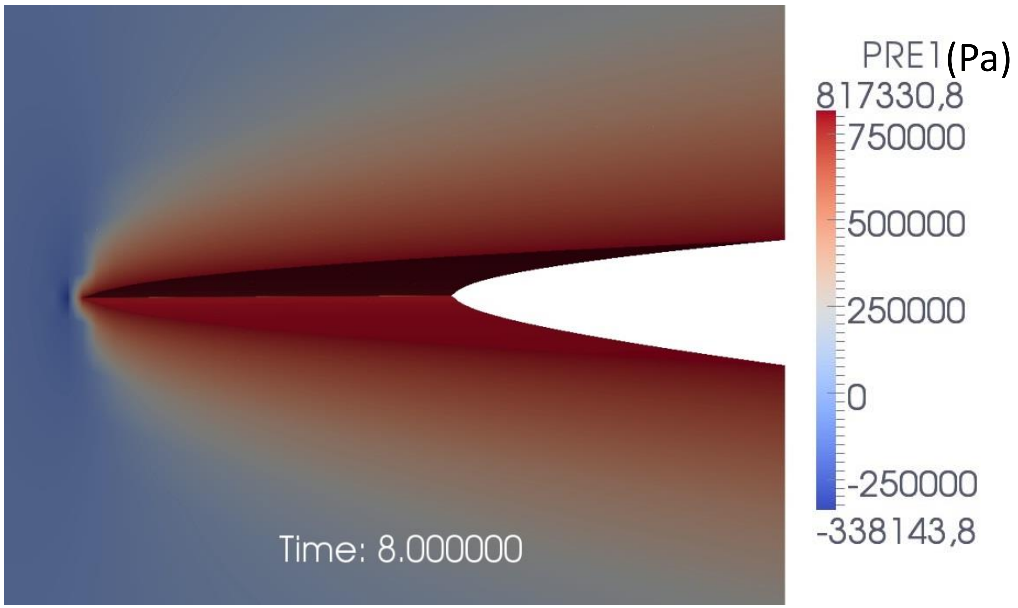

pore pressure and amplified deformed shape

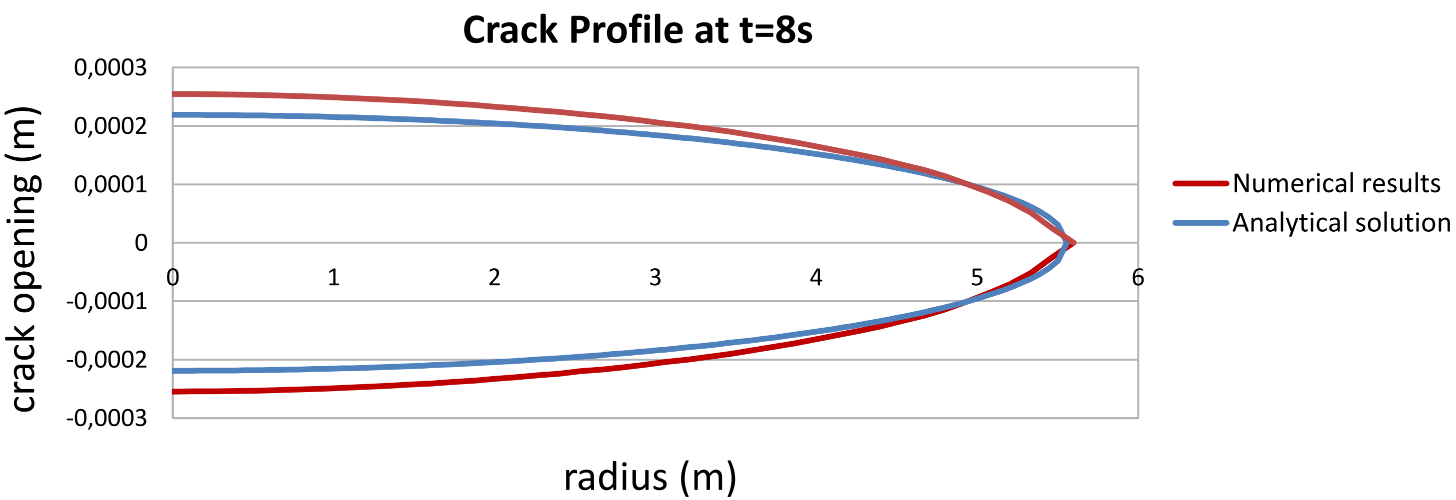

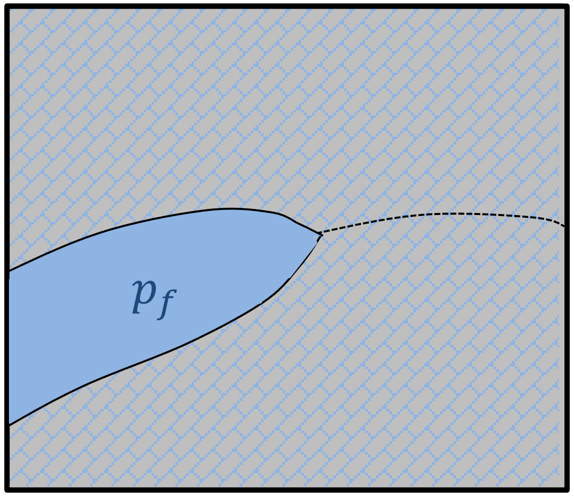

Crack reorientation

Potential crack surfaces

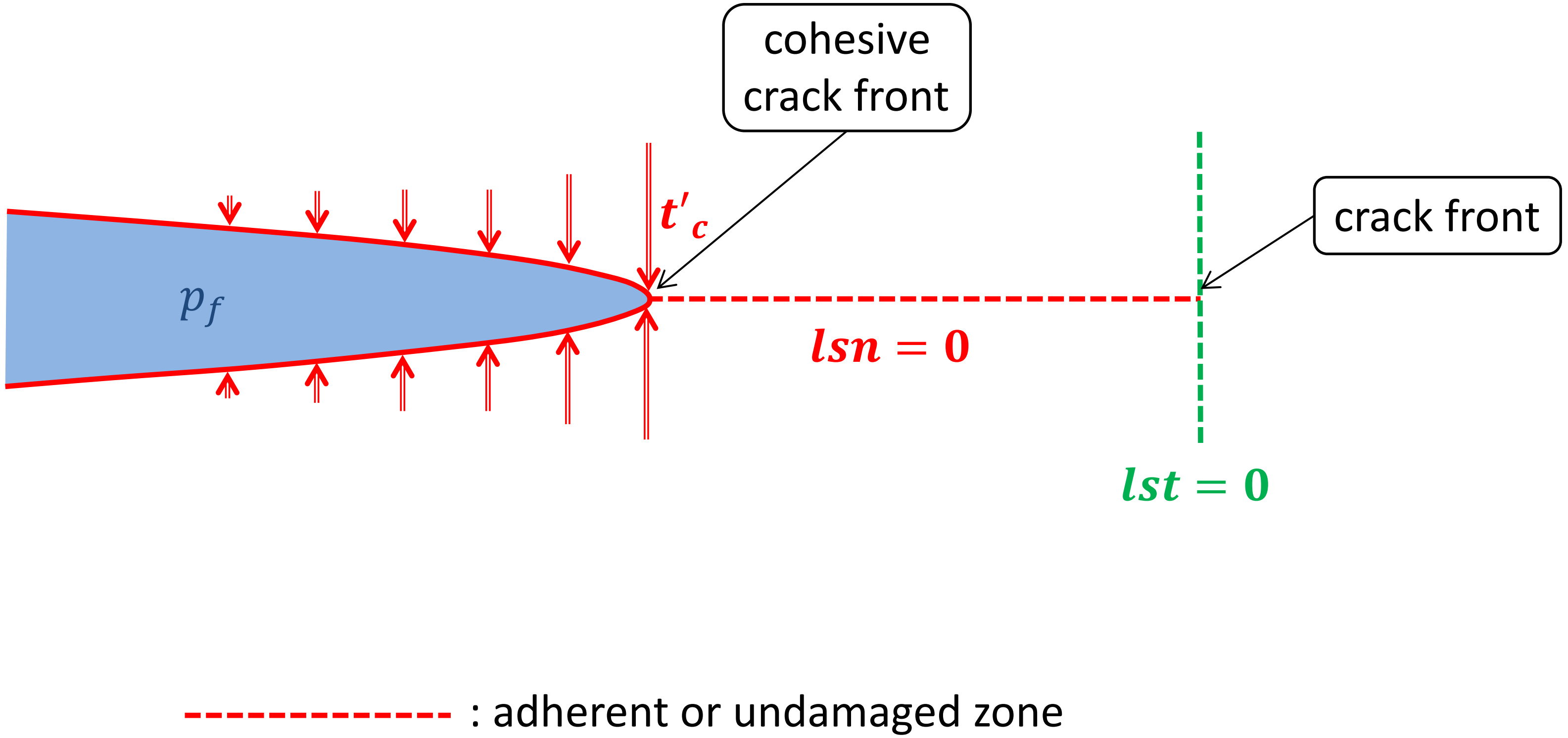

Potential crack surfaces

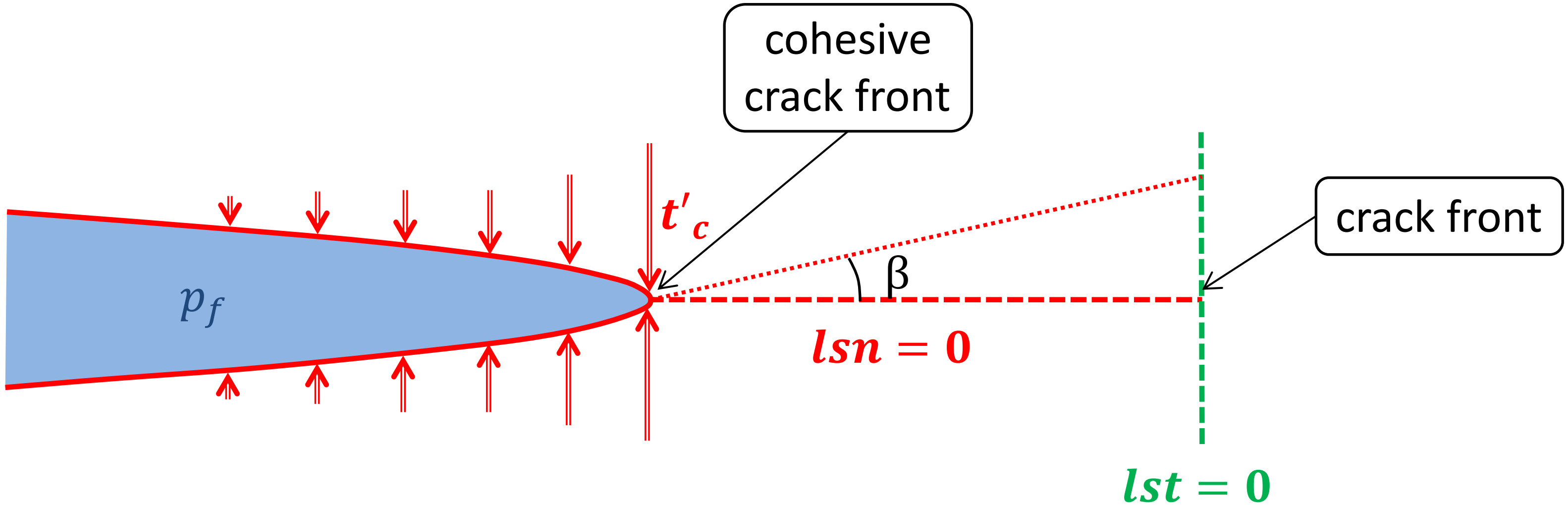

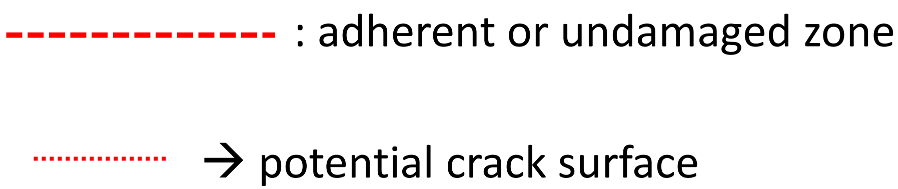

Potential crack surfaces

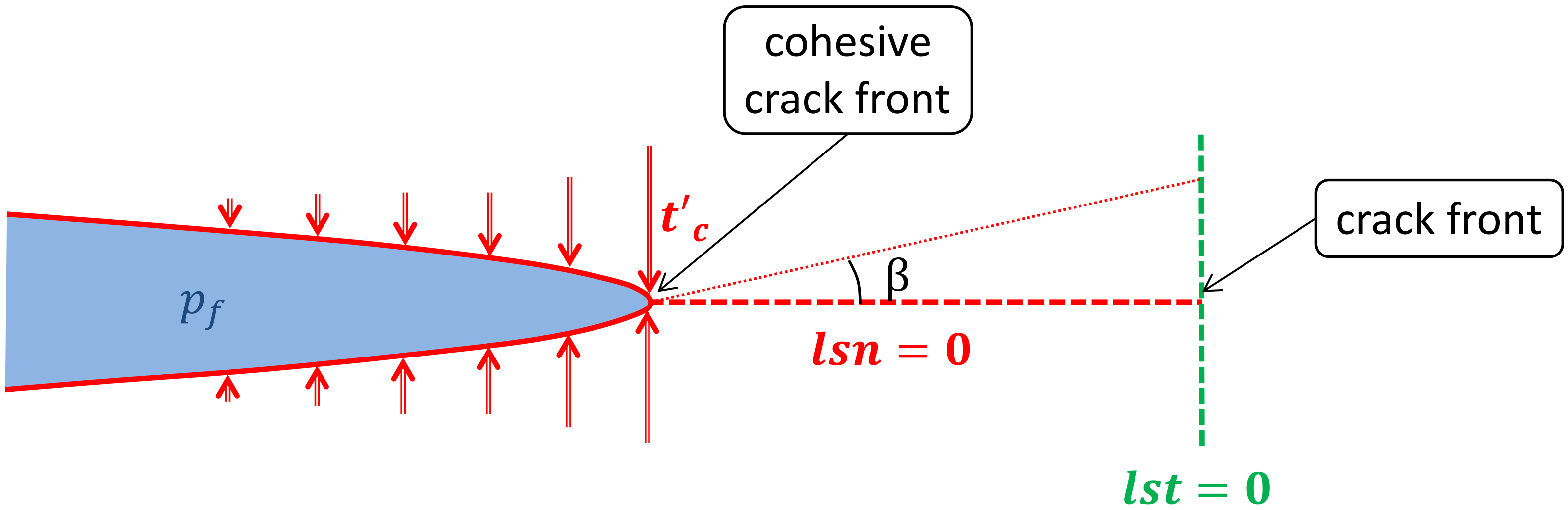

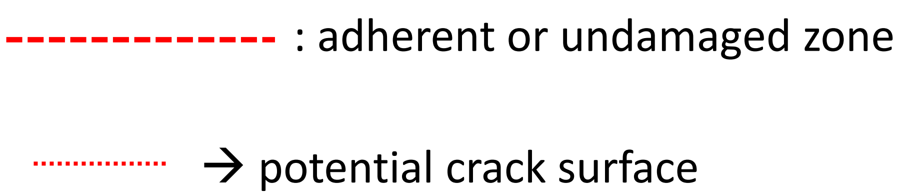

- Based on the work of Ferté (2016), we propose a procedure for the update of the potential crack surface.

- G. Ferté, P. Massin, N. Moës, *3D crack propagation with cohesive elements in the extended finite element method,* Comput. Meth. Appl. Mech. Eng., 2016

Stress intensity factors with a cohesive zone model

- According to Ferté (2016), we can still define a J-integral in the context of cohesive zone models:

$$\boxed{J = -\int_{\Gamma_c} \boldsymbol{t_c}.\nabla[\![\boldsymbol{u}]\!].\boldsymbol{\theta}\, d\Gamma_c}$$

- Furthermore: $$\boxed{J = G = \frac{1-\nu^2}{E}\left({K_I}^2 + {K_{II}}^2\right) + \frac{1}{2\mu}{K_{III}}^2}$$

- Finally, the stress intensity factors are identified as:

$$
\begin{aligned}
{K_I}^2 &= -\frac{E}{1-\nu^2}\int_{\Gamma_c} \frac{\partial[\![u_n]\!]}{\partial\theta}.(t'_{c,n} - p_f)\,d\Gamma_c \\
{K_{II}}^2 &= -\frac{E}{1-\nu^2}\int_{\Gamma_c} \frac{\partial[\![u_t]\!]}{\partial\theta} t'_{c,t}\,d\Gamma_c \\
{K_{III}}^2 &= -2\mu\int_{\Gamma_c} \frac{\partial[\![u_b]\!]}{\partial\theta} t'_{c,b}\,d\Gamma_c
\end{aligned}
$$

θ is a virtual extension of the crack:

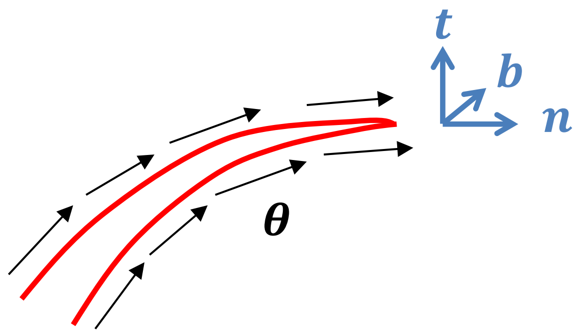

- G. Ferté, P. Massin, N. Moës, *3D crack propagation with cohesive elements in the extended finite element method,* Comput. Meth. Appl. Mech. Eng., 2016

Reorientation angle

- We adopt the maximum hoop stress criterion (Erdogan and Sih 1963):

$$\boxed{\beta = 2\arctan\left[\frac{1}{4}\left({K_I}/{K_{II}} - sign(K_{II})\sqrt{\left({K_I}/{K_{II}}\right)^2 + 8}\right)\right]}$$

→ it is expressed only in terms of the stress intensity factors K_I and K_{II}

→ it depends on global energetic quantities

- We do not account for the tilt. If we had, we would have got (Haboussa 2012):

$$\beta = 2\arctan\left[\frac{1}{4}\left(\frac{1 + x_I - (1 - x_{III})^p}{x_{II}} - sign(K_{II})\sqrt{\left(\frac{1 + x_I - (1 - x_{III})^p}{x_{II}}\right)^2 + 8}\right)\right]$$

with $x_i = \dfrac{K_i}{K_I + |K_{II}| + |K_{III}|}$ and $p = \dfrac{\sqrt{\pi} - 5\nu}{4}$

- D. Haboussa, *Modélisation de la transition traction-cisaillement des métaux sous choc par la X-FEM,* PhD INSA de Lyon 2012
- F. Erdogan, G.C. Sih, *On the crack extension in plane loading and transverse shear,* Journal Basic Engng 1963

Procedure for the propagation on non-predefined paths: an implicit approach

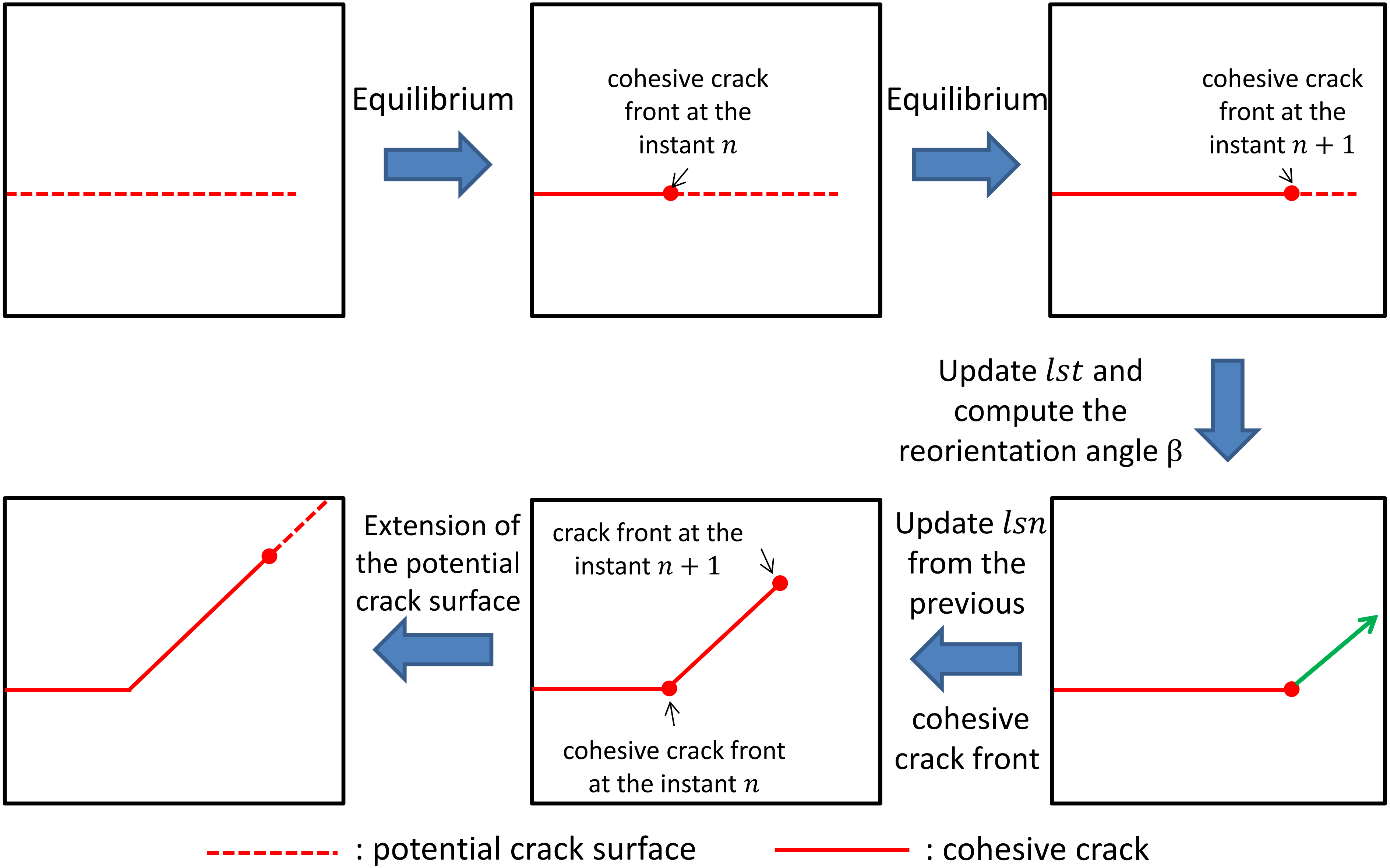

Competing nearby cracks

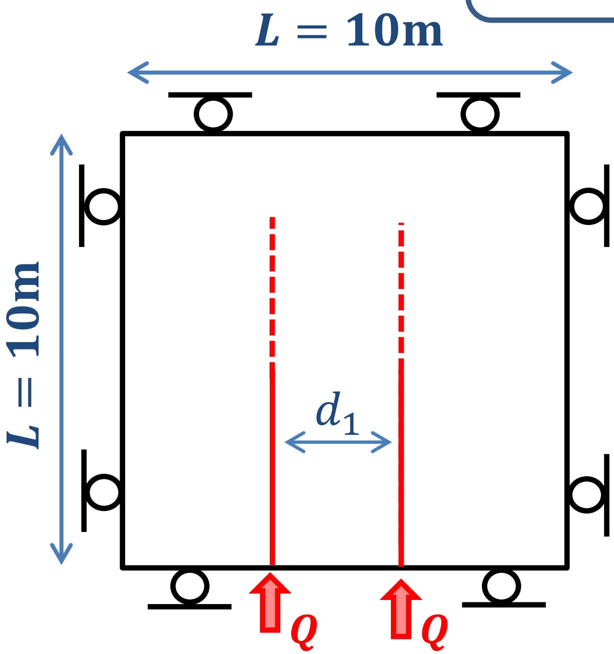

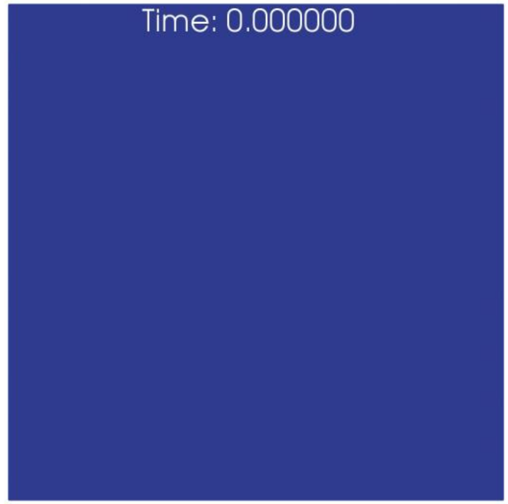

Pore pressure and amplified deformed shape

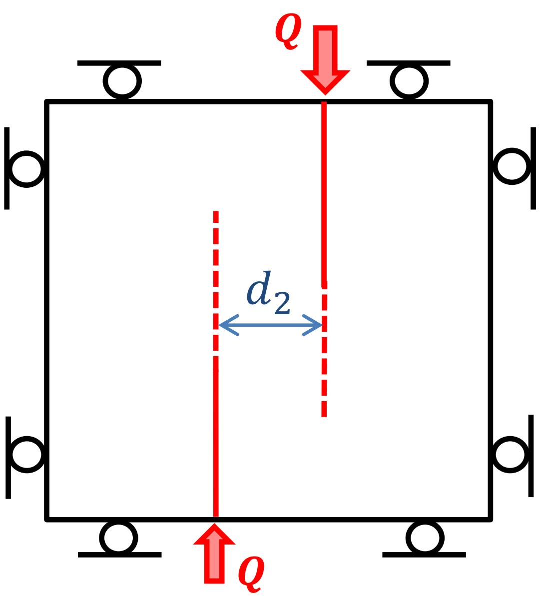

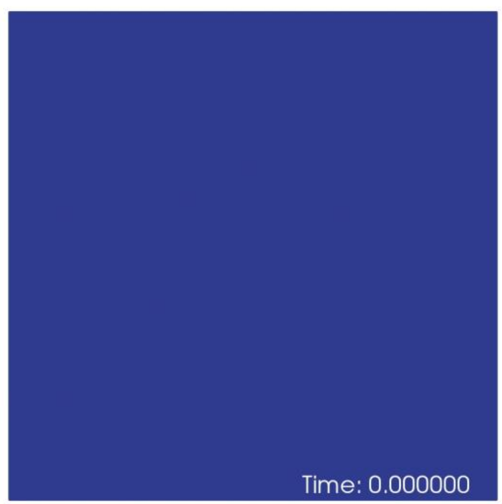

Pore pressure and amplified deformed shape

Material parameters

$E = 5800\ MPa$
$\nu = 0{,}2$
$\varphi = 0{,}1$
$k = 10^{-15} m^2$
$b = 0{,}8$
$1/K_l = 5.10^{-10} Pa^{-1}$
$\mu = 10^{-3} Pa.s$
$G_c = 900\ Pa.m$
$\sigma_c = 1{,}0\ MPa$

$Q = 0{,}0003\ m^2.s^{-1}$

$d_1 = 2{,}5m$
$d_2 = 1{,}5m$

3D crack reorientation

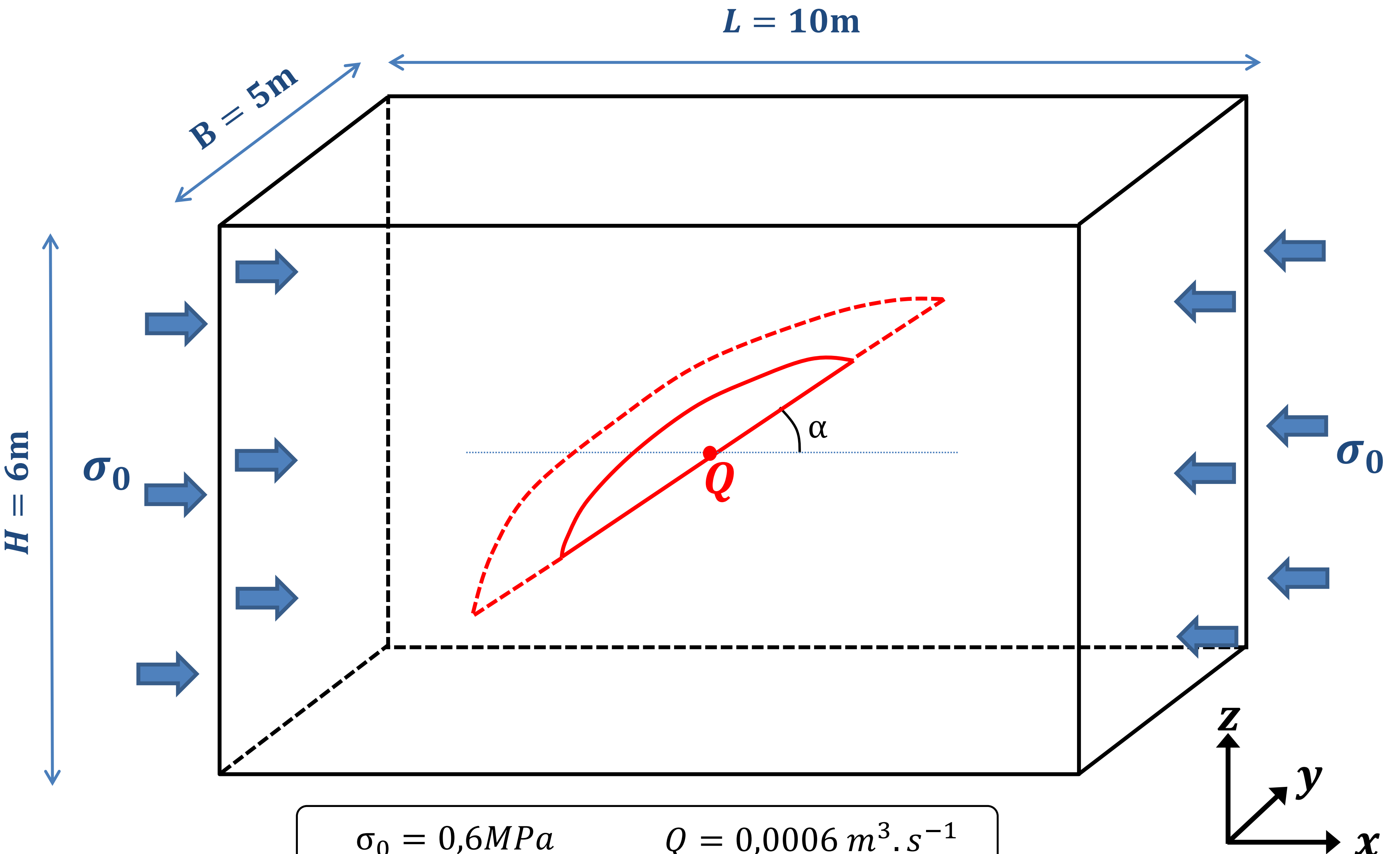

$\sigma_0 = 0{,}6MPa$ $\qquad Q = 0{,}0006\, m^3 . s^{-1}$

3D crack reorientation

Pore pressure and amplified deformed shape

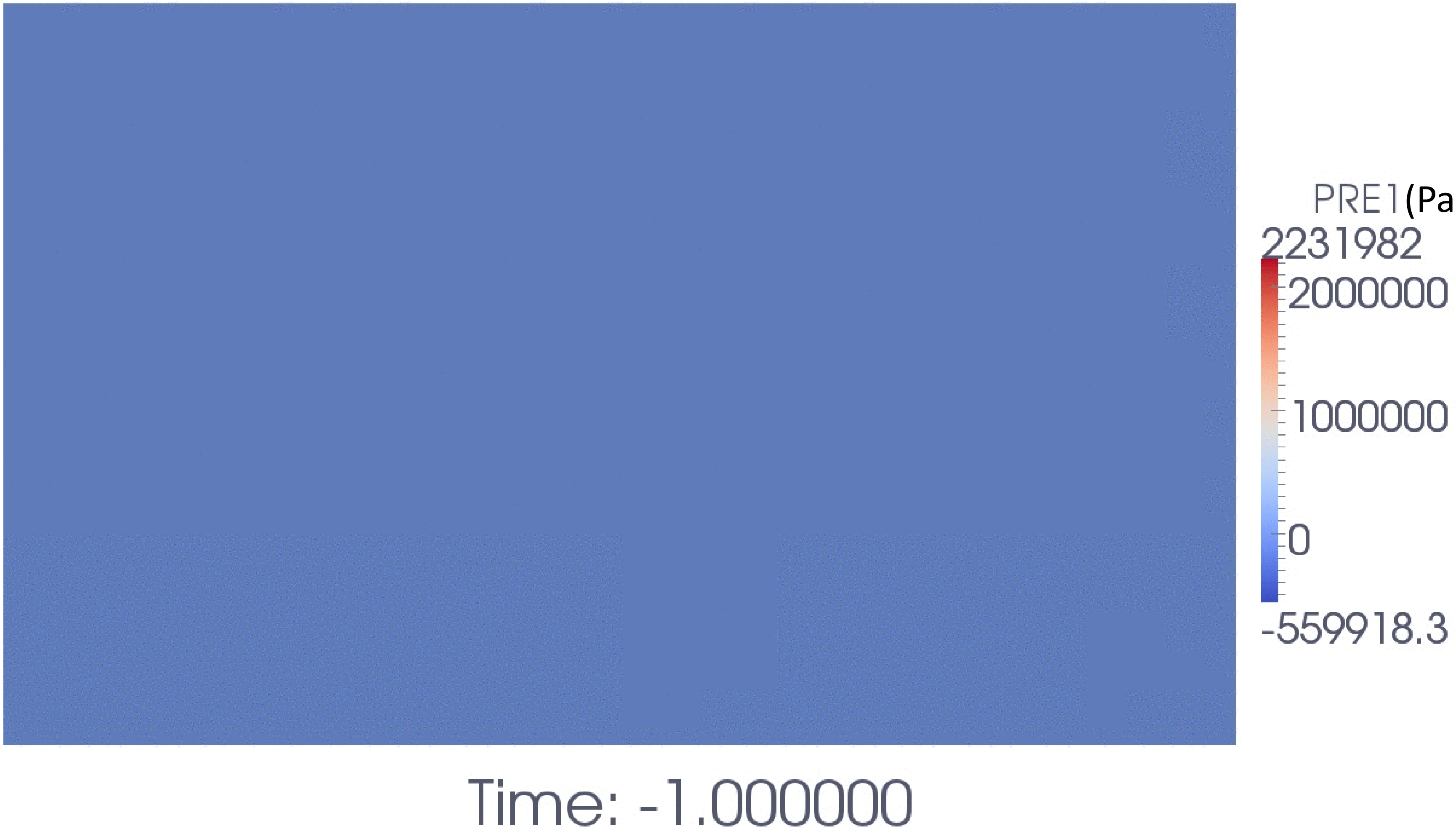

3D crack reorientation

Hydraulic fracture evolution

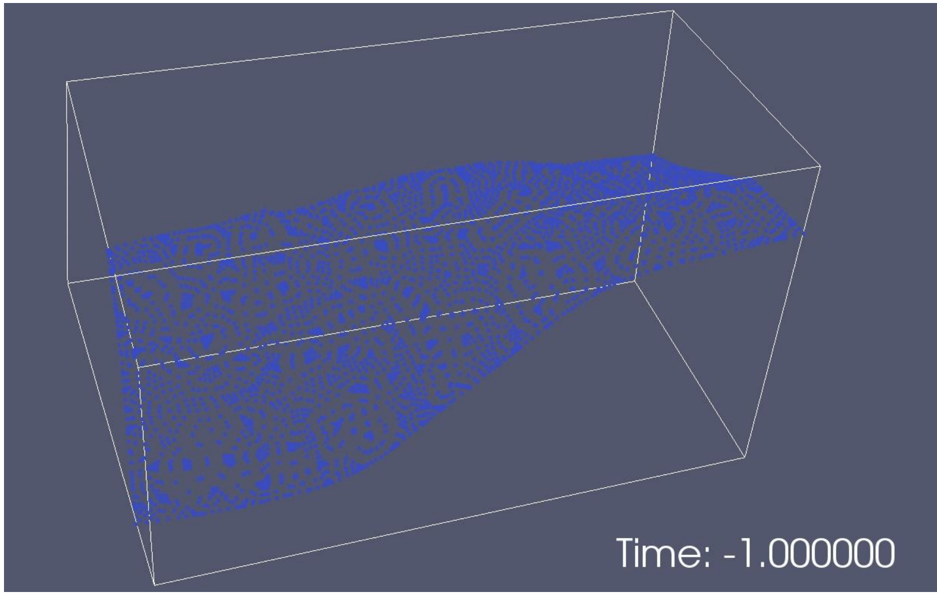

Initial crack surface and final crack surface

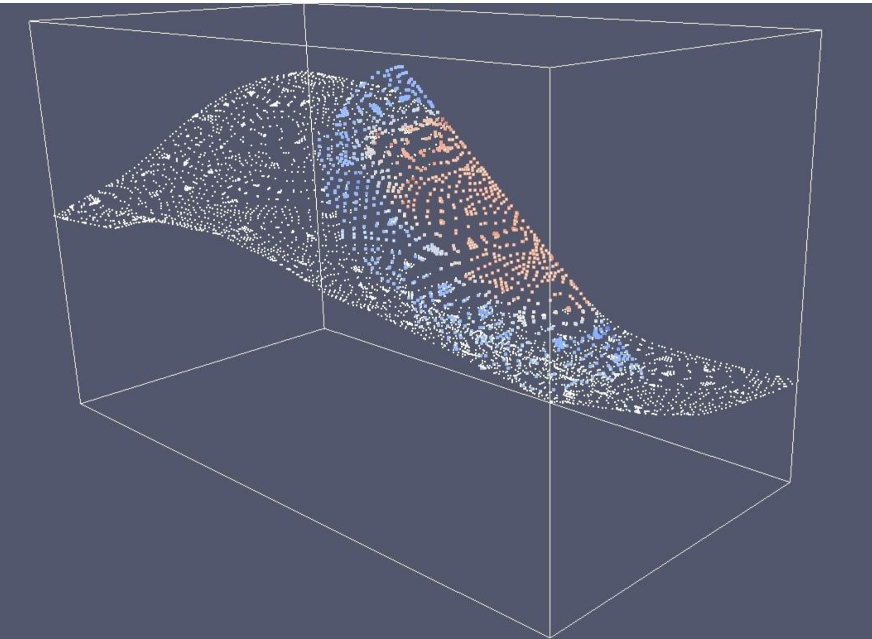

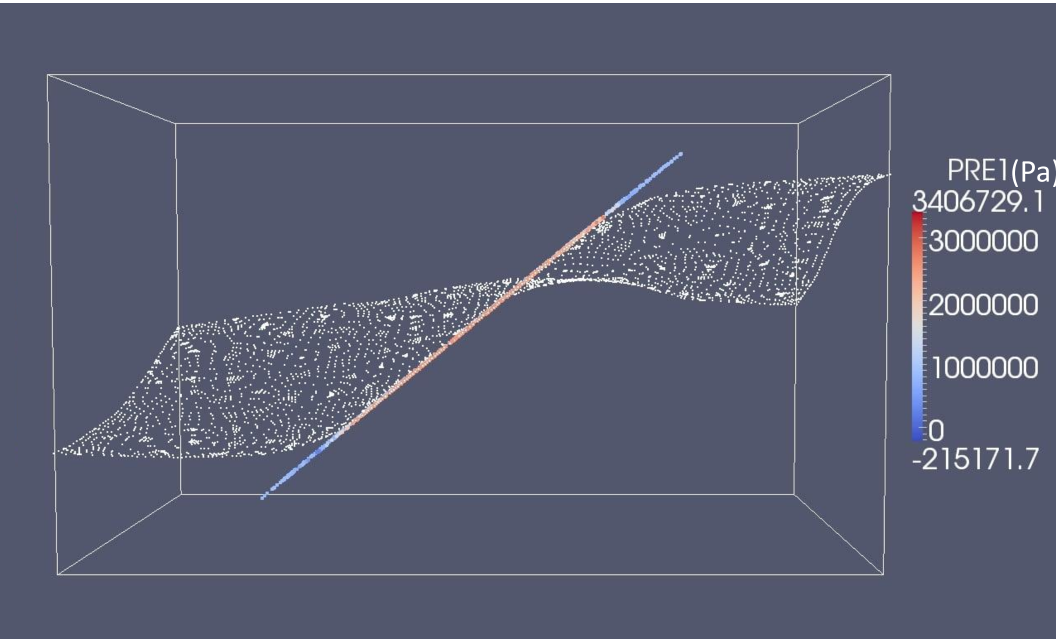

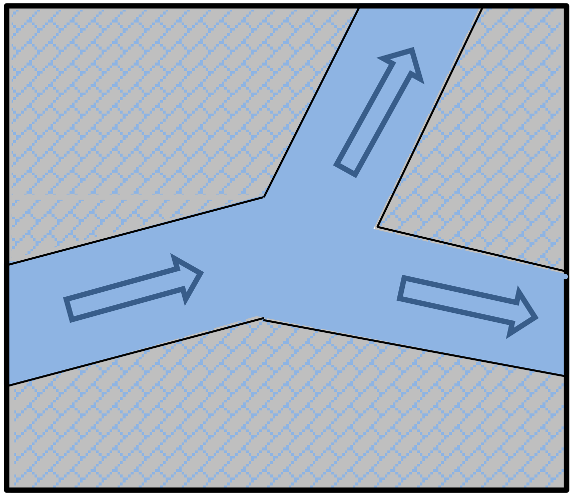

Fracture junction

Fracture junction

- A distinct approximation space is associated to each fracture branch:

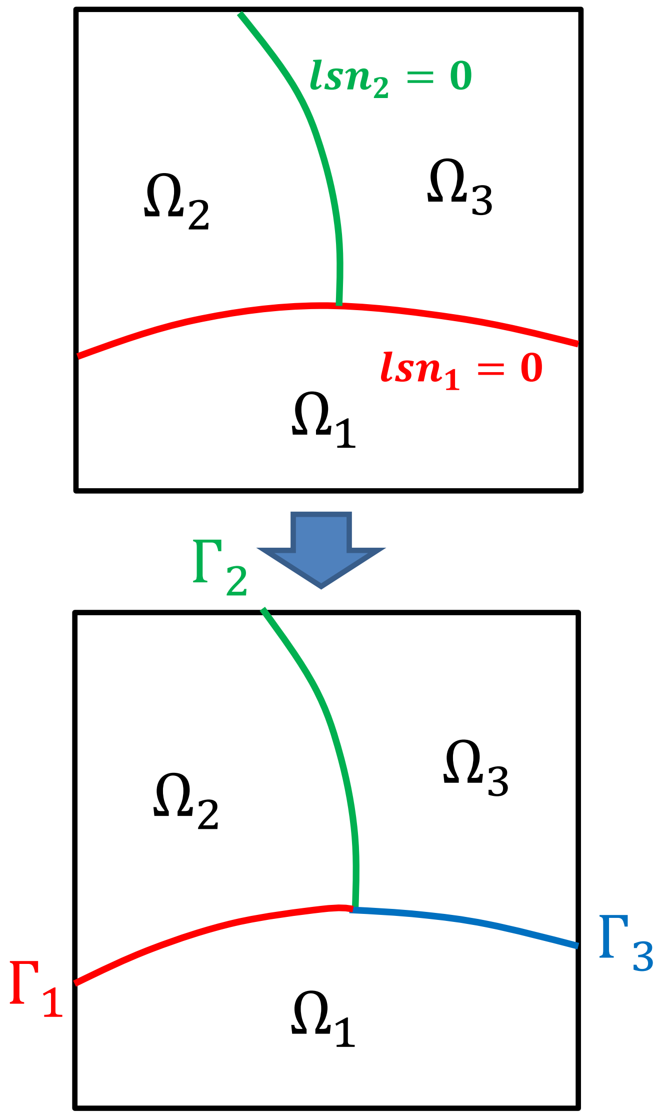

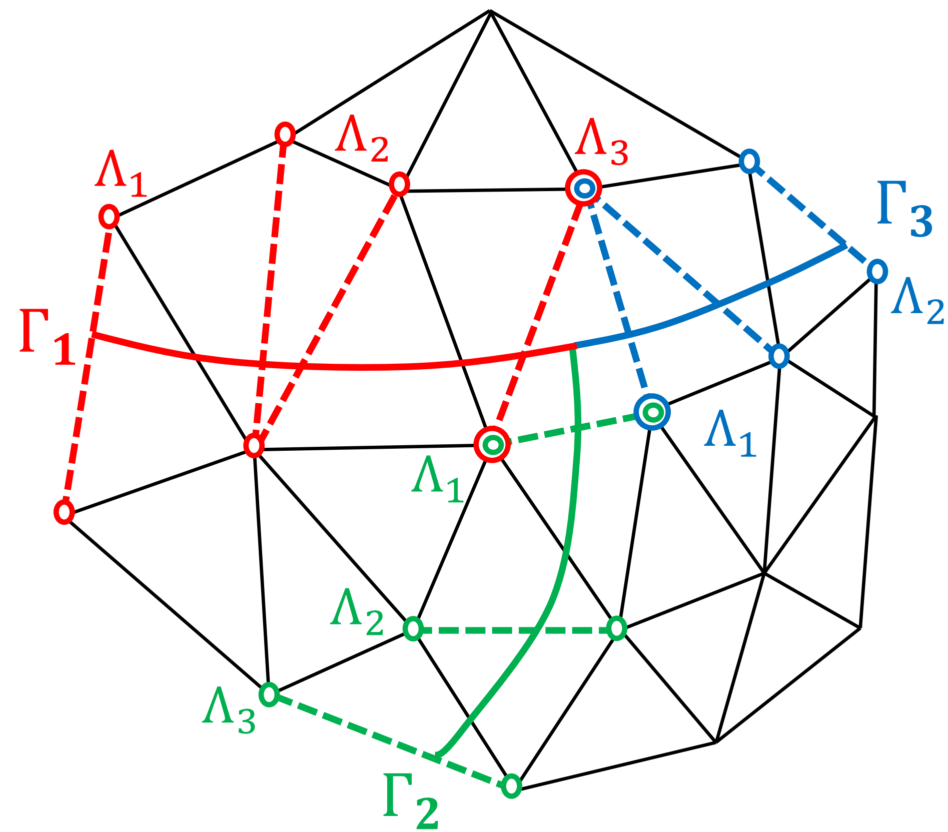

Fracture junction

- At the fracture junctions, we have two options:

  - imposing Neumann conditions: $\boxed{\underline{\boldsymbol{W}_1} + \underline{\boldsymbol{W}_2} + \underline{\boldsymbol{W}_3} = \underline{\mathbf{0}}}$

  - imposing Dirichlet conditions: $\boxed{p_{f,1} = p_{f,2} = p_{f,3}}$

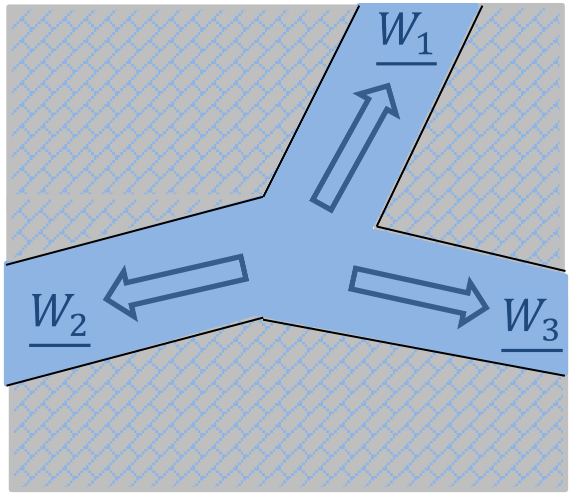

- We choose to impose Dirichlet conditions because the approximation space we use for p_f is too coarse to properly impose the Neumann conditions.

- The junction paths are systematically predefined. Furthermore, we have no appropriate criterion for the potential deviation at the fracture junctions. At a junction, each fracture branch is governed by the cohesive zone model

Multi-stage hydraulic fracturing

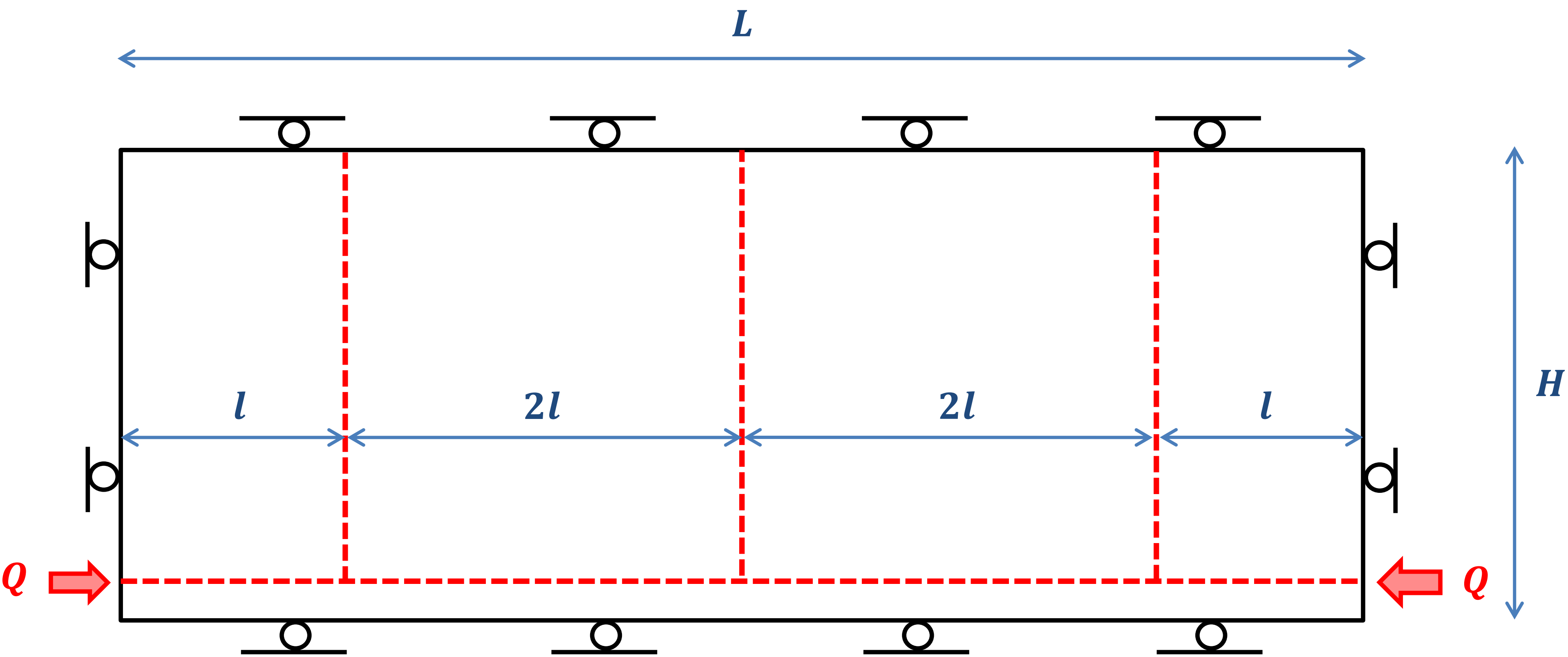

Material parameters

$E = 5800\ MPa$	$\varphi = 0{,}1$	$k = 10^{-17} m^2$
$\nu = 0{,}25$	$1/K_l = 5.10^{-10} Pa^{-1}$	$G_c = 500\ Pa.m$
$b = 0{,}8$	$\mu = 10^{-3} Pa.s$	$\sigma_c = 0{,}9\ MPa$

$L = 120m$

$H = 10m$

Multi-stage hydraulic fracturing

- Initial state:

- Various number n of vertical fractures

$n = 4$

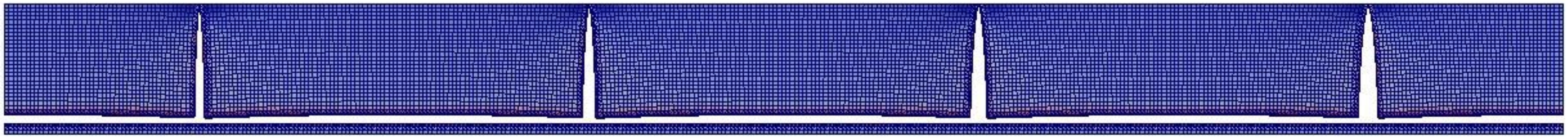

$n = 5$

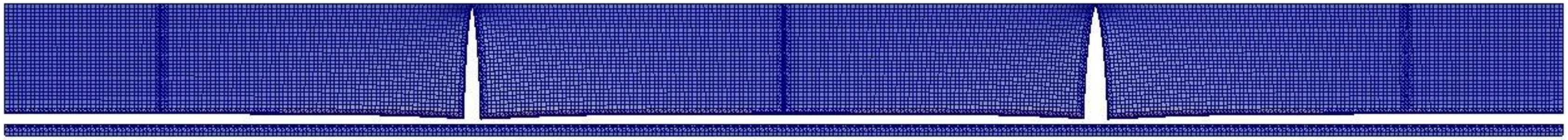

$n = 6$

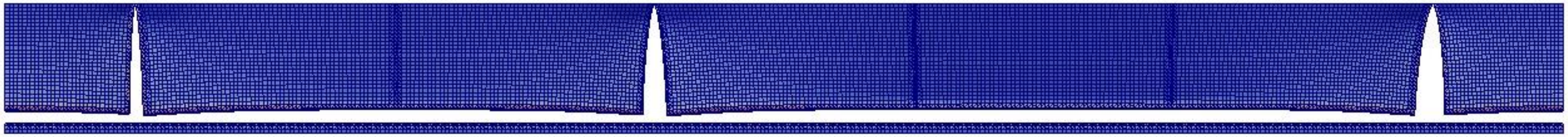

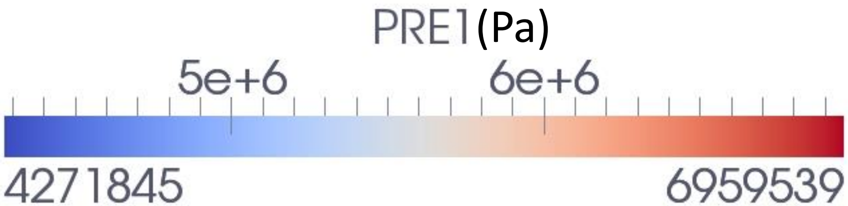

Multi-stage hydraulic fracturing

- Constant number of vertical crack (4 vertical cracks)
- $24m < 2l < 25m$

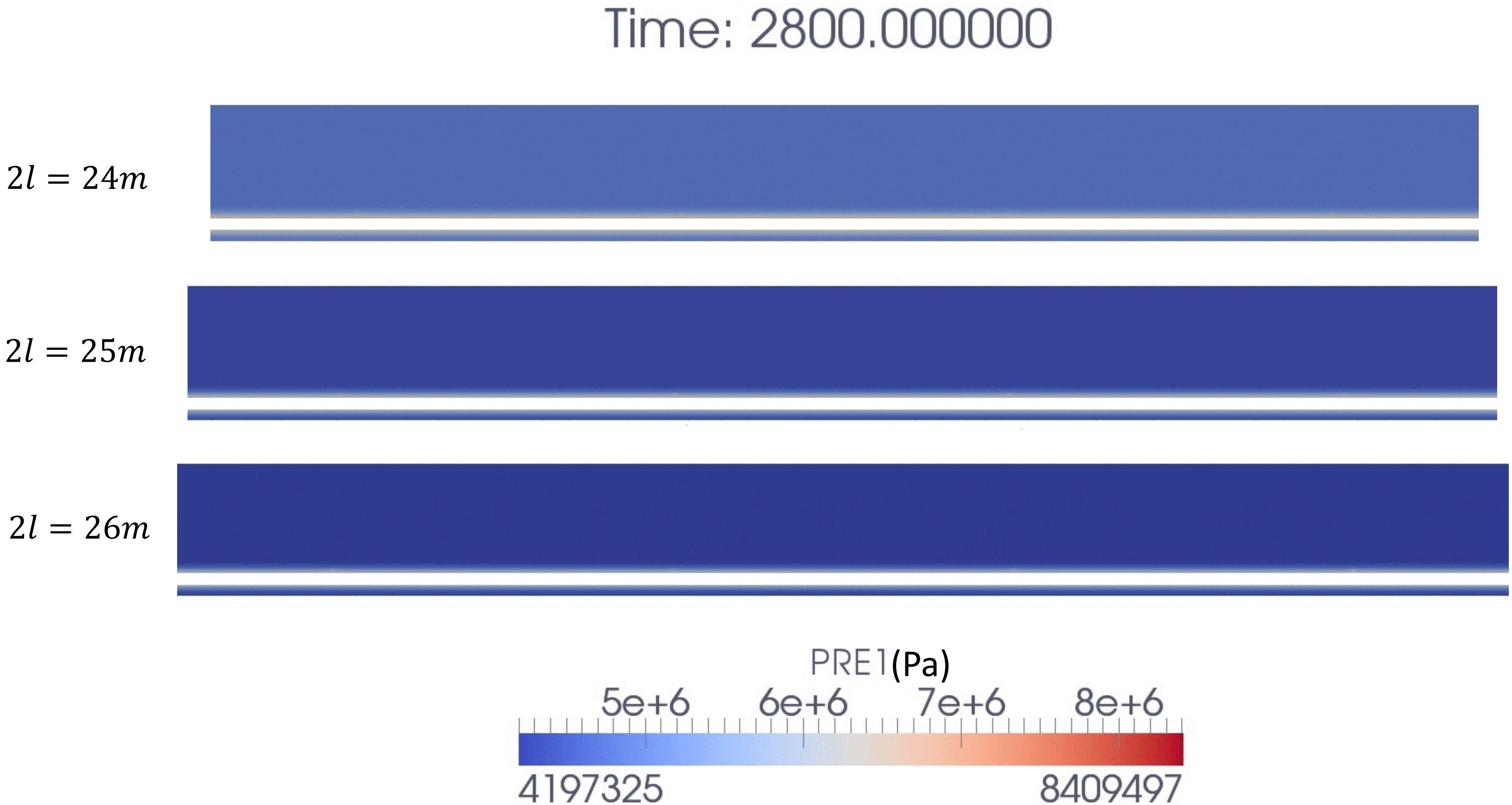

Multi-stage hydraulic fracturing

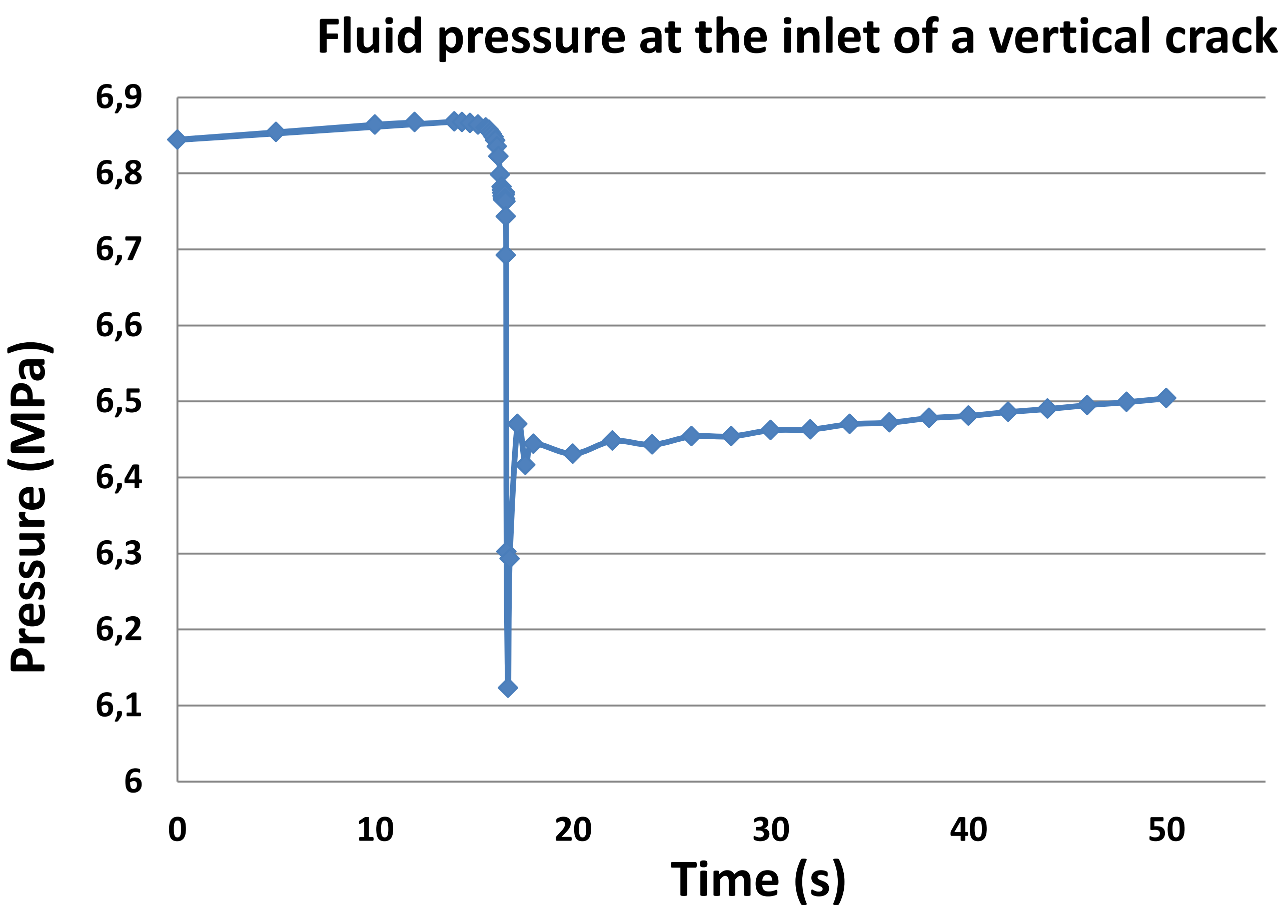

Conclusion and prospects

- Ambitious project that aimed at modeling 3D fluid-driven fracture networks.
- It relies on the latest advances of the extended finite element method.
- It offers a reliable numerical tool for a wide range of industrial applications.
- Potential improvements:

  - self-sustained crack propagation procedure.
  - cohesive zone parameters for fluid-driven cracks in porous media.

- Prospects (ANR HYDROGEODAM 17-CE06-0016) :

  - multiple phases
  - thermohydromechanical coupling.
  - anisotropy

→ I. DJOUADI, Ph.D EDF R&D - GéoRessources 2016-2019, *Accounting for anisotropy in the instantaneous response of geomaterials for undergraound structures.*

→ S. MOOSAVI, Ph.D GéoRessources 2015-2018, *Crack initiation and propagation in anisotropic medium accounting for Hydro-Mechanical couplings.*

Merci pour votre attention

Material parameters Bakken field

$$depth \sim 2200m$$

$$50GPa < E < 75GPa$$

$$0{,}05 < \nu < 0{,}25$$

$$\varphi \sim 0{,}08$$

$$1.10^{-15}m^2 < k < 3.10^{-15}m^2$$

$$\sigma_c \sim 10MPa$$

$$18MPa < \sigma_{regional} < 28MPa$$

- E. Eseme, J.L. Urai, B.M. Kroos, R. Littke, *Review of mechanical properties of oil shales: implications for exploitation and basin modelling,* Oil Shale *2007*
- R. Varga, A. Pachos, T. Holden, J. Pendrel, R. Lotti, I. Marini, E. Spadafora, *Seismic inversion in the Barnett shale successfully pinpoints sweet spots to optimize wellbore placement and reduce drilling risks,* SEG Annual Meeting 2012

Approximation space for the interface

Géniaut (2012)

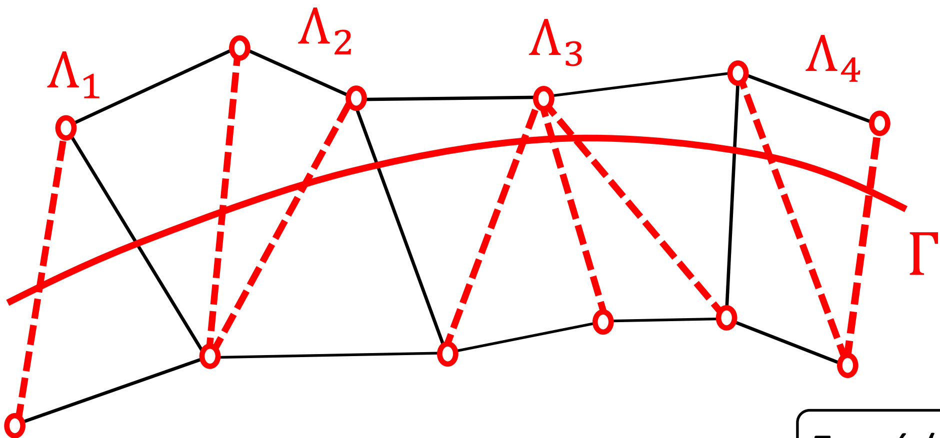

o : node carrying the fields associated to the fluid-filled fracture.

: intersected edge whose vertex nodes are submitted to equality relations for the fields associated to the fluid-filled fracture.

Ferté (2014)

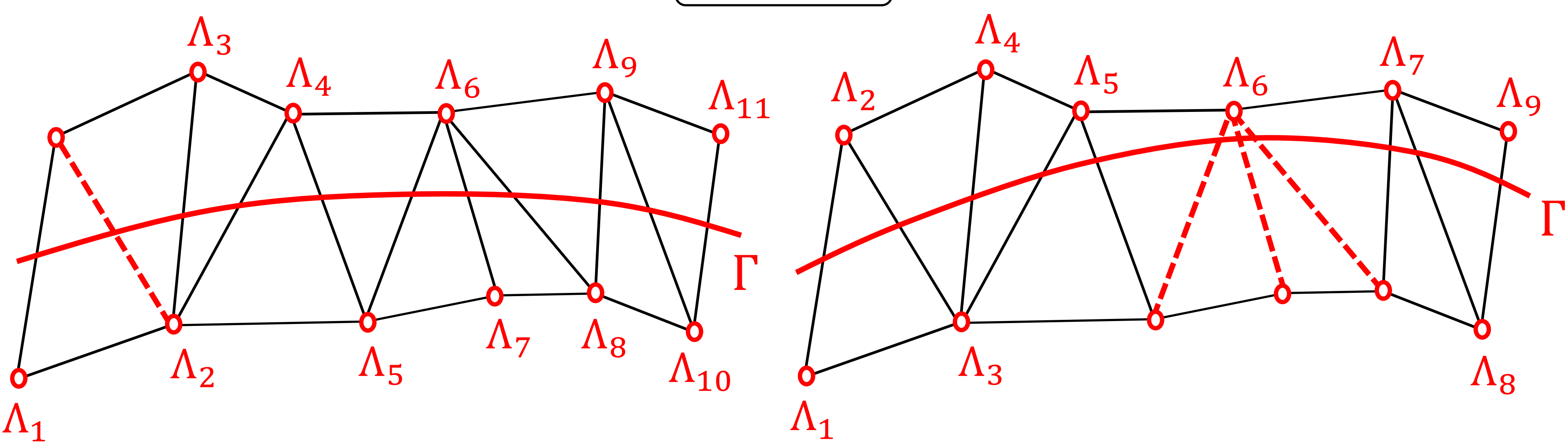

- S. Géniaut, P. Massin. N. Moës, *A stable 3D contact formulation using XFEM,* European Journal of Computational Mechanics, 2012
- G. Ferté, P. Massin. N. Moës, *Interface problems with linear or quadratic x-fem: design of a stable Lagrange multiplier space and error analysis,* Int. J. Numer. Meth. Eng., 2014

Fluid lag

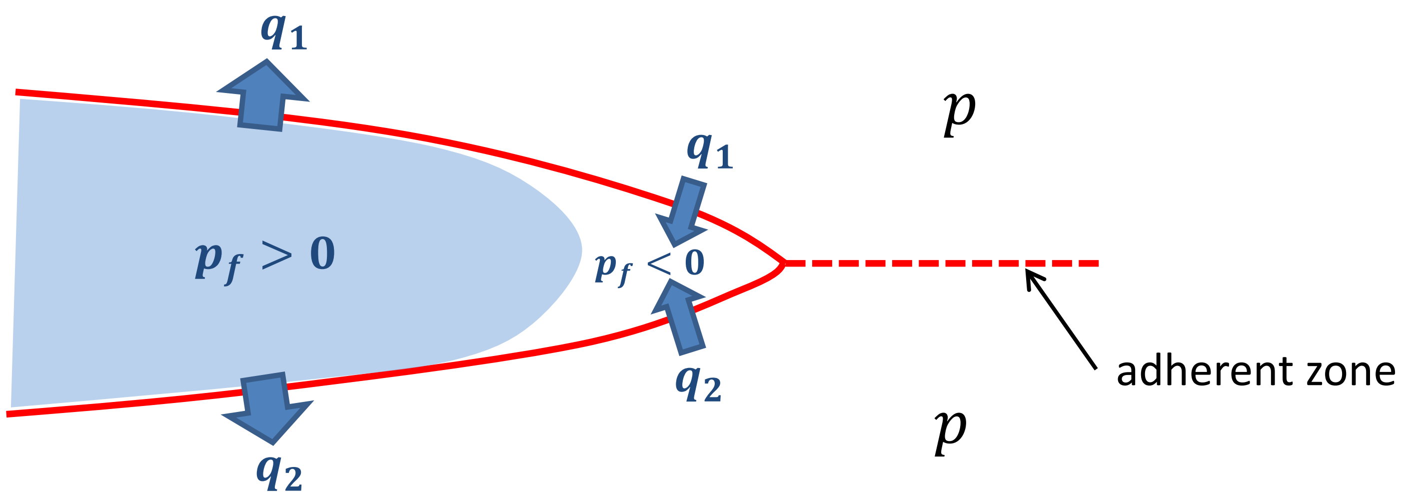

First formulation for the cohesive zone model

- The total energy of the system is:

$$\mathrm{E}(\boldsymbol{u},\boldsymbol{\delta}) = \underbrace{\frac{1}{2}\int_\Omega \boldsymbol{\varepsilon}(\boldsymbol{u}):\boldsymbol{C}:\boldsymbol{\varepsilon}(\boldsymbol{u})d\Omega}_{\text{elastic energy}} - \underbrace{\int_{\Gamma_t} \boldsymbol{t}.\boldsymbol{u}d\Gamma_t}_{\text{external loads}} + \underbrace{\int_{\Gamma_c} \Pi(\boldsymbol{\delta})d\Gamma_c}_{\text{cohesive energy}}$$

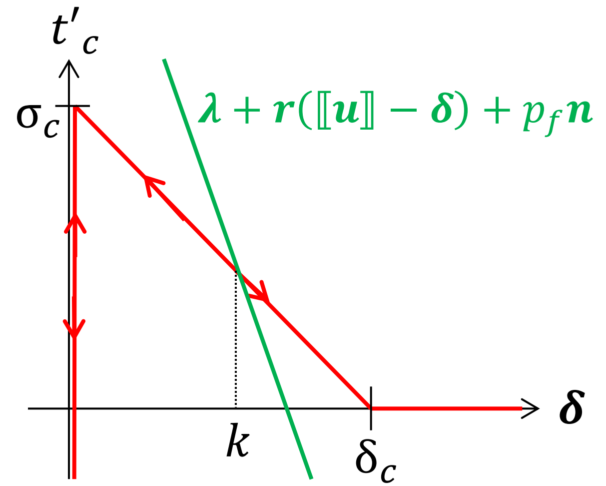

$$\boxed{\boldsymbol{t}'_c = \frac{\partial \Pi}{\partial \boldsymbol{\delta}}} \qquad \boxed{k = sup\|\boldsymbol{\delta}\|}$$

- Augmented Lagrangian (Lorentz 2008):

$$\boxed{\mathcal{L}_r(\boldsymbol{u},\boldsymbol{\delta},\boldsymbol{\lambda}) = \frac{1}{2}\int_\Omega \boldsymbol{\varepsilon}(\boldsymbol{u}):\boldsymbol{C}:\boldsymbol{\varepsilon}(\boldsymbol{u})d\Omega - \int_{\Gamma_t} \boldsymbol{t}.\boldsymbol{u}d\Gamma_t + \int_{\Gamma_c} \Pi(\boldsymbol{\delta})d\Gamma_c + \int_{\Gamma_c} \boldsymbol{\lambda}.([\![\boldsymbol{u}]\!] - \boldsymbol{\delta})d\Gamma_c + \int_{\Gamma_c} \frac{r}{2}([\![\boldsymbol{u}]\!] - \boldsymbol{\delta})^2 d\Gamma_c}$$

$$\int_{\Gamma_c} \boldsymbol{\delta}^*.[\boldsymbol{t_c} - \boldsymbol{\lambda} - \boldsymbol{r}([\![\boldsymbol{u}]\!] - \boldsymbol{\delta})]d\Gamma_c = 0 \quad \forall \boldsymbol{\delta}^* \in \boldsymbol{M_0} \quad \Rightarrow \quad \boldsymbol{t_c}(\boldsymbol{\delta},k) = \boldsymbol{\lambda} + \boldsymbol{r}([\![\boldsymbol{u}]\!] - \boldsymbol{\delta})$$

Asumption of Biot effective stress: $\boldsymbol{t_c} = \boldsymbol{t}'_c\text{-}p_f\boldsymbol{n} \Rightarrow \boxed{\boldsymbol{t}'_c(\boldsymbol{\delta},k) = \boldsymbol{\lambda} + \boldsymbol{r}([\![\boldsymbol{u}]\!] - \boldsymbol{\delta}) + p_f\boldsymbol{n}}$

- Augmented multiplier $\boxed{\boldsymbol{\beta} = \boldsymbol{\lambda} + \boldsymbol{r}[\![\boldsymbol{u}]\!] + p_f\boldsymbol{n}}$

- E. Lorentz, *A mixed interface finite element for cohesive zone models,* Comp. Meth. Appl. Mech. Eng. 2008

First formulation for the cohesive zone model

- Weak formulation of the mechanical problem:

$$\boxed{\int_{\Omega} \boldsymbol{\sigma}(\boldsymbol{u}) : \boldsymbol{\varepsilon}(\boldsymbol{u}^*) d\Omega - \int_{\Gamma_t} \boldsymbol{t}.\boldsymbol{u}^* d\Gamma_t + \int_{\Gamma_c} [\boldsymbol{\lambda} + \boldsymbol{r}(\llbracket \boldsymbol{u} \rrbracket - \boldsymbol{\delta})].\llbracket \boldsymbol{u}^* \rrbracket d\Gamma_c = 0 \quad \forall \boldsymbol{u}^* \in \boldsymbol{U}_0}$$

$$\boxed{\int_{\Gamma_c} \boldsymbol{\lambda}^*.(\llbracket \boldsymbol{u} \rrbracket - \boldsymbol{\delta}(\boldsymbol{\beta})) d\Gamma_c = 0 \quad \forall \boldsymbol{\lambda}^* \in \boldsymbol{M}_{\boldsymbol{0}}}$$

with $\boldsymbol{\beta} = \boldsymbol{\lambda} + \boldsymbol{r}\llbracket \boldsymbol{u} \rrbracket + p_f \boldsymbol{n}$

Equivalent leak-off coefficient

$$g(r,t) = \frac{2C_L}{\sqrt{t - t_0(r)}}$$

$g(r,t)$: fluid flux transiting from the fracture to the porous matrix per unit area

C_L: leak-off coefficient

$t_0(r)$: time it takes for the fracture to reach r

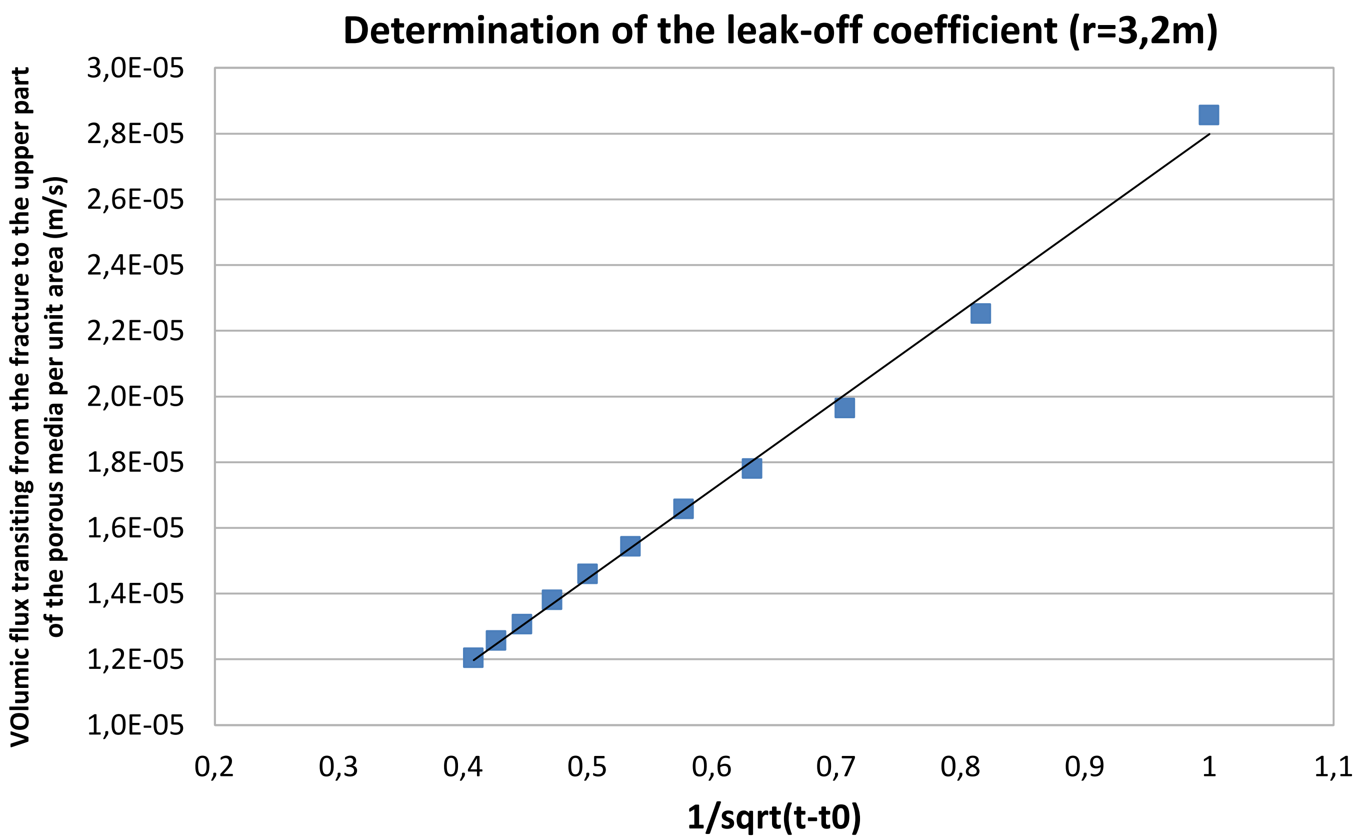

Curved competing hydraulic fractures

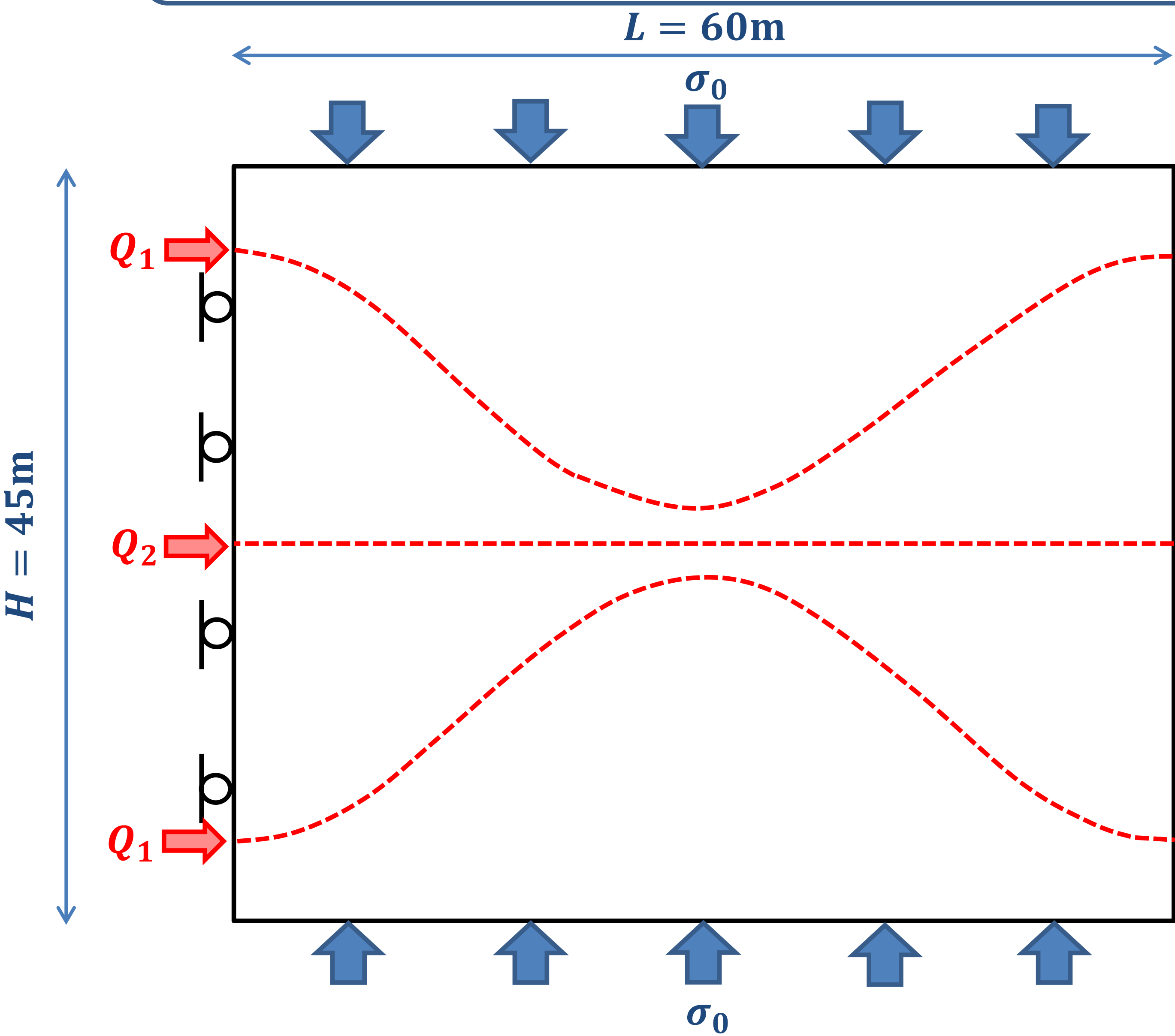

Material parameters

$E = 17\ GPa$
$\nu = 0{,}2$
$\varphi = 0{,}2$
$k = 10^{-16} m^2$
$b = 0{,}75$
$1/K_l = 0 Pa^{-1}$
$\mu = 10^{-4} Pa.s$
$G_c = 120\ Pa.m$
$\sigma_c = 1{,}25\ MPa$

Loadings

$Q_2 = 0{,}001 m^2.s^{-1}$
$Q_1 = 0{,}0014 m^2.s^{-1}$
$\sigma_0 = 3{,}7 MPa$

$\Delta t = 40s$

Pore pressure and amplified deformed shape

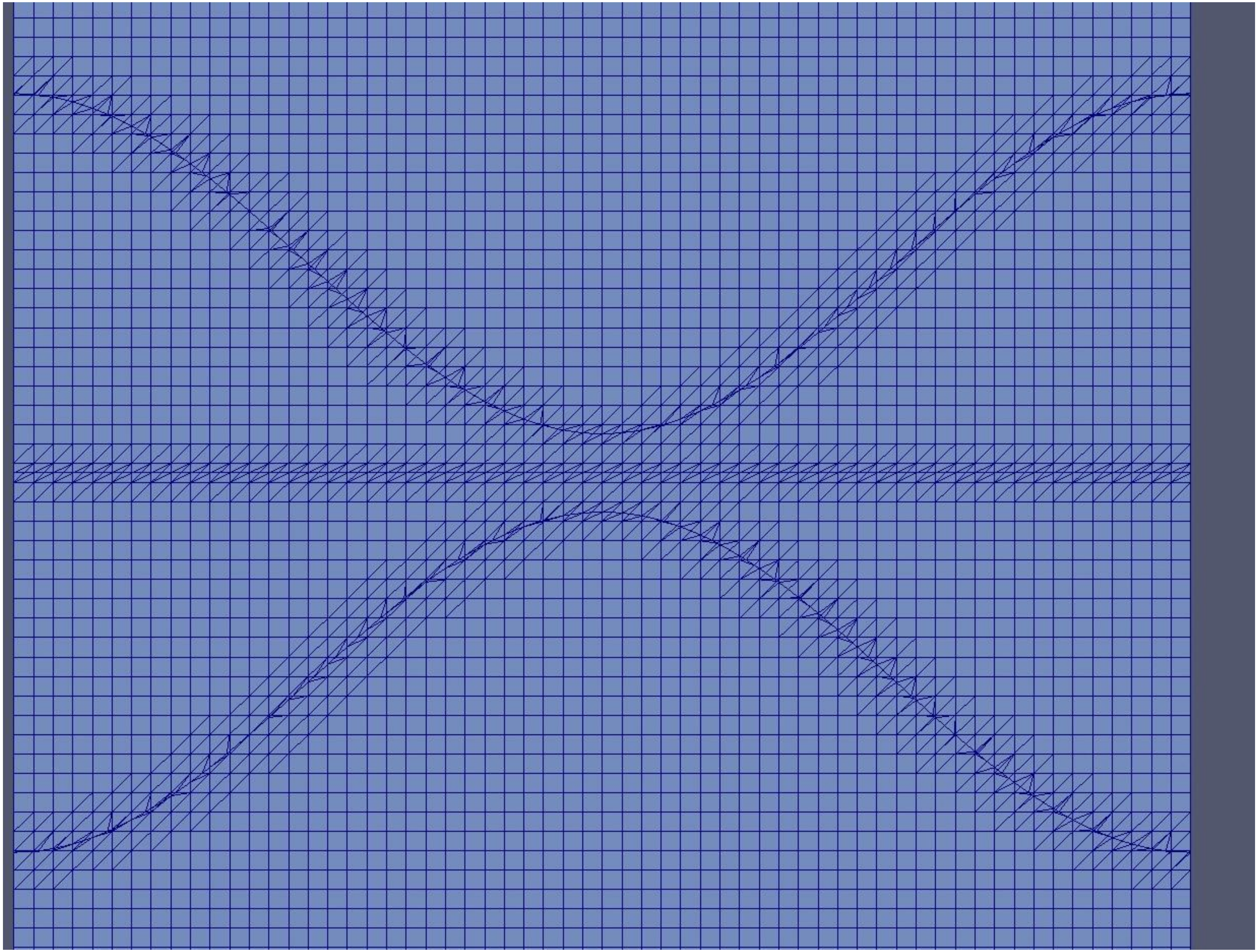

Procedure for the propagation on non-predefined paths

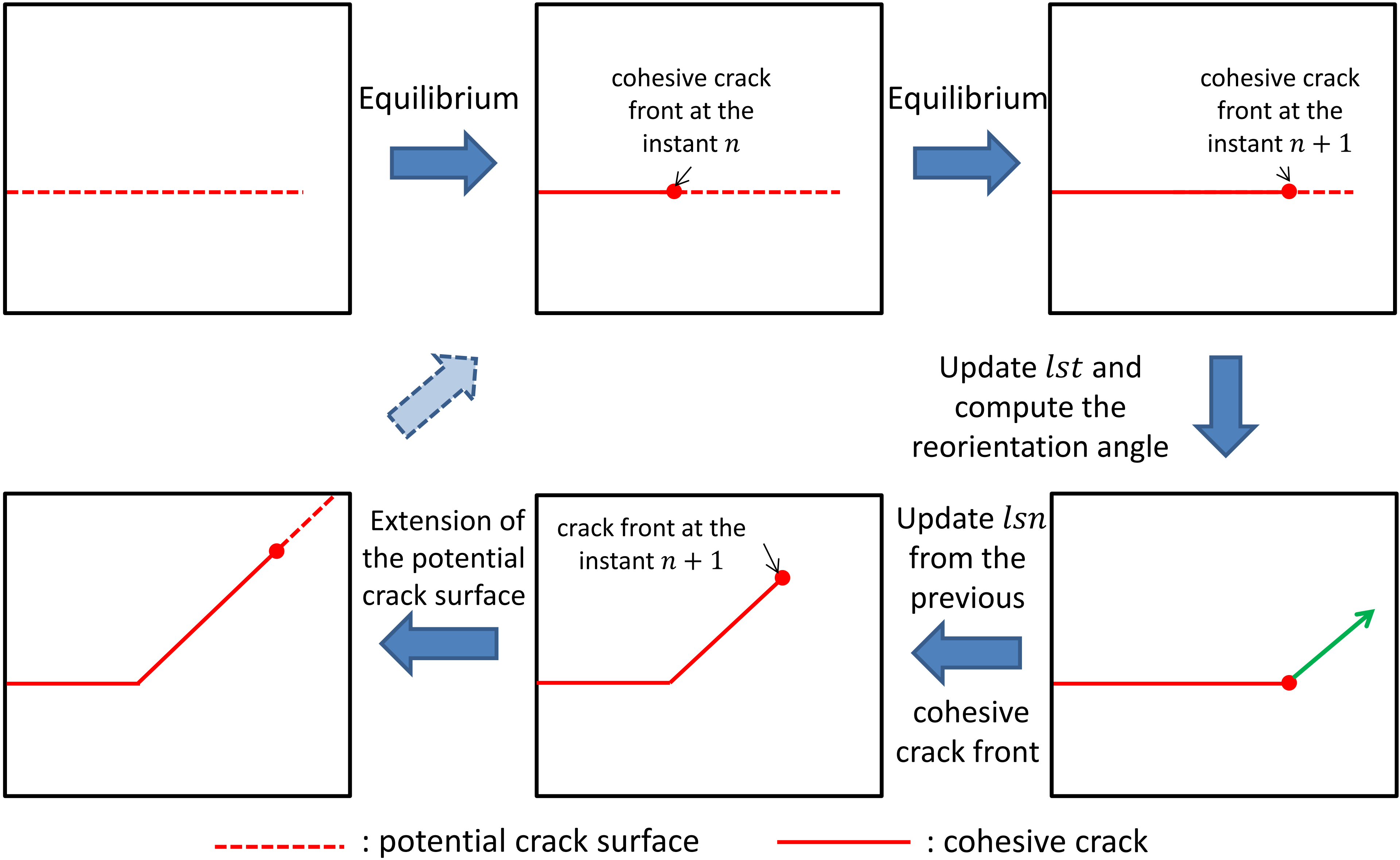

Self-sustained procedure?

- Projection of the fields from one model to another:

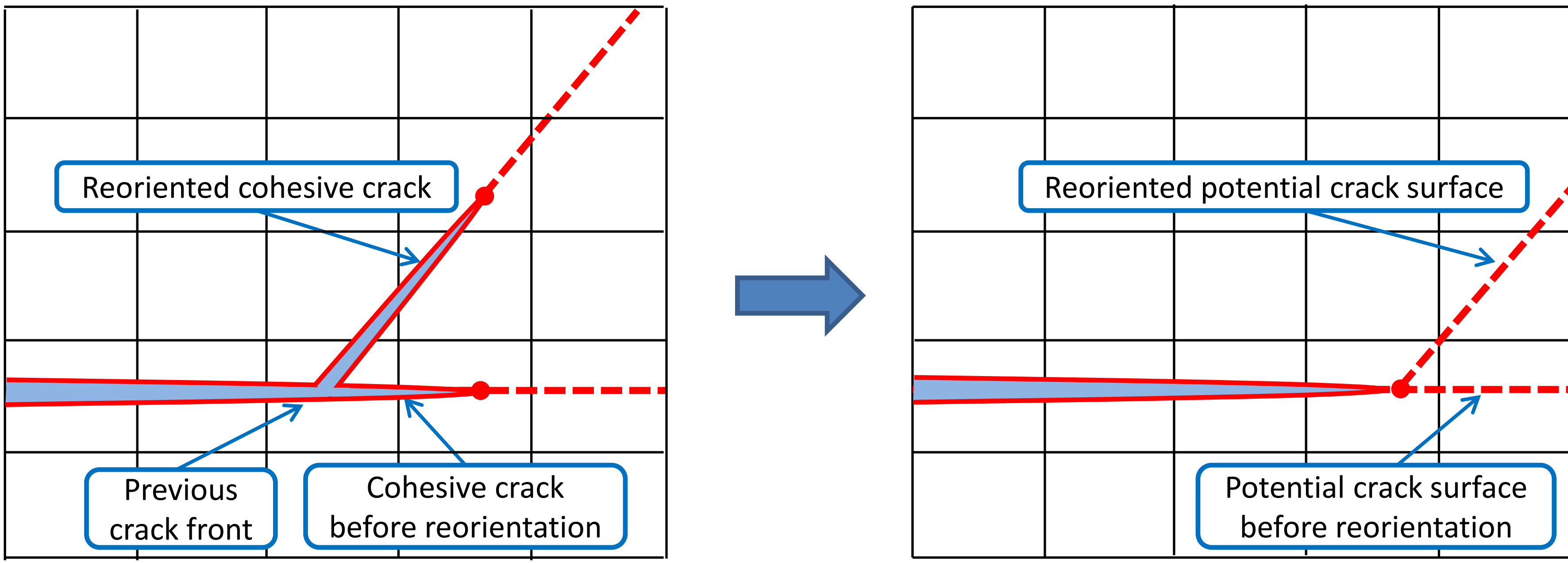

implicit update

explicit update

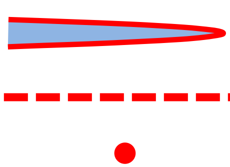

: cohesive crack

: potential crack surface

: cohesive crack front

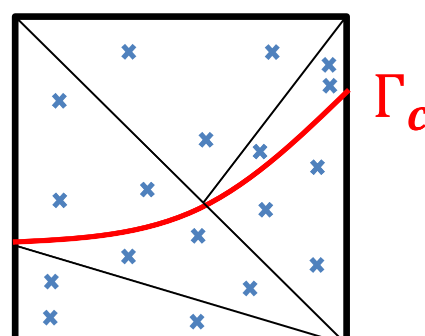

: integration point

Detection of the cohesive crack front

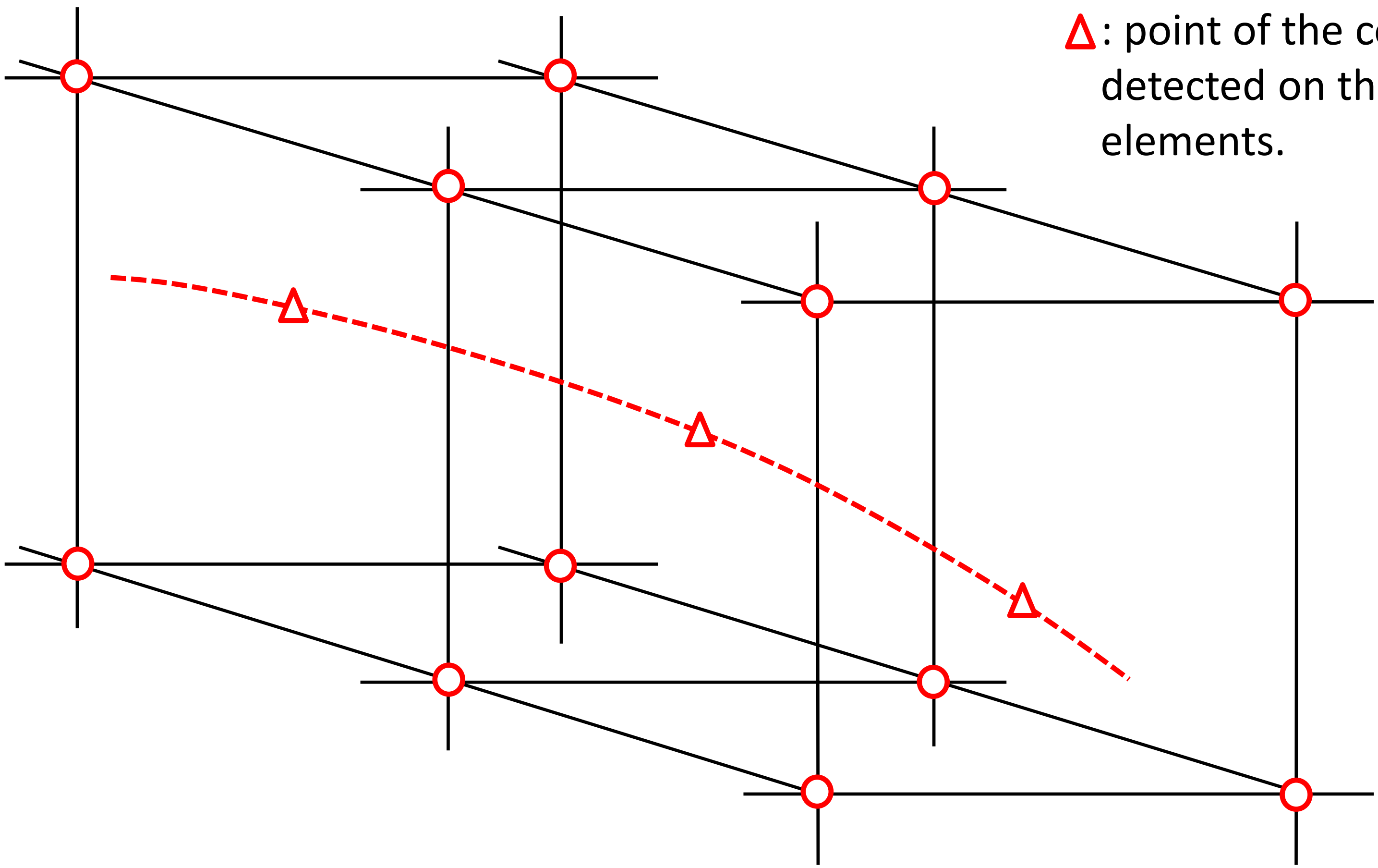

: vertex node carrying λ, w, μ and thus the internal variable of the cohesive zone model α.

: iso-zero of the internal variable α.

: point of the cohesive crack front detected on the faces of the 3D elements.

Update of the tangential level set

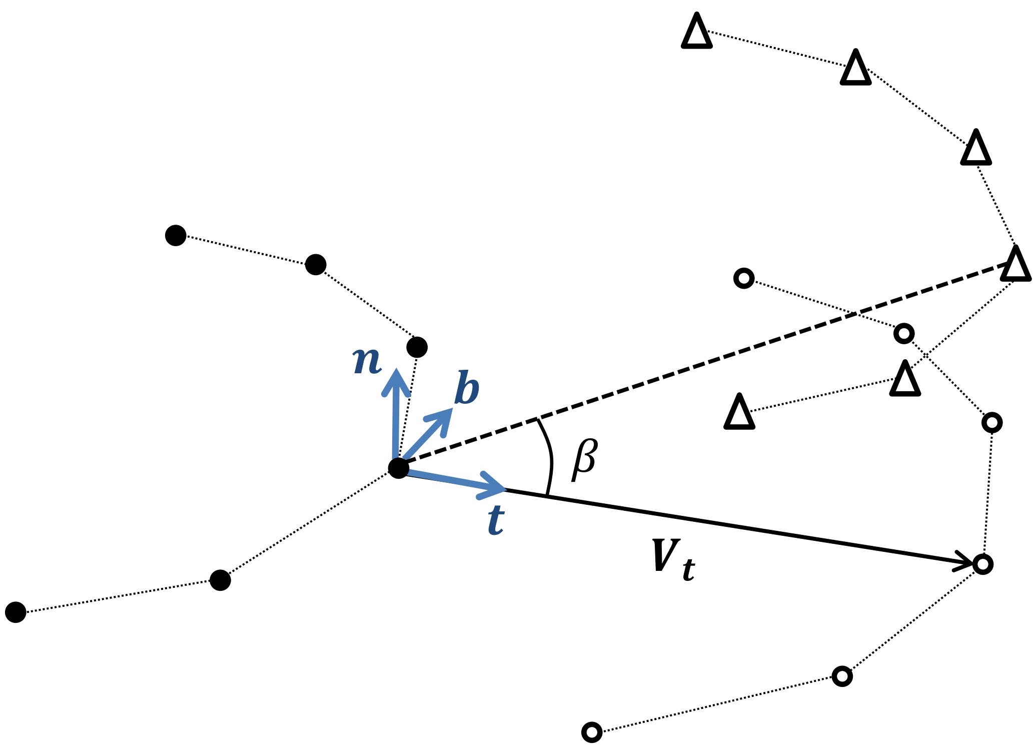

● : point of the cohesive crack front at the instant n

○ : point of the detected cohesive crack front at the instant $n+1$

Δ : point of the final crack front at the instant $n+1$

Sign of the bifurcation angle

$$\beta \quad \text{has the sign of} \ -\int_{\Gamma_c} \frac{t_{c,t}\left|\frac{\partial [\![u_t]\!]}{\partial \theta}\right| - \frac{\partial [\![u_t]\!]}{\partial \theta}\left|t_{c,t}\right|}{2} \Gamma_c$$

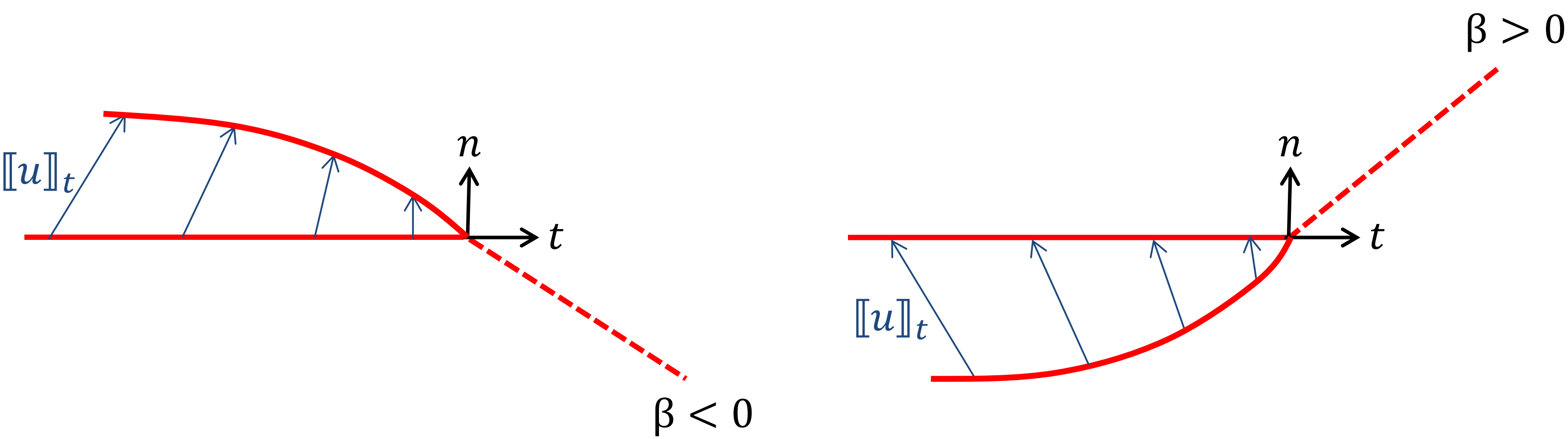

$$\boxed{\frac{\partial [\![u]\!]_t}{\partial \theta} < 0}$$

$$\boxed{\frac{\partial [\![u]\!]_t}{\partial \theta} > 0}$$

2D crack reorientation

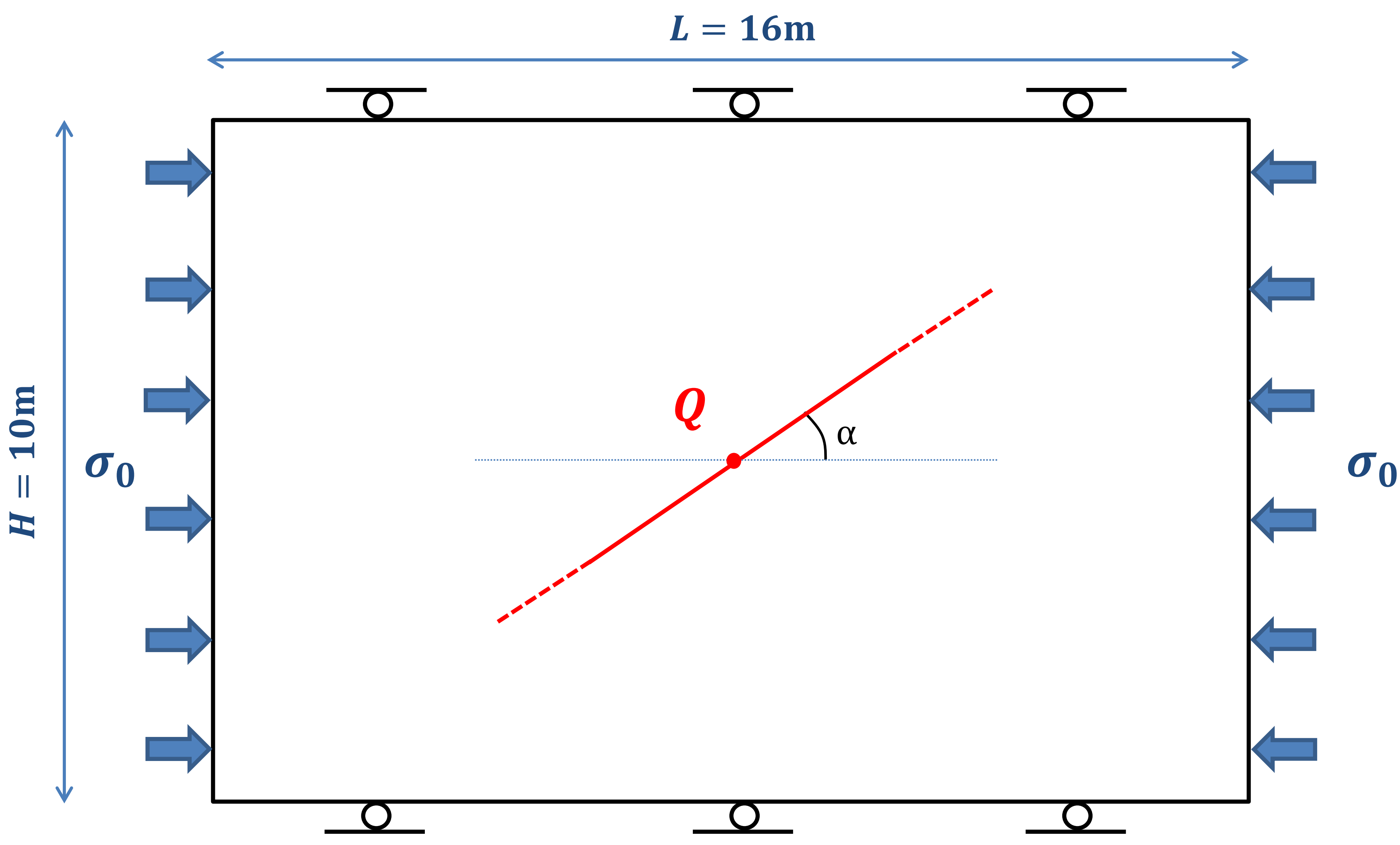

$\sigma_0 = 0{,}6 MPa$ $\quad Q = 0{,}00016\ m^2.s^{-1}$

2D crack reorientation

Pore pressure and amplified deformed shape

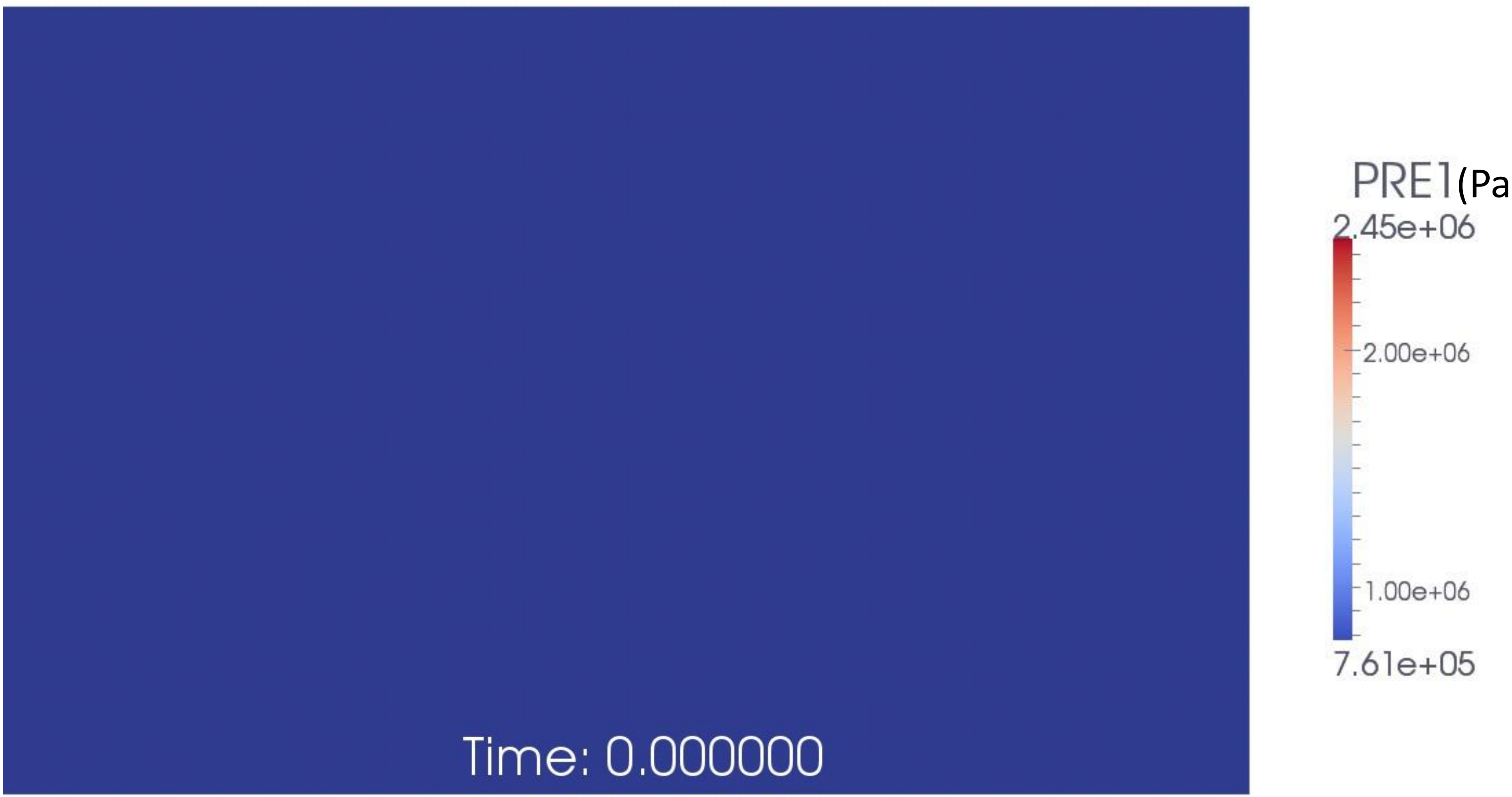

3D crack reorientation

Lateral displacement and amplified deformed shape at t=2,5s (left) and t=17s (right)

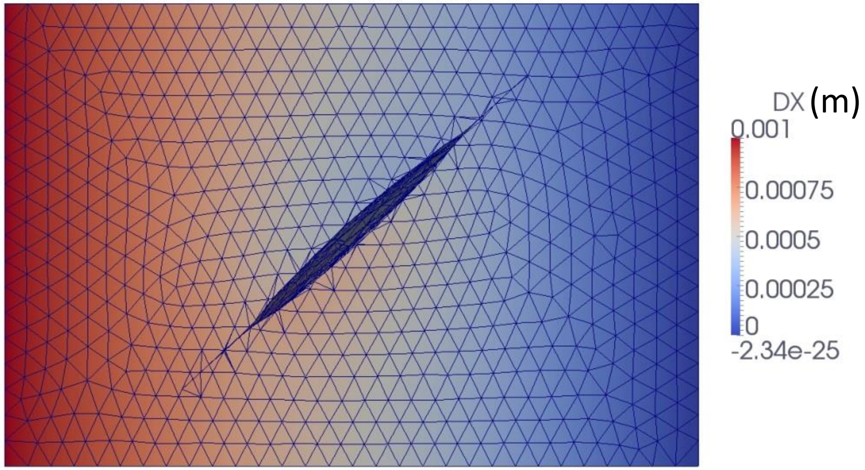

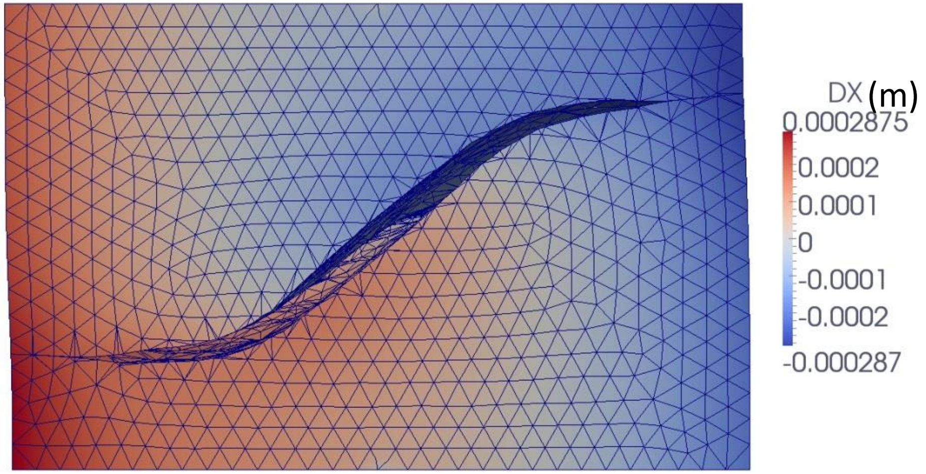

Pore pressure and amplified deformed shape at t=2,5s (left) and t=17s (right)

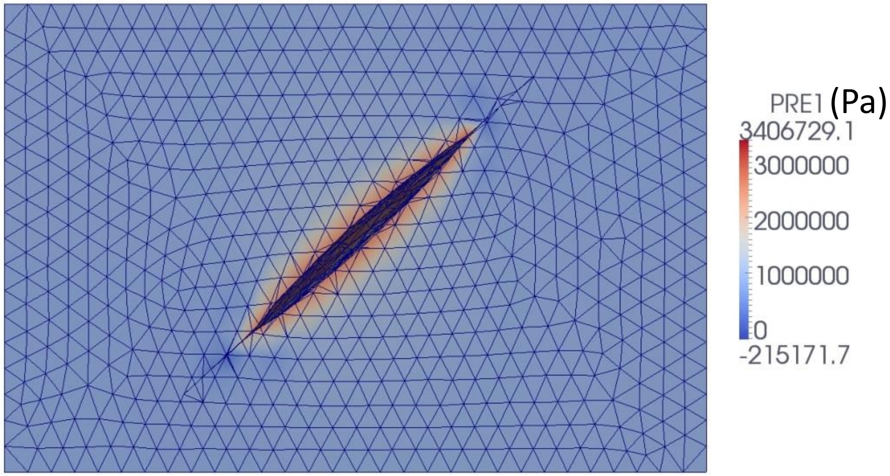

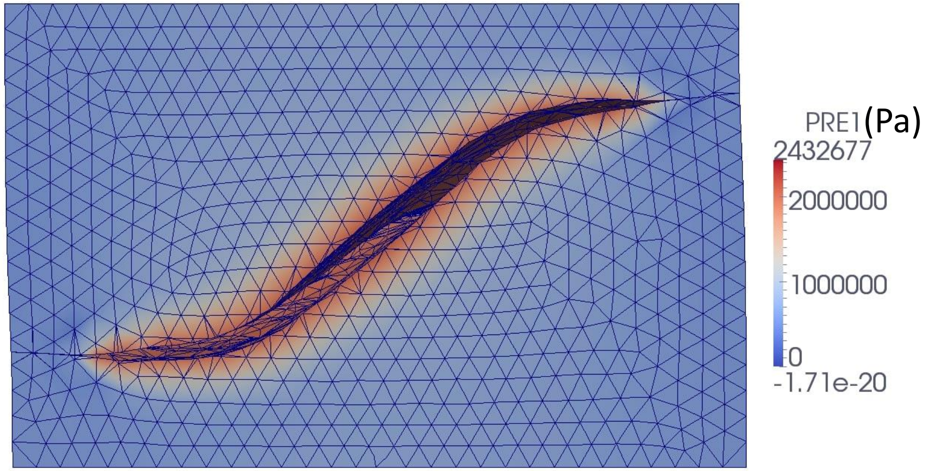

Experiments

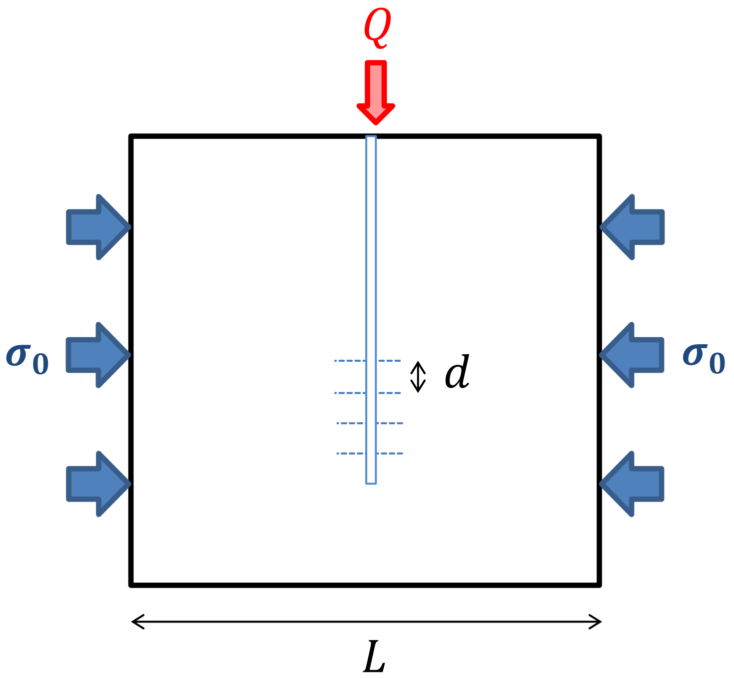

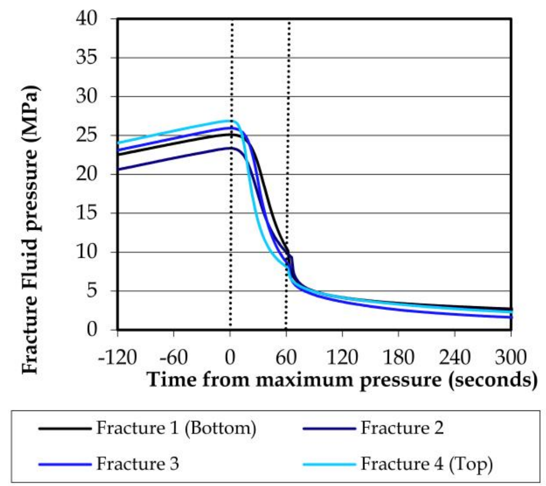

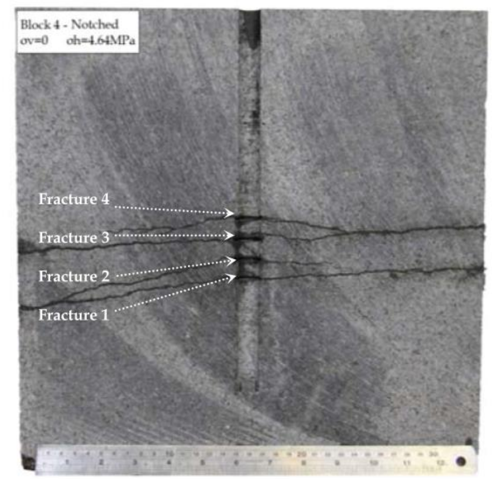

Bunger (2013)

<u>material</u>: Adelaide black granite

$E = 102\ GPa$	$\sigma_0 = 4{,}6\ MPa$	$L = 40cm$
$\nu = 0{,}27$	$Q = 0{,}19\ ml.min^{-1}$	$d = 15mm$
$K_{IC} = 2{,}3\ MPa.m^{0{,}5}$		

- A. P. Bunger, J. McLennan, R. Jeffrey, *Three dimensional forms of closely spaced hydraulic fractures*, 2013

Competing nearby cracks

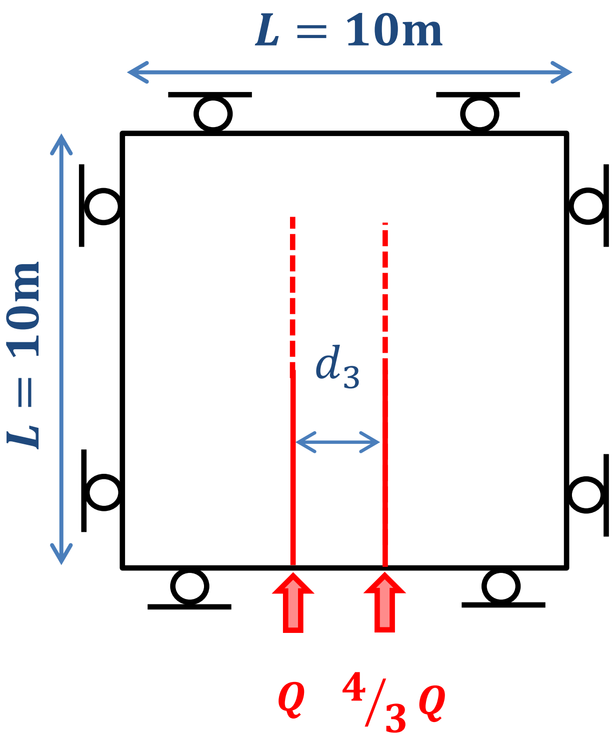

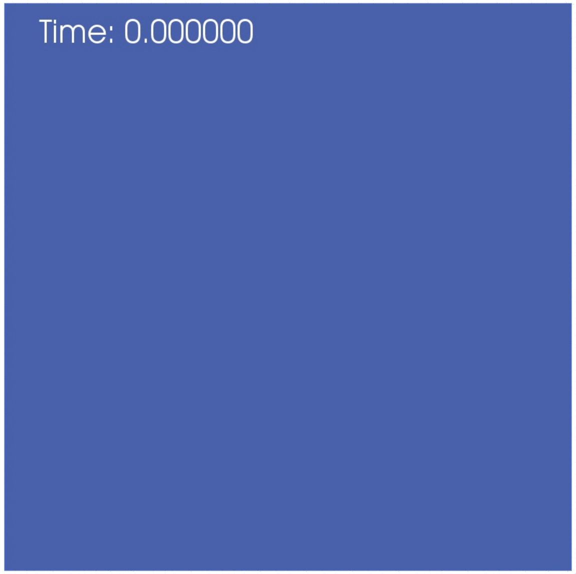

Pore pressure and amplified deformed shape

Material parameters

$E = 5800\ MPa$

$\nu = 0{,}2$

$\varphi = 0{,}1$

$k = 10^{-15} m^2$

$b = 0{,}8$

$1/K_l = 5.10^{-10} Pa^{-1}$

$\mu = 10^{-3} Pa.s$

$G_c = 900\ Pa.m$

$\sigma_c = 1{,}0\ MPa$

$Q = 0{,}0003\ m^2.s^{-1}$

$d_3 = 1{,}5m$

Hydraulic connection at a junction

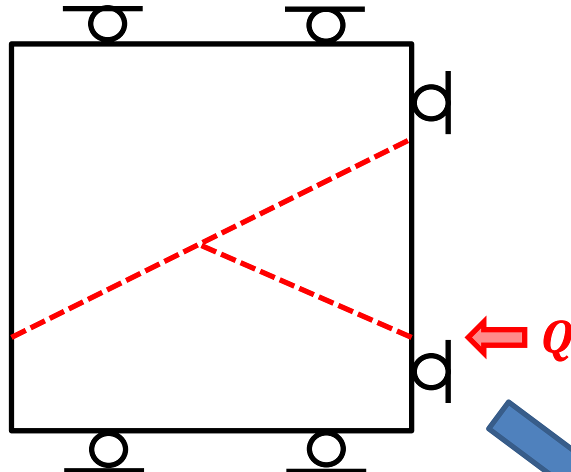

continuity of p_f imposed at the junction

continuity of p_f not imposed at the junction

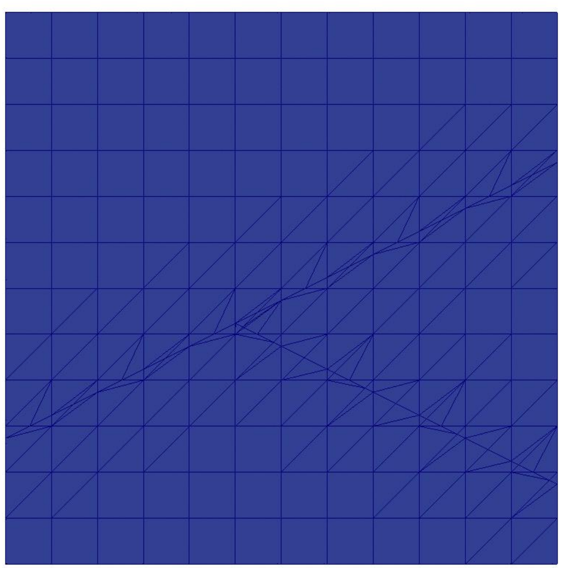

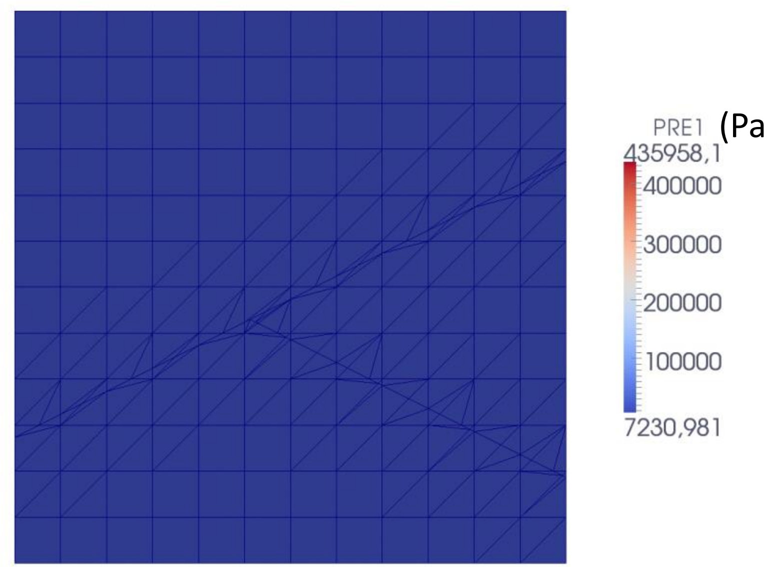

Hydraulic fracture junction

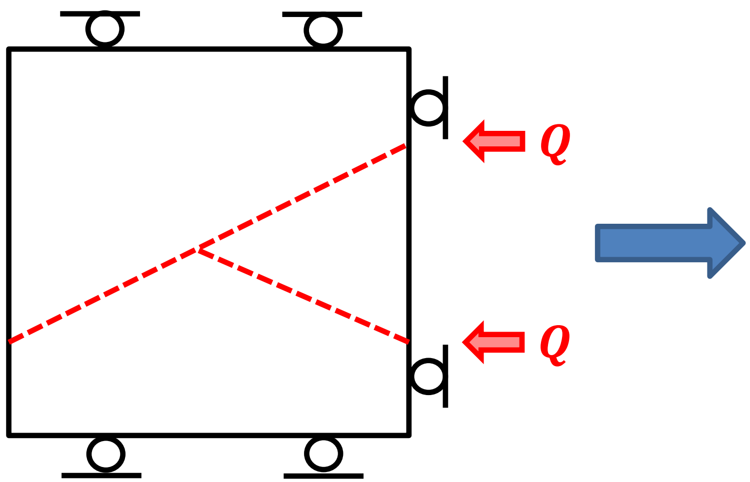

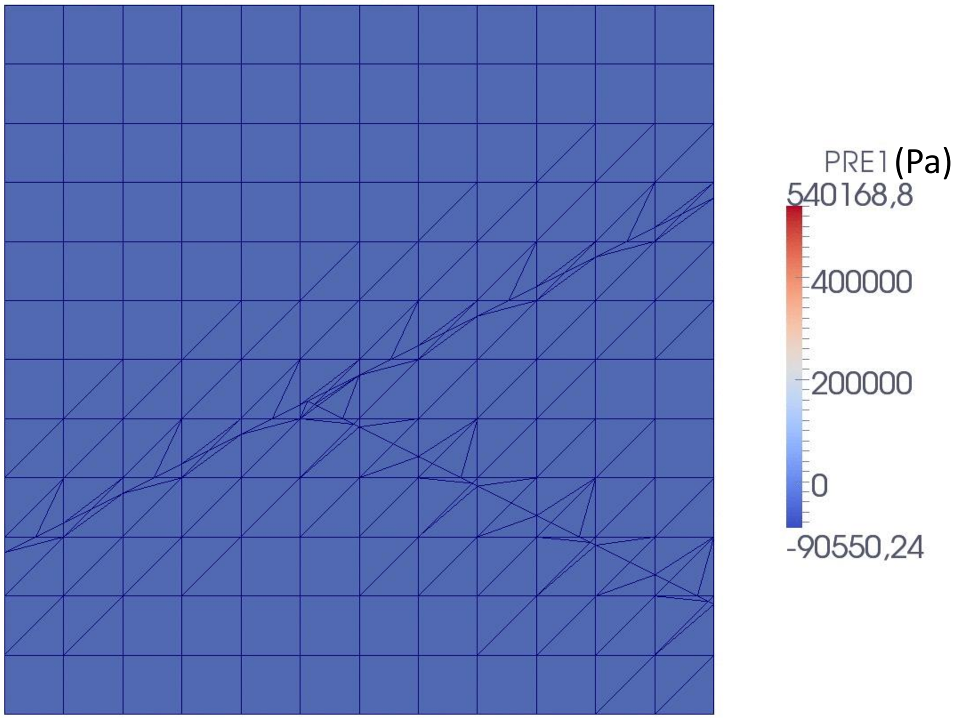

Hydraulic fracture junction

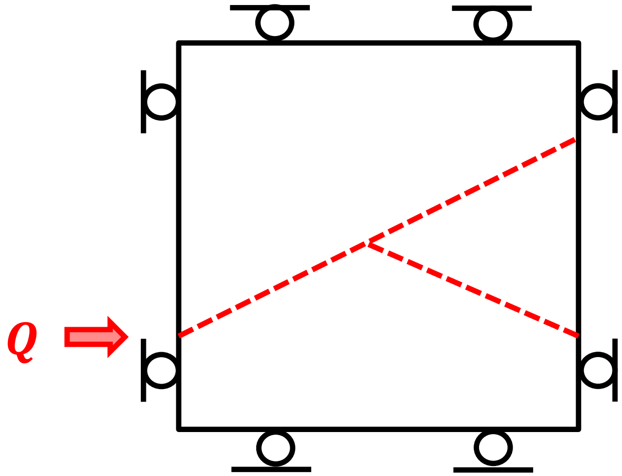

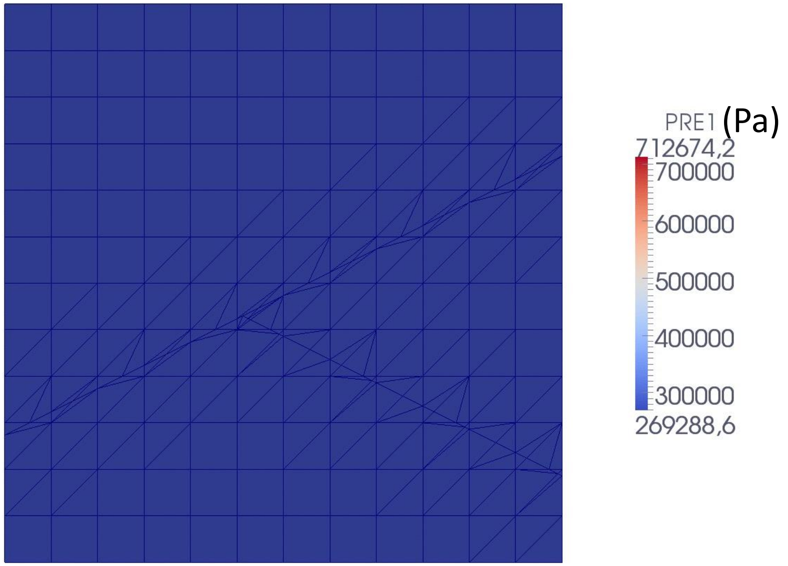

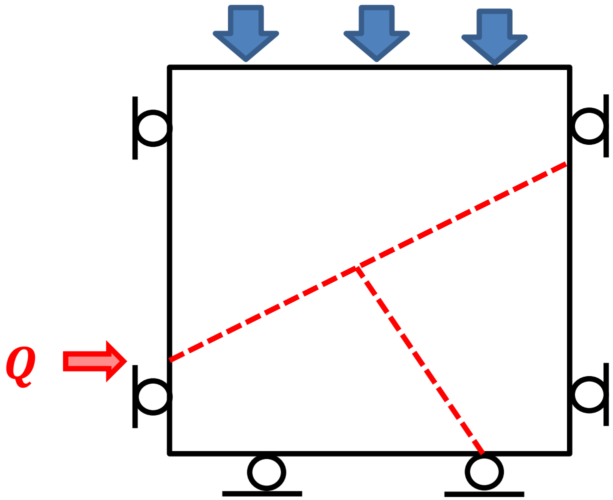

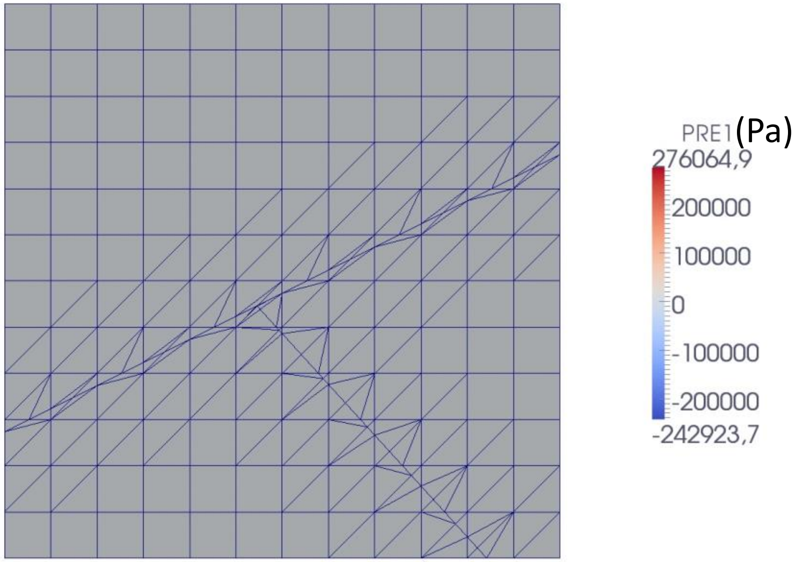

Imposing a fluid flux in a fracture (3D case)

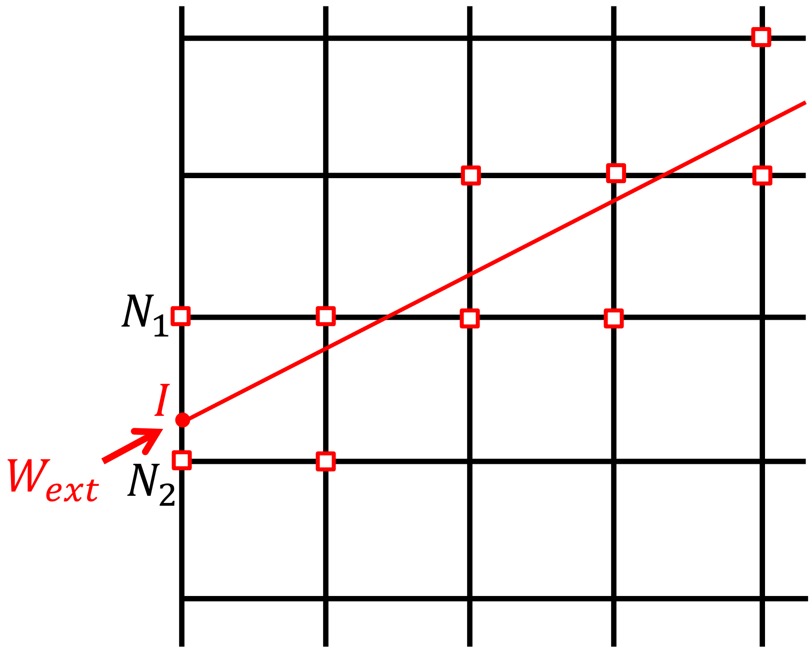

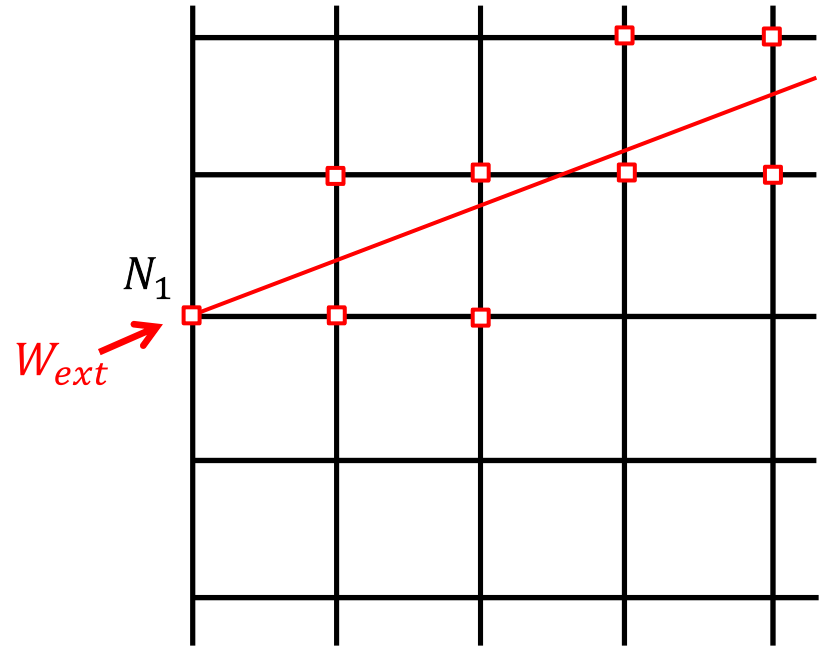

Imposing a fluid flux in a fracture (3D case)